A baculovirus-mediated expression system for the analysis of HaSV RNA packaging

A thesis submitted in the fulfilment of the requirement for the degree of

Master of Science
(Microbiology)

At

Rhodes University

By

Adriano Mendes

February 2012

Abstract

The *Helicoverpa armigera stunt virus* (HaSV) is a member of a family of small non-enveloped (+) ssRNA insect viruses currently known as the *Tetraviridae*. This family is unique in terms of the *T*=4 quasi-symmetry of its capsid particles and the unusually narrow host range and tissue tropism. Assembly of tetraviral particles has been well characterised and involves the combination of 240 copies of a single capsid precursor protein (VCap) into a procapsid followed by autoproteolytic cleavage to yield the major (β) and minor (γ) capsid subunits within the mature particle. HaSV has two genomic RNAs, RNA 1 encoding the replicase and RNA 2 encoding VCap and p17, the ORF of which lies upstream of and overlaping with the 5' end of the *VCap* ORF. Prior to this study, Vlok (2009) used a plasmid expression system to study RNA packaging in HaSV VLPs assembled in *Spodoptera frugiperda* 9 (*Sf9*) cells co-expressing p17 and VCap. The study showed that the *p17* ORF was required for the packaging of RNA 2 during capsid assembly but it was unclear whether p17 expression was required for packaging. In addition, expression from the transfected plasmids was sub-optimal affecting both the yield of VLPs and the detection of p17. The aim of this study was to use the plasmid system to test whether p17 expression was required for plasmid-derived VLP RNA packaging and then develop a baculovirus-mediated system to test this hypothesis.

By using a plasmid in which the start codon of *p17* was mutated, it was shown that p17 expression was required for RNA 2 packaging into plasmid-VLPs. For the baculovirus system, four recombinant baculoviruses based upon the pFastBac Dual expression system, were constructed. These included Bac20, expressing wild type RNA 2, Bac21, RNA 2 with *p17* silenced, Bac23, RNA 2 and *p17* expressed on a separate transcript and Bac24, RNA 2 with *p17* silenced plus *p17* expressed on a separate transcript. Assembly of VLPs was more efficient using the baculovirus expression system and p17 expression was observed in cells infected with Bac20, Bac23 and Bac24, but not Bac21. In contrast to the plasmid-VLPs, bac-VLPs did not require p17 for the encapsidation of RNA 2. In addition to RNA 2, Bac23 and Bac24 packaged the *p17* mRNA transcribed separately from RNA 2. This insinuated that

bac-VLPs may be packaging RNA non-selectively. It was proposed that p17 may play a role in packaging in an RNA-limiting environment (plasmid system) but functioned differently when viral RNA was in excess (baculovirus system). This data points to the importance of developing a replication system for the analysis of the packaging pathways of these viruses and this study has laid down the foundations for such a system in which RNA 1 and RNA 2 can be introduced into a single cell by means of a single recombinant virus.

Table of Contents

List of Figures

List of Tables

List of Abbreviations

Viruses:

AcMNPV	*Autographica californica multicapsid nuclear polyhedrosis virus*
AMV	*Alfalfa mosaic virus*
BMV	*Brome mosaic virus*
CCMV	*Cowpea chlorotic mottle virus*
DpTV	*Dendrolimus puncatatus tetravirus*
EeV	*Euprosterna elaeasa virus*
FHV	*Flock House virus*
HaSV	Helicoverap *armigera stunt virus*
HIV	*Human immunodeficiency virus*
NβV	*Nudaurelia capensis beta virus*
NωV	*Nudaurelia capensis omega virus*
PrV	*Providence virus*
TaV	*Thosea asigna virus*
TMV	*Tobacco mosaic virus*

General:

(+)	positive sense
amp^R	ampicillin resistance gene
ARM	arginine-rich motif
bac-VLPs	virus-like particles derived from the infection of recombinant baculoviruses
bp/s	base pair/s
BSA	bovine serum albumin
C1	bromovirus RNA-protein complex 1
cDNA	complementary deoxy-ribonucleic acid
CDS	coding sequence
Cryo-EM	cryo-electron microscopy
dddwater	triple distilled water
DI RNA	defective-interfering RNA
DIG	digoxygenin
DNA	deoxyribonucleic acid

E. coli	*Escherichia coli*
eGFP	enhanced green fluorescent protein
ER	endoplasmic reticulum
gent^R	gentamycin resistance gene
HC	hairpin cassette ribozyme
hr:AcMNPV	hyprid insect promoter from the *Autographica californica multi capsid nuclear polyhedrosis virus*
Hsp90	Heat shock protein 90
IPTG	isopropyl β-d-1 thiogalacto-pyranoside
kan^R	kanamycin resistance gene
kb	kilobase
KCl	potassium chloride
kDa	kiloDalton
LA	Luria-Bertani agar
LB	Luria-Bertani broth
MOI	multiplicity of infection
MOPS	4-morpholine-propane sulphonic acid buffer
M_R	relative molecular weight
mRNA	messenger RNA
Na$_2$EDTA	disodiumethylenediaminetetra-acetic acid
NaCl	sodium chloride
NC	nucleocapsid protein
NP-40	octyl phenoxypolyethoxylethanol
Nt	nucleotide
ORF	open reading frame
P	pseudo-triangulation number
PCR	polymerase chain reaction
pfu	plaque forming units
pfu/ml	plaque forming units per millilitre of baculovirus innoculum used per well
plasmid-VLPs	virus-like particles derived from the transfection of plasmids
RNA	ribonucleic acid
SDM	site-directed mutagenesis
SDS-PAGE	sodium dodecyl sulphate – polyacrylamide gel electrophoresis
Sf21	*Spodoptera frugiperda* midgut cell line 21

Sf9	*Spodoptera frugiperda* midgut cell line 9
ss	single stranded
SV40	*Simian virus 40* origin of replication
T	triangulation number
TEM	transmission electron microscopy
Tris	tris(hydroxymethyl)aminomethane
UTR	untranslated region
UV	ultraviolet
v/v	volume per volume
VCap	virus capsid protein
VLPs	virus-like particles
w/v	weight per volume
X-Gal	5-brome-4-chloro-3-indolyl-β-d-galactopyranoside

<u>Acknowledgments</u>

I would like to express my gratitude to the following people:

- My supervisor, Prof. R.A. Dorrington for introducing me to scientific research, garnering my passion for this field and developing my skills as a scientist. I consider myself privileged to have gained from your vast knowledge and expertise and am thankful for the enthusiastic support you have always provided.

- Val Hodgson, without which mine and any other projects would not be possible.

- Members of lab 417 both past and present. In particular, Dr James Short. It was a pleasure having such a wise colleague to both work with and sometimes argue against, we make a formidable partnership.

- My parents Alida and Telmo Mendes and my brother Alessandro, who sought not to understand what I was working on but rather to support me unequivocally. I owe all my success to my loving family.

- Jess Watermeyer, whose constant love and affection kept me afloat during trying times.

- My friends and especially those individuals whom I lived with in Grahamstown for the last six years. I am grateful to you guys for showing me that there is life outside the laboratory.

- Our collaborators at the Scripps Research Institute for kindly supplying us with an additional baculovirus.

Chapter 1

Literature review

1.1   Introduction

In the classical definition of the infectious life cycle, a virus must attach to and enter the host cell, express its genes and set up replication factories, replicate the viral genome, assemble new virus progeny and then release the progeny to infect the next cell. Unfortunately for the cell but fortunately for the virus, there are virtually an unlimited number of ways in which these steps may be modified to infect any cell type on the planet, but in general this definition represents a handy framework within which to compare the life cycles of seemingly unrelated viruses.

Since the 1970s, virus assembly has been an extensively studied area of the viral life cycle, due in part to availability of the technology of the time, i.e. X-ray crystallography and electron microscopy (Rossmann and Johnson, 1989). According to a review on virus assembly by Casjens and King in 1975, assembly of a virus particle involves the following basic steps: (1) protein subunits coming together to form a closed shell, (2) the packaging of nucleic acids into this shell, (3) any other steps required to make the newly formed particle infectious and (4) the regulation of both the structure and information encoded by these particles by various processes. In addition, the authors motivated for the study of virus assembly by maintaining that effective anti-viral therapy could only be achieved when factors influencing assembly were well understood (Casjens and King, 1975). Although this is a rather dated review, the reasons behind the analysis of viral assembly mechanisms are still as important today as they were more than 30 years ago.

Icosahedral viruses have always been at the forefront of the study of assembly pathways. Indeed Rossmann and Johnson (1989), stated that the elucidation of the structure of *Tomato Bushy stunt virus* (Harrison *et al*., 1978) and *Tobacco mosaic virus* (TMV), (Bloomer *et al*., 1978) themselves icosahedral single-stranded (ss)RNA viruses, "initiated high-resolution structural virology". The structure of plant viruses

was studied by Crick and Watson as early as 1956, in a paper in which they elegantly outlined how regular polyhedrons may be an accurate representation of the shape of virus particles (Crick and Watson, 1956). They proposed that the small amount of information encoded on a viral nucleic acid would be sufficient for a protein which had a molecular weight of only a fraction of the whole capsid. Multiple copies of this protein would thus have to be repeated in order to fully encapsulate the nucleic acid without any gaps and thus only a regular polyhedron shape could realistically adhere to these conditions (Crick and Watson, 1956).

In 1962 Casper and Klug advanced the theory developed by Crick and Watson, by showing that in order for one protein to produce a regular polyhedron, each of its copies had to take up a "quasi-equivalent" environment in relation to its neighbour. An icosahedron of quasi-equivalent proteins was predicted as the most favourable polyhedron and this has proven accurate given the number of icosahedral viruses isolated to date (Natarajan *et al.*, 2005). Furthermore Casper and Klug noted that when more than one protein makes up each face of an icosahedral virus, a triangulation number (T) should be used to identify the number of quasi-equivalent units, therefore, making $60T$ the number of proteins making up an icosahedral capsid particle. During these studies, another important element of virus assembly came to light in the realisation that in order to assemble a capsid, several different types of non-equivalent contacts are needed to complete the shell (Harrison, 2001). This means identical subunits need to make non-identical contacts in a quasi-symmetrical icosahedral structure and somehow the virus needs to make a choice as to which contacts to make and when in order to achieve the most optimal arrangement (Harrison, 2001). The accurate assembly of these contacts as well as the incorporation of the genome within represent the major challenges that have moulded the specificity with which viruses assemble icosahedral particles.

1.2   <u>Assembly of icosahedral viruses</u>

The mechanism of assembly of a virus is determined by its capsid proteins and in the past the major emphasis has been on determining how a similar set of these proteins is able to arrange a symmetrical icosahedral structure (Schneemann, 2006).

In fact, the protein-protein interactions are but one third of the process of assembling viruses. According to Fox *et al.* (1994) both sequence specific RNA-protein interactions (generally responsible for initiation and regulation of assembly) and sequence independent RNA-protein interactions (responsible for stabilizing packaged RNA), must take place before the formation of a capsid shell around RNA viruses. In addition, the ability of the virus to select and package only viral RNA from the slew of cellular RNA is essential for efficient assembly. A review of some of the basic systems available for the study of the assembly of icosahedral viruses is presented in Table 1.1. High resolution protein structural data was extremely useful in these systems and traditionally *in vitro* assembly experiments were favoured. Due to the limitations of molecular techniques in the past, the protein-nucleic acid interactions have only recently become the focus of attention and there is now increasing structural data relating to how these two molecules combine to form viruses (Schneemann, 2006). There is however, still limited information on how the RNA is specifically packaged into icosahedral virus particles and there are even fewer studies that have delved into the specific intracellular events involved.

Table 1.1: Model systems available for the study of icosahedral RNA virus assembly

Virus	RNA genome	Capsid proteins	*In vitro* assembly system	Identification of packaging signal	High resolution structure
Plant					
Cowpea chlorotic mottle virus	Multiple	Single	Yes	No	Yes
Turnip crinkle virus	Single	Single	Yes	Yes	Yes
Bacteria					
Phage R17	Single	Single	Yes	Yes	No
Animal					
Hepatitis B pregenome	Single	Single	No	Yes	No
Sindbis virus	Single	Single	Yes	Yes	No

(Adapted from Fox *et al.,* 1994)

Icosahedral ssRNA viruses have been organised into three categories based upon the similarity of their capsid structure and assembly mechanisms. The first category is the ssRNA plant viruses. These viruses tend to exhibit the traditional *T*=1 or *T*=3

capsid symmetry, with the only exception being the *Comovirus* group that is more similar to the picornaviruses (Casjens and King, 1975; Chen *et al.,* 1989). The positive sense (+) ssRNA bacteriophages represent the second structural group as these viruses package their RNA plus an A protein into distinctive icosahedral head structures with varying symmetries (Hohn and Hohn, 1970). Perhaps the best studied in terms of structure and molecular biology is the third group, the animal picornaviruses (Wien *et al.*, 1996). These viruses have been shown to exhibit a pseudo-*T*=3 capsid symmetry or *P*=3, as each protein in the asymmetric unit does not have the same amino acid sequence but still takes up a quasi-equivalent environment in the capsid particle (Rossmann and Johnson, 1989). A diagrammatic representation of the comparison between the *T* symmetry of the plant viruses versus the *P* symmetry of the picorna and comoviruses is presented in Fig. 1.1.
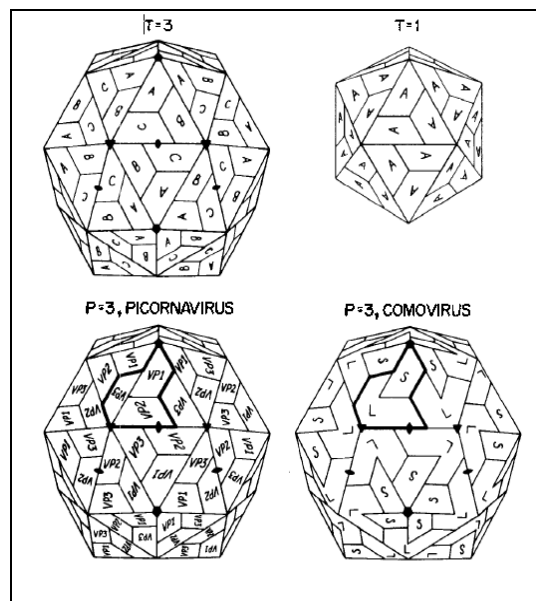
Figure 1.1: Structure of icosahedral RNA viruses. The majority of plant and insect viruses are represented in the top tier as their capsid structures tend to exhibit *T*=3 or *T*=1 symmetry. *T*=1 viruses contain only one capsid protein (**A**) per asymmetric capsid face, while *T*=3 viruses require three of the same proteins (**A**, **B** and **C**) each in a quasi-equivalent environment. The picornaviruses and the plant group, the comoviruses, are represented in the bottom tier. The symmetry in this instance is described as *P*=3, as the proteins are quasi-equivalent but VP1, 2 and 3 are not the same protein. Comoviruses combine two large subunit proteins (L) and a small subunit protein (s) to resemble the *P*=3 symmetry (Taken from Rossmann and Johnson, 1989).

1.3   RNA packaging

The mechanisms by which all the viruses in the above mentioned groups assemble both the protein and RNA components together have been generalised into two basic pathways. The first is called the procapsid pathway, in which there is the initial assembly of a procapsid (partially assembled capsid particle) into which the RNA is inserted. The second insinuates a greater responsibility on the RNA and involves viral RNA-protein complexes being formed, which then initiate the assembly of additional protein components around the RNA to form a closed shell (Fox *et al*., 1994). Although by no means a rule, many phages and picornaviruses utilise the procapsid pathway while many plant viruses make ribonucleoprotein complexes (Fox *et al.,* 1994). These pathways provide a basis behind what is known as packaging.

Packaging refers to the point in the assembly process when nucleic acids are to be incorporated into the capsid and in general, it is largely the responsibility of the capsid protein to identify specific signals on viral RNA and carry out this process (Liljas, 1999). The capsid proteins of many icosahedral RNA viruses surprisingly share a major similarity in that the shell forming unit of these viruses is essentially the same eight antiparallel β-strands in a "jelly roll" formation (Rossmann and Johnson, 1989). There are a variety of ways that domains have been inserted between and around the β-strands of the jelly-roll core, but RNA viruses all tend to incorporate largely positively charged N or C-terminal residues on the interior face of the capsid in order to bind negatively charged RNA (Schneemann, 2006). Although the structure of the RNA within the capsid is becoming clearer, the mechanisms by which capsid proteins identify viral RNA as opposed to cellular RNAs are not as well understood and a variety of factors have been shown to play a role.

RNA secondary structure is generally an important element for recognition by capsid proteins. For example the *Hepatitis B virus* (*Hepnaviridae*) utilises a stem-and-loop region known as the ε site as a packaging signal for pregenomic RNA to be packaged into the nucleocapsid core (Kramvis and Kew, 1998). Despite differing primary sequences, it has been predicted that all hepanaviruses not only require this structure for selectively packaging subgenomic RNA, but also for the activation of

reverse transcription (Fallows and Goff, 1995). A general feature of RNA packaging is that it is difficult to differentiate the requirements for packaging from other viral processes that may be tightly coupled to packaging, such as reverse transcription (in hepnaviruses) and replication (linked in nodaviruses and bromoviruses) (Fallows and Goff, 1995; Venter and Schneemann, 2007). Other examples of RNA viruses that utilise stem-and-loop packaging signals are the togavirus, *Sindbis virus* and the coronavirus, *Mouse hepatitis virus* (Frolova *et al.*, 1997; Molenkamp and Spaan, 1997). Whether these signals play a role in other processes within the lifecycle of these viruses is yet to be determined.
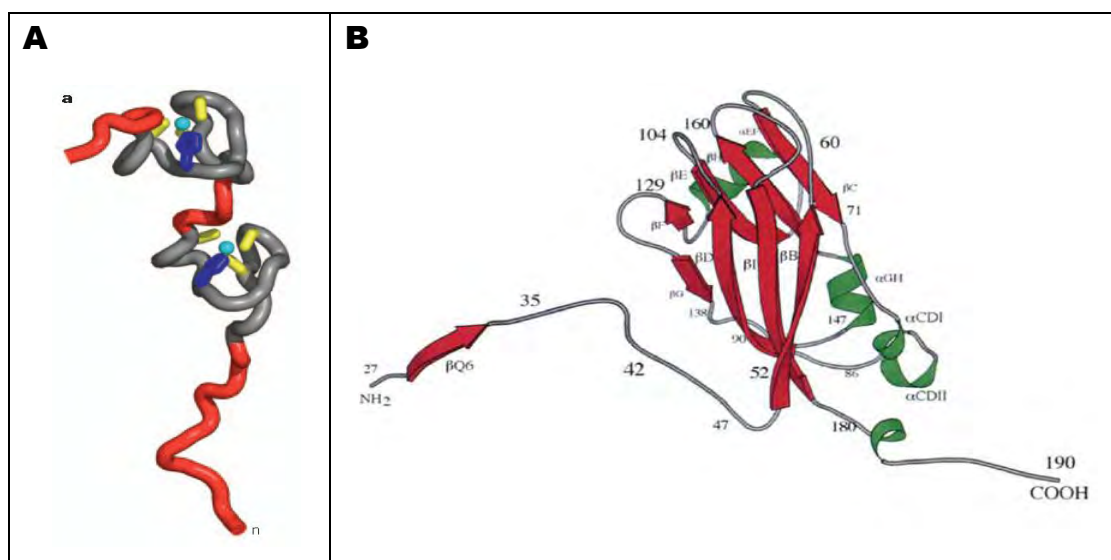
Figure 1.2: Structure of the HIV nucleocapsid protein (NC) and the CCMV capsid protein. (**A**) Ball and stick model of the HIV-1 NC protein, showing the two zinc-knuckle domains bound to zinc atoms (cyan) towards the middle of the protein (backbone – grey, Cys – yellow, His – blue, flexible tail – red) (D'Souza and Summers, 2005). (**B**) Ribbon diagram of the CCMV coat protein (β sheets – red and α helices – green). The N terminal region prior to the first β sheet contains an ARM which is critical in RNA recognition (Taken from Speir *et al.*, 2006).

Viral RNA is recognised by many common motifs found on the capsid proteins of unrelated viruses and therefore, the capsid protein itself is another important element in RNA packaging although, many capsid proteins have been observed to lack a specific RNA binding motif and still bind RNA. This is probably due to the fact that with the structural diversity of RNA comes a large degree of diversity in the way proteins can bind to it (Draper, 1995). The arginine-rich motif (ARM) is an example

of a widely used RNA recognition motif (Fig. 1.2 B). It is used by the capsid protein of the nodavirus *Flock House virus* (FHV) to package RNA 1 (Venter *et al*., 2009), the capsid proteins of members of the *Bromovirus* genus, *Brome mosaic virus* (BMV) and *Cowpea chloritic mottle virus* (CCMV) to package their RNAs (Annamalai *et al*., 2005) and by the *Human Immunodeficiency virus* (HIV) REV and TAT proteins for their separate functions in regulating HIV gene expression (Draper, D. 1995). Zinc-finger or zinc-knuckle domains are another example of RNA binding domains (Fig. 1.2 A). The HIV nucleocapsid protein (NC) domain of the GAG polyprotein contains one or two such zinc-fingers that aid in the selective packaging of the RNA dimer into the nucleoprotein core (D'Souza and Summers, 2005).

Other factors over and above protein-RNA interactions can play equally important roles in RNA packaging. Both the RNA and the capsid protein may need to be in close proximity in order to facilitate binding and this makes the site of assembly another key consideration. An example of this comes from the nodaviruses, where it has been shown that targeting to the mitochondria may represent a key process in the sequential packaging of RNA 1 and RNA 2 (Venter *et al*., 2009). Cellular proteins can also be involved in RNA packaging, an example of which is the heat shock protein 90 (Hsp90). Hsp90 is involved in binding to the ε site of *Hepatitis B virus* and could have some effect on the packaging of both the polymerase and the RNA into the nucleocapsid (Kramvis and Kew, 1998).

In summary, packaging and assembly of icosahedral RNA viruses involves a variety of viral and cellular elements combining to make an infectious particle. In the past, there has been a trend to separate these into separate bodies of work, involving either packaging or assembly pathways. In reality these pathways are heavily interlinked and very often it is the interaction of protein and RNA that simultaneously initiates assembly and packaging in the first place.

1.4 <u>Tetraviruses</u>

The family of interest in this study is the *Tetraviridae,* a family of viruses that infect exclusively insect hosts and thus the question arose as to where insect viruses fitted in, in terms of their strategies for assembly and packaging. In 1998 Christian and Scotti categorised the RNA viruses that infect insects into four key families: the *Picornaviridae*, *Dicistroviridae*, *Nodaviridae* and *Tetraviridae*. When one examines these families closely it would seem that the insect picornaviruses assimilate into the *P*=3 picornavirus assembly group (Knowles *et al*., 2011). On the other hand, the dicistroviruses (which have a *T*=3 symmetry despite formally being part of the family *Picornaviridae*), the nodaviruses (*T*=3) and tetraviruses (*T*=4) bear the most similarity to the first assembly category, the ssRNA plant viruses, based on their capsid symmetry and varying degrees of similarity in genome organisation as well (Chen *et al*., 2011; Thiéry *et al*., 2011; Dorrington *et al*., 2011). This literature review will focus on the specific packaging and assembly of (+) ssRNA into the first assembly category, the ssRNA plant viruses and by extension the insect viruses. The review will highlight what is known about assembly and packaging of the *Bromoviridae*, a family of *T*=3 plant viruses, continue through the *Nodaviridae,* a family of *T*=3 insect viruses ending off with what little is known about tetravirus packaging, in the hope that by contrasting structurally similar viruses, some clues will be will discovered as to which of the packaging factors are important in the *Tetraviridae*.

The tetraviruses are a relatively underexplored family of non-enveloped insect (+) ssRNA viruses. It is surprising that so little research has been done on this family given the peculiar properties of these viruses. Tetraviruses were the first *T*=4 icosahedral viruses to be discovered and it is for this reason that the family has been named the *Tetraviridae* (Finch *et al*., 1974). Tetravirus particles are relatively small, ranging from 32 – 42 nm in diameter (Dorrington *et al*., 2011). Both the host range and tissue tropism of these viruses is very narrow, to date they have only been found to infect the larvae of moths and butterflies belonging to the order *Lepidoptera* and can only be isolated from the midgut tissue of their host species (Finch *et al*., 1974; Dorrington *et al*., 2011; Brooks *et al*., 2002). In addition, only one tetravirus species,

Providence virus (PrV), has been shown to replicate in tissue cultured cells despite numerous attempts with various cell lines (Pringle *et al*., 2003; Bawden *et al*., 1999). The genome organisation and current classification are interlinked, as the two genera are defined by the monopartite (*Betatetravirus*) or bipartite (*Omegatetravirus*) nature of encapsidation (Fig 1.3 A). Members of the *Betatetravirus* genus express the replicase (5' ORF) and the capsid protein precursor α (3' ORF) from one RNA strand, utilising a sub-genomic RNA for expression of the capsid protein precursor (VCap), which may also be encapsidated (Fig 1.3 A). The type species of this genus is the *Nudaurelia capensis beta virus* (NβV) while PrV is unique in that it encodes a third open reading frame (ORF), designated p130, which is the first ORF at the 5' end of the viral genome (Fig 1.3 A and C). Whether p130 is expressed and how it functions in the viral life cycle, is unknown (Gordon *et al*., 1999; Walter *et al*., 2010).

In species belonging to the genus *Omegatetravirus*, the replicase and VCap are encoded by two separate genomic RNAs, RNA 1 and RNA 2 respectively, both of which are encapsidated within the same particle (Fig 1.3 A). In addition to the replicase, the RNA 1 of the omegatetraviruses also encodes three small proteins overlapping with the *replicase* ORF at its 3' end (Dorrington *et al*., 2011). The expression of these proteins and their function in the viral lifecycle is yet to be elucidated. A further ORF encoding a protein of 17 kDa (p17) is found upstream and overlapping with the *VCap* ORF on RNA 2 (Dorrington *et al*., 2011). The position of the *p17* ORF and its amino acid sequence is conserved in all three omegatetraviruses, alluding to a common function (Du Plessis *et al*., 2005; Hanzlik *et al*., 1995; Yi *et al*., 2005). The *p17* ORF is preceded by a poor translation context and the predicted amino acid sequence contains a high proportion of Pro-Glu-Ser-Thr amino acids, collectively known as PEST signals (Reichsteiner and Rogers, 1996; Kozak; 1987; Hanzlik *et al*., 1995). This data prompted Hanzlik and colleagues to propose that p17 might be a movement protein or function in regulating viral replication (Hanzlik *et al*., 1995). The *Dendrolimus punctatus tetravirus* (DpTV) p17 has been shown to bind RNA. The study by Zhou *et al*. (2008) showed that recombinant p17 bound viral RNA 2, but also exhibited non-specific binding to non-viral ssRNA, dsRNA and DNA. The authors speculated that the protein was involved in regulating viral RNA replication (Zhou *et al*., 2008).

As mentioned, the name *Tetraviridae* is derived from the *T*=4 capsid symmetry of the particles (Finch *et al*., 1974). Yet despite commonality regarding the structure of the capsids, the replicase proteins used by different species within the family can be separated into three major families. For this reason the *Tetraviridae* is being re-classified into three new families based on the sequence of the replicase proteins (Fig. 1.3). The new families are as follows: (1) The *Alphatetraviridae* (Fig 1.3 A), which will consist of the two genera mentioned previously, *Betatetravirus* (monopartite) and *Omegatetravirus* (bipartite); (2) the *Permutotetraviridae* (Fig 1.3 B), which will only contain two species, *Thosea asigna virus* (TaV) and *Euprosterna elaeasa virus* (EeV), and have been separated from the alphatetraviruses on the basis of an internal permutation on the replicase and the lack of methyl transferase and helicase domains on the protein and (3) the *Carmotetraviridae* (Fig 1.3 C), which will comprise the monopartite PrV and also lack the methyl transferase and helicase domains but encodes a carmo-like replicase (Dorrington and Short, 2010).
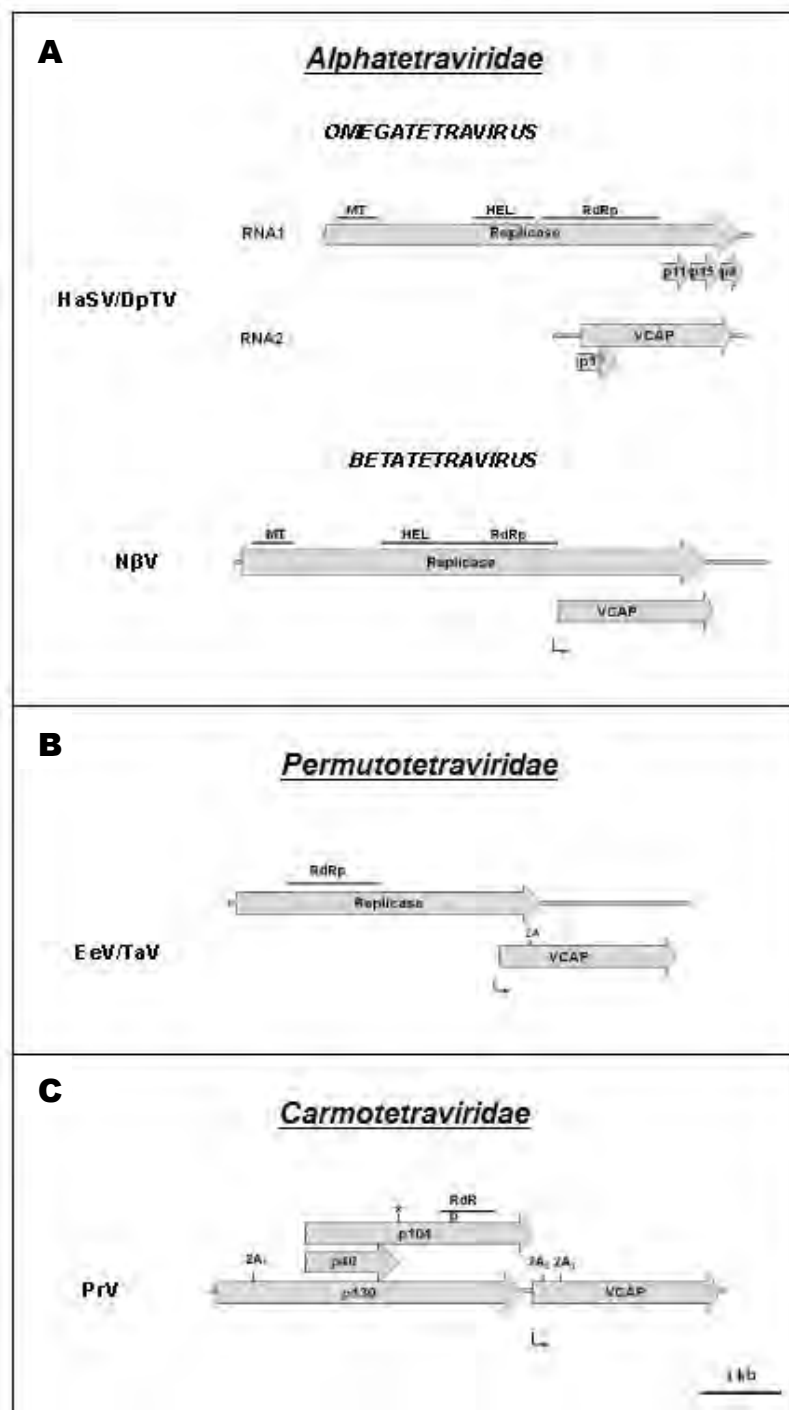
Figure 1.3: Genome organisation of the re-classified *Tetraviridae*. (2A) refers to the 2A-like processing sequences and (*) the read through stop codons. The conserved domains of the replicase proteins are refered to as MT for methyl transferase domain, HEL for the helicase domain and RdRp for the RNA-dependant RNA polymerase domain. Bent arrows indicate the start of a subgenomic RNA species. HaSV – *Helicoverpa armigera stunt virus*, DpTV – *Dendrolimus punctatus tetravirus*, NβV – *Nudaurelia capensis beta virus*, EeV – *Euprosterna elaeasa virus*, TaV – *Thosea asigna virus*, PrV – *Providence virus* (Adapted from Dorrington and Short, 2010).

Capsid assembly

The novel nature of the structure of the *T*=4 tetravirus capsid has meant that a great deal of research has been undertaken regarding capsid assembly. The first tetravirus crystal structure was developed by Cavarelli and colleagues in 1991. The structure of the *Nudaurelia capensis omega virus* (NωV) capsid at 2.8 Å resolution was the first description of a virus in which 240 copies of a single protein made up a capsid with *T*=4 symmetry (Fig. 1.4). The *T*=4 nature of the particle thus means that there are four separate conformations of the capsid proteins, described as subunits A, B, C and D. Therefore, when compared to the other viruses in the *T*=3 assembly category mentioned above, tetraviruses contain one extra conformation (Cavarelli *et al.*, 1991).
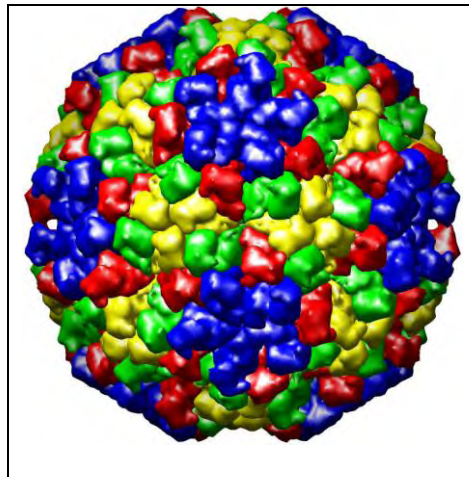
Figure 1.4: Structure of NωV. NωV is the current type species of the genus *Omegatetravirus* and the capsid is characterised as *T*=4 due to the four separate quasi-equivalent conformations that the capsid protein takes up. These are designated A (blue), B (red), C (green) and D (yellow). A complete particle is assembled from pentamers, formed by the interaction of A subunits (blue) to each other, and quasi-hexamers, formed by the pairing of B (red), C (green) and D (yellow) subunits (Carillo-Tripp *et al.*, 2009; NωV: http://viperdb.scripps.edu/info_page.php?VDB=1ohf).

During assembly, tetravirus capsid dimers assemble into an alternating series of pentamers and quasi-hexamers to form the capsid shell. Five copies of the A subunit form the pentamers while pairs of B, C and D subunits form the quasi-hexamers (Fig. 1.4). Initially this particle exhibits a swollen immature form called a procapsid. The procapsid then undergoes maturation which coincides with a drop in

pH, which in turn promotes the protonation of specific residues on VCap (Canady *et al.*, 2000). The orientation of these residues in relation to an Asp-Phe pair within the capsid core is thus changed, making this bond sterically unfavourable. Maturation thus occurs via the autoproteolytic cleavage of the Asp-Phe peptide bond in all 240 copies of the capsid protein, resulting in major (β) and minor (γ) capsid proteins that remain part of the mature particle (Dorrington *et al.*, 2011).

Extensive analysis of the tetravirus procapsid using cryo-EM has shown that NωV procapsids are rounder, larger in diameter, perforated and contained different conformations of the internal and external protein domains when compared to the mature capsid (Canady *et al.*, 2000). In this regard, a link was made to the swollen form of the bromoviruses TBSV and CCMV and it was noted that these viruses also utilise a protein dominated molecular switch (Canady *et al.*, 2000). X-ray scattering was used to analyse the unique properties of the procapsid (Canady *et al.*, 2001). From these experiments it was shown that the procapsid is an independent stable structure at pH 7.6 and undergoes a complete maturation at pH 5.0 within seconds. The conformational change seems to facilitate the cleavage reaction and conversely this reaction can take as long as 96 hours to complete but is irreversible if more than 15 % of the residues are already cleaved per capsid (Canady *et al.*, 2001). Specific mutations at key residues around the cleavage site have shown that these capsids are able to revert back to the procapsid state when the pH is reversed back to 5 from 7.6 (Taylor *et al.*, 2002).

The experiments described above have prompted the maturation reaction to be described as a "pH-driven machine" involving the molecular switch (schematically represented in Fig. 1.5). The C-terminal region of the C and D subunits which will represent the wedge between flat contacts (molecular switch) acts as the engine, while the remainder of the capsid subunits act as the cargo (Taylor *et al.*, 2002). After a drop in pH, these key helices are converted to coils via the protonation of amino acids around this area. The coils are consequently small enough to act as the wedge between capsid subunits and thus flat instead of bent contacts are created. Taylor *et al.* (2002) proposed that this may also explain the evolution of the cleavage

reaction post-assembly, as it uncouples the engine from the cargo and thus when the particle has been formed into a mature capsid, the pH has no bearing on its structure and it is thus "locked" in place. Evidence from experiments where the pH of maturation was carefully controlled via titration have shown that pH is not necessarily required for the chemistry of the cleavage reaction but is required for the protonation of the domains around the active site, thus ensuring that it is accessible for the auto-proteolytic reaction (Matsui *et al*., 2009).
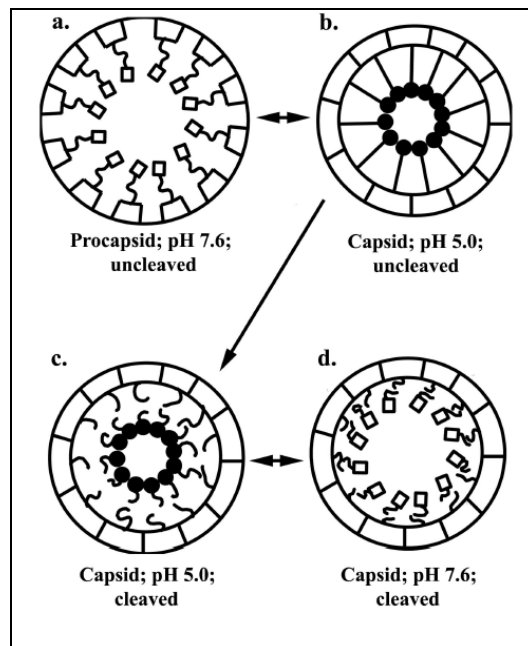
Figure 1.5: Representation of the "pH-driven machine" controlling maturation of tetravirus particles. The region of the helical domain responsible for maturation in NωV is residues 1 – 44 and 571 – 644. The core of the capsid precursor protein is represented by an empty rectangle. The internal helical region is either represented as a helix (empty square) or a coil (filled in circle). (**a**) The procapsid is a porous structure isolated at pH 7.6 in which the internal helical regions are in the helix conformation. (**b**) Upon reduction to pH 5, protonation of key residues institutes conformational changes in the internal region that result in the helices being converted to coils. (**c**) Without cleavage the procapsid to capsid state is reversible but upon cleavage the engine (γ peptide) of the "machine" is separated from the cargo (rest of the protein). (**d**) The capsid is thus locked in position and shifts in pH between 5 and 7.6 can alter the state of the internal helical region without affecting the capsid structure (Reproduced from Taylor *et al*., 2002).

Unfortunately, further analysis of the assembly of tetraviruses is hampered by the fact that they are not infectious in cell culture. For this reason a variety of alternate strategies and systems have been employed to produce virus-like particles (VLPs)

that can be used to map the *T*=4 structure of the capsids. Non-infectious NωV VLPs that are structurally indistinguishable from the wild type particle have been produced by the baculovirus mediated expression of the *VCap* ORF in insect cells (Agrawal and Johnson, 1995; Taylor *et al*., 2002; Maree *et al*., 2006). HaSV VLPs (which are also non-infectious) have also been produced from yeast as well as plant expression systems, involving *Nicotiana plumbaginifolia* protoplasts (Tomasicchio *et al*., 2007; Gordon *et al*., 2001).

Tetravirus research has progressed to a point in which the structure of the particles and mechanisms of assembly are relatively well understood. Despite this, the mechanisms behind specific packaging are unclear. It is therefore, important to look at other examples of viruses in which assembly and packaging have been analysed side by side, to establish some idea of how tetraviruses may encapsidate their genomes.

1.5   **Bromoviruses**

Plant viruses have historically been effective systems for studying virus assembly and thus packaging for four major reasons. Firstly, their particles were some of the first for which near atomic resolution structures were acquired; secondly, their assembly mechanisms are simple enough to manipulate when compared to their animal counterparts; thirdly, their assembly and packaging mechanisms can be studied *in vitro*, data of which has been shown to be applicable *in vivo* and, finally, the full length cDNA of these viruses is infectious and many constructs are available (Fox *et al.,* 1994). Investigations into how the structure and assembly of bromoviruses affected the packaging of their genomic RNA represents one of the largest bodies of packaging literature to date (Yi *et al*., 2009; Kao *et al*., 2011)

Bromoviruses have been at the vanguard of assembly and packaging for many years. They are (+) ssRNA plant viruses with *T*=3 capsid symmetry (Fox *et al*., 1994). The family *Bromoviridae* forms part of the alphavirus-like superfamily and consists of six genera (Bujarski *et al*., 2011). The genome of these viruses is

segmented into three separate messenger sense RNAs. RNA 1 and 2 encode 1a and 2a proteins that together are essential in RNA replication. RNA 3 is dicistronic, encoding both the movement protein, known as the 3A protein (5' ORF) and the capsid protein (3' ORF) (Alquist, 1994). The capsid protein is expressed via a subgenomic RNA which is co-encapsidated with RNA 3. RNA 1 and 2 are encapsidated into separate particles (Rao, 2006). The assembly and packaging pathways of these viruses is thus complicated by the fact that not only do they need to select viral RNA but they need to ensure that four separate viral RNAs are packaged into separate particles. It would appear that assembly is RNA dependant due to the fact that no empty virus particles have been documented in wild type preparations (Kao *et al.,* 2011). The majority of the understanding of the assembly and packaging mechanisms of this family has come out of the study of two viruses; BMV (Fig. 1.6 A) and CCMV (Fig. 1.6 B).
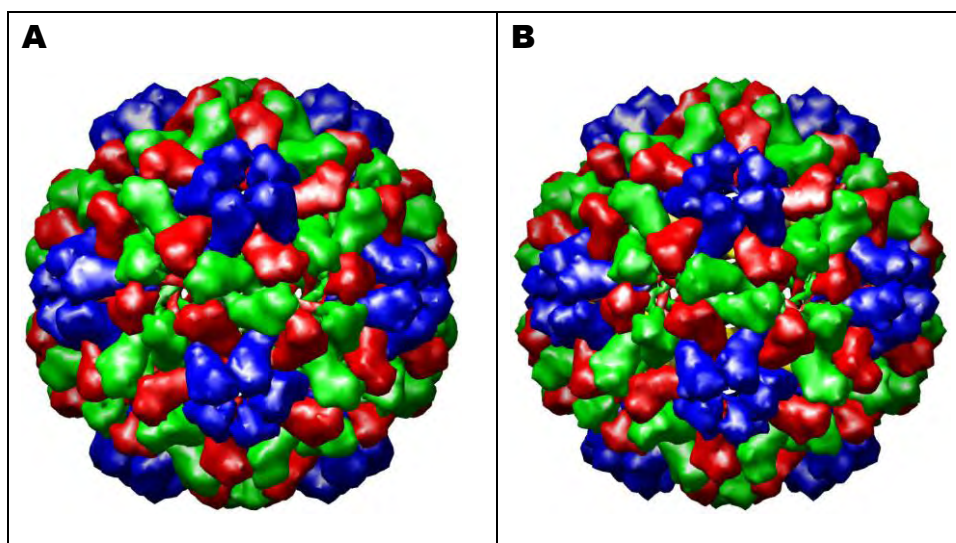
Figure 1.6: Structure of BMV (A) and CCMV (B). Similar subunit conformations of the capsid proteins are depicted in the same colour coding as Fig. 1.4; ie. subunit A – blue, B – red and C – green. Both bromoviruses are made up of pentemers formed between the A subunits and hexamers between B and C. Each protein is quasi-equivalent to its neighbour (Carrillo-Tripp *et al*., 2009; BMV: http://viperdb.scripps.edu/info_page.php?VDB=1js9; CCMV: http://viperdb.scripps. edu/info_page.php?VDB=1za7).

Capsid assembly

CCMV was the first virus to be fully assembled *in vitro* and this work effectively kick-started the study of virus assembly (Bancroft *et al.,* 1969). It was observed that generally, particles were stable at low pH (5.0) and high ionic strength but that when the pH was increased to 7.0 while lowering the ionic content, a swollen form of the particles resulted and upon further increase in pH (above 7.5), the particles completely disassembled into 40S ribonucleoprotein complexes and capsid protein dimers (Bancroft *et al.,* 1969). This study represented the initial framework on which to model bromovirus assembly and was the first indication that a ribonucleoprotein complex and capsid protein dimers may represent the basic assembly units.

Some years later, high resolution structures for both CCMV and BMV were resolved at 3.2 Å and 3.4 Å, respectively (Speir *et al.,* 1995; Lucas *et al.*, 2002). The structure of both sets of viruses was similar in that 180 units of the capsid proteins were combined into sets of quasi-equivalent dimers (A/B, C/C) making up asymmetric pentamers and hexamers forming a *T*=3 particle (Fig. 1.6). The general structure of the viruses and the polymerization of their capsid proteins during assembly is similar to that of the tetraviruses and nodaviruses, as the N and C termini both play a role in tethering one protein subunit to the other (Speir *et al.,* 1995). This was independently corroborated by Zhou *et al.* (1995) who were able to show that N and C termini deletion mutants of CCMV capsid proteins expressed in *Escherichia coli* (*E. coli*) resulted in a variety of assembly defects when assembled *in vitro*. Taken together and given the evidence of many subsequent studies, it is hypothesised that assembly starts with dimerization of the capsid proteins, which itself involves interaction between the C terminal 179 – 190 amino acids of each subunit which are then clamped together and stabilised by the first 49 amino acids of the N terminal (Speir *et al.*, 1995). The dimers then combine to form hexamers between the B and C subunits or pentamers between the A subunits, to which additional dimers are added (Fig. 1.7). The hexmeric structures are known as β-hexamers. RNA binding is thought to occur early on in the process at either the dimer or β-hexamer interface and acts as the molecular switch to induce curvature at certain contacts (Kao *et al.,* 2011). In this way the addition of RNA or nonRNA-bound subunits effectively

initiates the choice between either a bent or straight contact between the capsid subunits allowing for the assembly of a closed shell, while simultaneously packaging the genome.
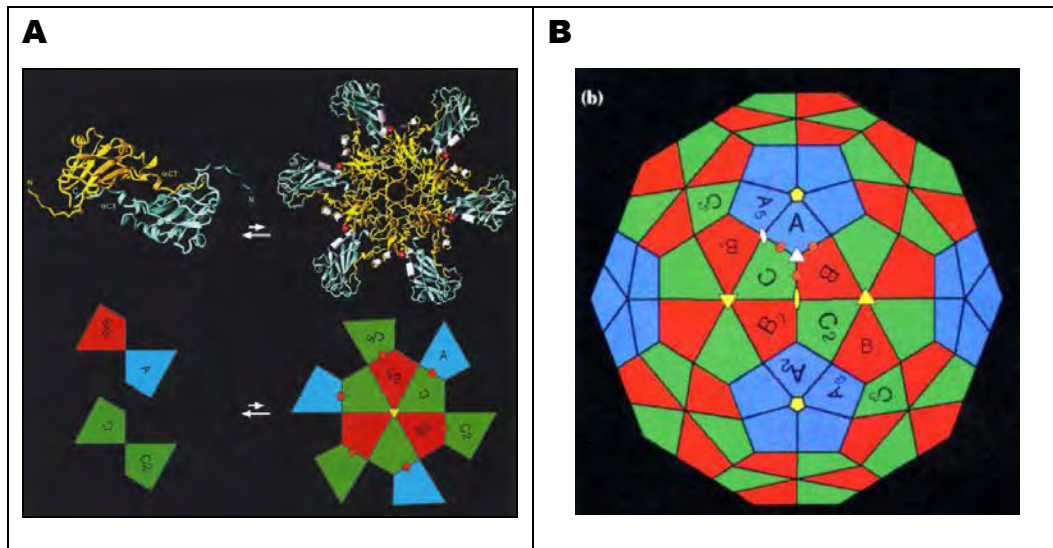
Figure 1.7: Structure and assembly of CCMV. The same colour coding strategy is used as for Fig. 1.4. (**A**) The basic assembly unit is made up of dimers of the same 19.4 kDa capsid protein (shown between subunits B and A or C and C) that combine to form a β-hexamer structure. The top half of (**A**) depicts a ribbon diagram of the process (note the N and C terminal tails extending away from the jelly-roll core in order to facilitate binding to the next subunit), while the bottom half is a diagrammatic representation. (**B**) Diagrammatic representation of the final T=3 capsid particle. (Reproduced from Speir *et al.,* 1995)

The interaction between RNA and protein plays an essential role in the formation of the infectious particle, yet interestingly the same induction of particle formation in bromoviruses can be mimicked by many polyanions, including various RNAs and dextran (Bancroft *et al.,* 1969). Following on from this work, Cuillel *et al.* (1979) was able to show that *Alfalfa mosaic virus* (AMV) 12S RNA could effectively replace *Bromegrass mosaic virus* subgenomic RNA in capsid particles indistinguishable from the wild type, although it was noted that when placed in direct competition for encapsidation the wild type subgenomic RNA effectively outcompeted 12S AMV RNA to the extent that only 20 % of the heterologous RNA was packaged *in vitro* (Cuillel *et al.,* 1979). This indicated that the ionic characteristics of the molecule being packaged play a role in the initiation of assembly, but that selective packaging

mechanisms are present to ensure that the bromoviruses encapsidate the correct RNA (Cuillel *et al.,* 1979).

Packaging

As mentioned earlier, the N-terminus of the capsid proteins of both BMV and CCMV contain regions rich in positively charged arginine residues, known as ARMs (Speir *et al*., 1995; Lucas *et al.,* 2002). These regions have been implicated in ensuring that each capsid particle contains either RNA 1, 2 or 3 and the subgenomic RNA. Despite this, evidence using whole plant infection assays has been somewhat contradictory. When plants were infected with functional RNA 1, 2 and 3 as well as mutant subgenomic RNA in which the codons for four of the arginines in the ARM were mutated to prolines, packaging defects of only the subgenomic RNA were observed (Choi and Rao 2000a). The well-established *in vitro* system was used to reassemble these mutant viruses and it was shown that despite assembling into *T*=3 particles, the subgenomic RNA packaging defect was maintained *in vitro*. As mentioned before, icosahedral virus assembly is dependent on the interaction of the capsid protein with the RNA and thus it was interesting to note that without the ARM the capsid was still able to assemble RNA 1, 2 and 3 particles. Instead of disrupting total RNA packaging, only the signal required for RNA 4 packaging was disrupted (Choi and Rao 2000a). This data implies that the selection of RNA is distinct from the assembly mechanism. These conclusions were supported by the observation that chimeric TMV (family: *Tobamoviridae)* with BMV coat proteins effectively packaged all the subgenomic RNAs generated by the TMV genome (Choi and Rao 2000b). The results suggested that the ARM must be able to recognise a region (of which both primary and secondary structure may be important) contained on its own open reading frame and that RNA 1, 2 and 3 must have similar regions in order to be packaged (Choi and Rao 2000b). The binding of the RNA to the ARM is not necessarily specific and thus the virus requires some other mechanism to ensure RNA specificity (Choi and Rao 2000b).

In 2003, a dynamic model for the packaging of CCMV was postulated, based on *in vitro* RNA binding assays and gel shift data (Johnson *et al.,* 2003). By combining

RNA 1 with varying concentrations of the capsid dimers, two distinct shift profiles were observed: (1) a fast pathway occurring after just twenty minutes at approximately stoichiometric binding of ninety dimers and (2) a slow pathway, only being evident after twenty-four hours. The fast pathway resulted in a characteristic nucleoprotein complex that resembled wild type RNA binding, while the slow pathway had a bimodal gel shift in which some RNA formed wild type complexes while another portion migrated quicker than RNA 1 alone. This was called complex 1 (C1) and it was concluded that RNA folding instead of degradation must have been responsible for its formation and migration (Johnson *et al.,* 2003).
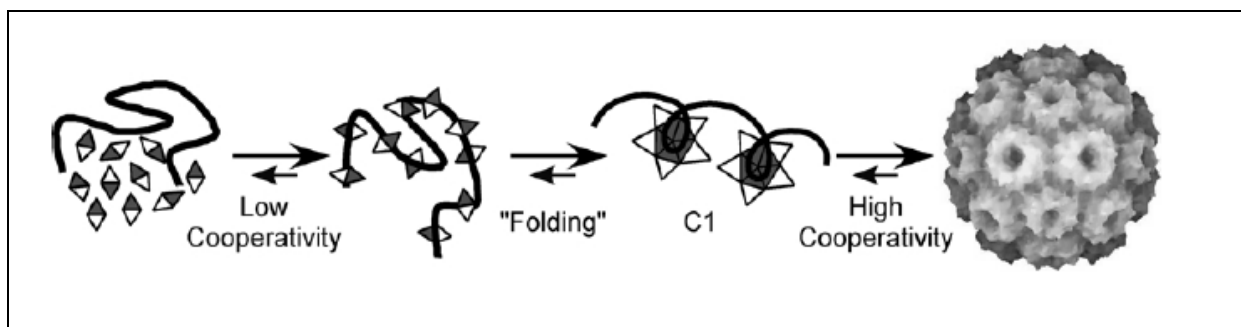
Figure 1.8: Model for the specific packaging of RNA 1 into CCMV particles. The diamonds represent capsid protein dimers and the single line RNA 1. At low protein concentrations, the dimers find high affinity RNA binding sites on the viral RNA and bind. This allows the ribonucleoprotein complex to fold into C1. This initial binding is at low cooperativity, given the lower capsid protein concentration and therefore progresses slowly. Once viral RNA is "labelled" as C1, then a high cooperativity binding of additional dimers results and the assembly of the capsid particle can be completed (Taken from Johnson *et al.,* 2003).

A model which takes advantage of the differing concentrations of RNA and capsid protein at differing points during infection has been proposed by Johnson *et al.* (2003). According to the model (see schematic diagram depicted in Fig. 1.8), at the initial stages of infection, when the RNA concentration is high but the coat protein dimer concentration is limiting, the conditions, are conducive for the coat proteins to scan RNA to find high affinity viral RNA binding sites. As the dimers find viral RNA, they slowly fold into C1. This allows time for the capsid protein concentration to increase, while viral RNA is "tagged" by its formation of a C1 complex. Capsid dimers thus preferentially bind C1 over other RNA molecules and the addition of subsequent dimers and hexamers to C1 will form a virus particle. In this way coat

protein effectively labels viral RNA, described as a "structural identifier" (Johnson *et al.,* 2003). In separate studies there is evidence that the coat proteins of CCMV and BMV have been proposed to regulate replication and translation by binding other regions of the RNAs (Yi *et al.*, 2009; Zhu *et al.,* 2007). Although it is not clear how all these processes may function together, it is interesting to note that assembly, replication and translation have been linked to RNA-capsid protein binding. Future experiments may elucidate a linkage between all these processes. The C1/ "structural identifier" model predicts that it would be possible for heterologous RNA to initiate C1 (by non-specific binding to the capsid protein) and thus be incorporated into particles as was seen in a study with *Xenopus* elongation factor RNA and yeast tRNA by Krol *et al.* (1999). Yet it also predicts that in competition, capsid precursor dimers should select bromovirus RNA over heterologous RNA, as was observed by Cuillel *et al.* (1979). The advantage of the bromovirus packaging system would be that no specificity of the ARM is required for specific packaging of RNA. To date, no C1 complex with wild type RNA 2 and 3 has been detected, suggesting either that differing mechanisms are involved in their packaging or that there is some requirement for RNA 1 packaging first (Annamalai *et al.,* 2005).

Choi and Rao (2003) identified a bipartite signal on BMV RNA 3 that seems to be essential for its packaging into a virus particle. The tRNA-like structure, found on the 3'end of all bromoviral RNAs, was described as a nucleating element while a 187 nt double stem and loop region within the movement protein ORF represented the packaging element. It was shown that the combination of these signals was required for the packaging of RNA 3 into BMV particles. An intriguing feature of this observation is that all bromoviral RNAs share the tRNA-like structure on the 3' end of the RNA and thus its combination with a distinct signal on each viral RNA could act as a mechanism to incorporate separate RNAs into separate virions (Choi and Rao, 2003).

1.6   <u>Nodaviruses</u>

A variety of insect viruses have also recently been used as model systems to study packaging and assembly. The capsid structure and symmetry of the nodaviruses is relatively similar to that of the bromoviruses and tetraviruses, thus as could be expected, the basic mechanism of assembly is as well. Yet surprisingly, despite the similarities, the way in which insect viruses regulate the selective packaging of their genomic RNA appears markedly different. This could be because insect cells are inherently different to plant cells or that insect viruses do not traditionally encode movement proteins and thus there is a higher premium on effective packaging to ensure infectious particles. Either way, it is fascinating that the way in which two sets of capsid particles are formed can be the same but the packaging of the genomic RNA so different. The nodaviruses are insect *T=3* viruses that resemble the plant *T*=3 structure (Thiéry *et al*., 2011). This family is related to the tetraviruses via similarity in the amino acid sequence of the capsid proteins and consequently, despite the difference between *T*=3 versus *T*=4 capsid symmetry, the two families are structurally also related. Given this relationship, nodaviruses provide another potential source of clues for tetravirus packaging and it is thus fortunate that recently a great deal of focus has been placed on nodavirus assembly and packaging (Thiéry *et al*., 2011).

Nodaviruses are also (+) ssRNA viruses (Thiéry *et al*., 2011). These viruses infect a variety of insect species and have intriguingly also been isolated from fish (Mori *et al.,* 1992; Thiéry *et al*., 2011). The family is made up of only two genera, namely *Alphanodavirus* and *Betanodavirus*. The differentiating element between these two genera is that nodaviruses isolated from insects are placed into the *Alphanodavirus* genus whereas those isolated from fish are defined as betanodaviruses (Thiéry *et al.,* 2011). Nodavirus particles generally have a diameter of between 25 – 30 nm. The genome is bipartite, consisting of RNA 1 encoding Protein A (the replicase) and RNA 2, which encodes protein α (the capsid precursor protein) (Friesen and Rueckert 1981; Thiéry *et al*., 2011). A separate subgenomic RNA 3 has been detected in infections of both fish and insects and is synthesised from the 3' end of RNA 1. This strand is not packaged by the nodavirus particles (Eckerle and Ball,

2002). This RNA is responsible for the expression of two proteins, named B1 and B2. Recent evidence has revealed that despite very little sequence homology, the B2 protein of both alpha and betanodaviruses functions as a novel host immune system repressor (suppressing RNA silencing) while the function of B1 is unknown (Sullivan and Ganem, 2005; Qi *et al*., 2011). Both RNA 1 and 2 are packaged into a single particle made up of 180 subunits of protein α (Krishna and Schneemann, 1999). Like the tetraviruses, protein α is cleaved post-assembly into two mature capsid proteins, β and γ, that remain part of the capsid (Gallagher and Rueckert, 1988). This represents a distinctive difference between the assembly of the insect viruses and the symmetrically similar plant viruses. The story of assembly and packaging in nodaviruses is another example of how recently developed, sophisticated molecular techniques have been employed together with equally sophisticated classical structural biology to map out in detail the mechanism of nodavirus particle assembly.

<u>Capsid assembly</u>

The crystal structures of three alphanodaviruses have been determined to the same 3.0 Å level of resolution; these include *Black Beetle virus* (BBV – Fig. 1.9 A), *Flock House virus* (FHV – Fig. 1.9 B) and *Pariacoto virus* (PaV – Fig. 1.9 C) (Hosur *et al.,* 1987; Fisher and Johnson, 1993 Tang *et al.,* 2001). The structure of each of these particles is essentially the same in that it is made up of 180 subunits of the capsid precursor protein α. In the same way as the plant *T*=3 viruses, each protein occupies a quasi-equivalent environment distinguished by slightly different conformations, designated A, B and C (Fig. 1.9). However, unlike bromoviruses and similarly to the tetraviruses, the particle initially assembles into an immature particle or provirion, characterised by a porous capsid structure (Gallagher and Rueckert 1988; Schneemann *et al*., 1992) Once the provirion has formed, the immature particles undergo autoproteolytic cleavage between an Asn-Ala pair (Asn-Ser in PaV) at a site deep inside the virus core, which results in the mature β and γ capsid proteins (Hosur *et al.,* 1987; Tang *et al.,* 2001). The β protein is the larger of the two as the γ protein is only coded for by the last 40 - 50 amino acids of the precursor protein (Friesen and Rueckert, 1981). The cleavage is proposed to increase the

stability of the particle and also make it infectious (Schneemann *et al.,* 1993). Mutations, in which cleavage is abolished by changing the amino acids at the cleavage site of FHV, have resulted in non-infectious particles, implying that cleavage is also essential in assembly (Schneemann *et al.,* 1993).
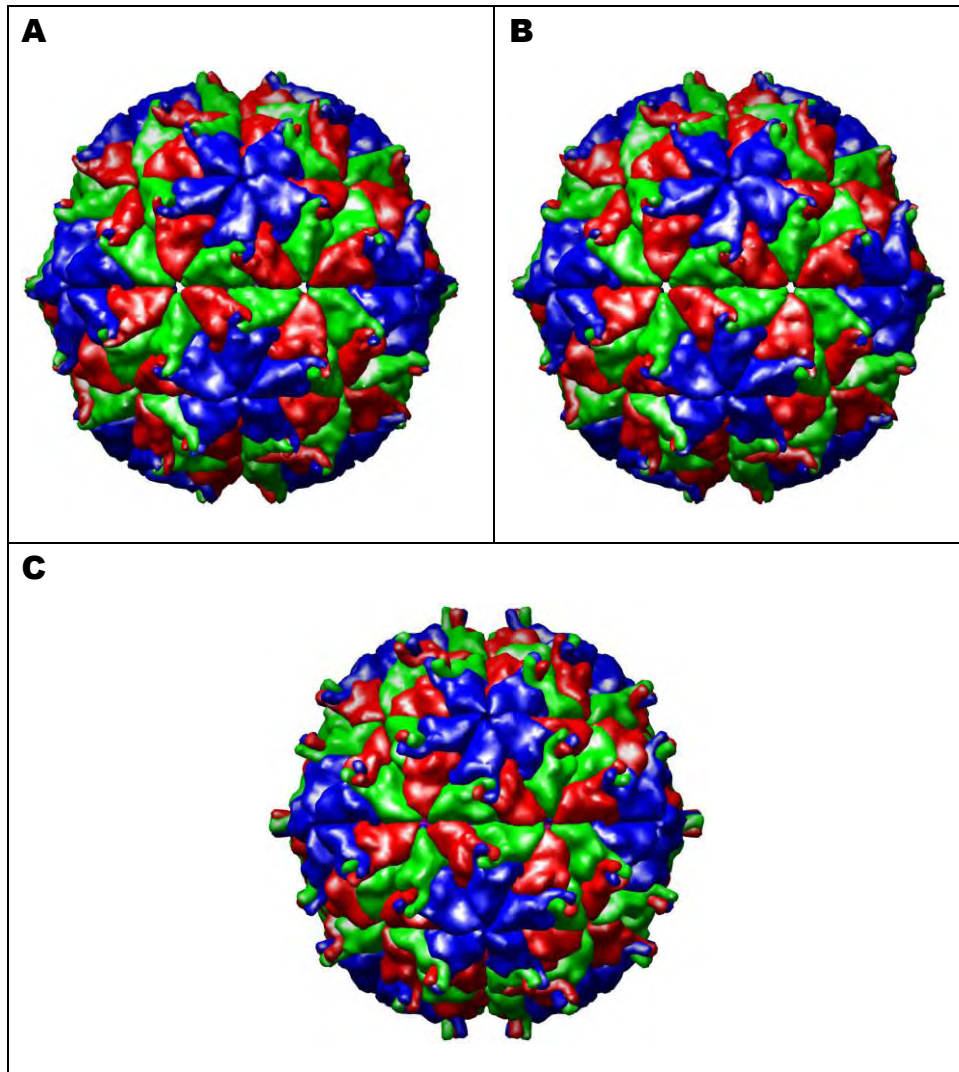
Figure 1.9: Structure of BBV (A), FHV (B) and PaV (C). The same colour coding strategy is used for the capsid proteins of Fig. 1.4. The structure and assembly of the nodaviruses shares the same *T*=3 symmetry of the bromoviruses and is thus also formed by pentamers of A subunits and hexamers of B and C (Carrillo-Tripp *et al.*, 2009; BBV: http://viperdb.scripps.edu/info_page.php?VDB=2bbv; FHV: http://viperdb.scripps.edu/info_page.php?VDB=2z2q; PaV: http://viperdb.scripps.edu/info_page.php?VDB=1f8v).

Despite the assembly of a provirus, the mechanism by which nodavirus particles assemble is similar to that of the bromoviruses discussed above (Dong *et al.,* 1998; Fisher and Johnson, 1993; Tang *et al.,* 2001). Essentially it is believed that a trimer of dimers (in the α conformation) makes up the basic assembly unit. At some point during dimerisation RNA is incorporated, therefore, even though nodaviruses form provirions/procapsids, the procapsid pathway of packaging is not utilised in favour of making ribonucleoprotein complexes. These complexes are formed when pentamers of capsid protein dimers, formed by the tethering together of subunits at their N-terminus, attach to RNA and then to one another. Just as in the bromoviruses, the N subunit of one of the capsid conformations, namely subunit A, folds around the trimer interface and fits into a groove between B or C in which it stabilises the RNA. The crystal structure and amino acid sequence also show that the C-termini (γ peptide) of each of the subunits have extensive interactions with the RNA, although whether this is the initial RNA binding site for each trimer is still to be determined (Fisher and Johnson, 1993; Tang *et al.,* 2001). Upon binding the RNA, the capsid proteins differentiate into either A, B or C conformations and are all connected by bent contacts. Interaction with the RNA results in some flat contacts forming instead of bent contacts and in this way, with the help of additional non-specific RNA interactions with more dimers, an icosahedral *T*=3 nodavirus particle is formed (Fig. 1.10) (Fisher and Johnson, 1993; Tang *et al.,* 2001; Thiéry *et al.*, 2011). Thus the RNA together with the N-terminal of the γ peptide is essential as the molecular switch in nodavirus assembly. This model is supported by evidence that when amino acids 1 – 50 of the N-terminus or the entire γ peptide of the capsid protein were deleted in FHV, no assembly of VLPs resulted (Schneemann and Marshall, 1998; Dong *et al.,* 1998).
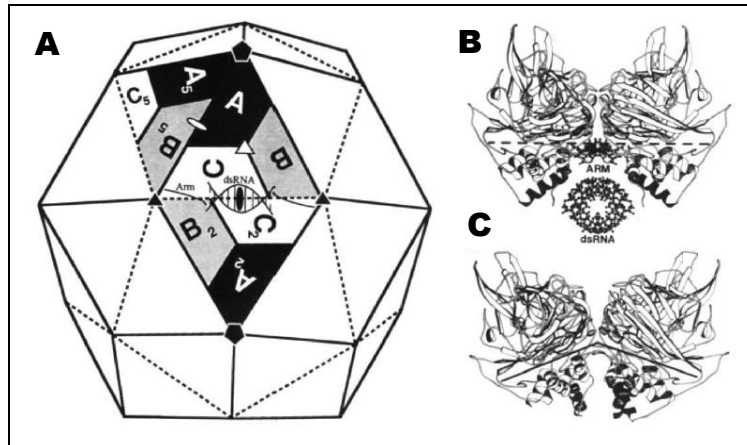
Figure 1.10: Capsid protein-protein and protein-RNA interactions essential in FHV assembly. (**A**) Schematic diagram of the FHV *T*=3 structure made up of the capsid protein in A, B and C conformations. The dsRNA duplex bound to the ARM of peptide C is depicted in the centre. (**B**) The dsRNA bound to the ARM of the γ peptides (dark black alpha helices), acts as a wedge thus ensuring that the contact between subunits C and B is flat. (**C**) Conversely the lack of RNA means that the A and C contact is bent (ribbon diagram below). This makes RNA the molecular switch during nodavirus assembly (Reproduced from Fisher and Johnson, 1993).

The high resolution structures of FHV and PaV have revealed the structure of the RNA within their capsids (Fisher and Johnson, 1993; Tang *et al.,* 2001). These have shown that the RNA forms an ordered duplex dodecahedral cage with its own symmetry mimicking the *T*=3 symmetry of the capsid (Fig. 1.11) (Fisher and Johnson, 1993; Tang *et al.,* 2001). The model generated for the structure of PaV showed furthermore that approximately 30 head to tail duplexes are connected to the capsid proteins (and thus could be seen in the crystal structure) and make up 35% of the packaged RNA, while the remaining 65% bulk RNA was connected to the cage but lay in the interior (Fig. 1.11) (Tang *et al.,* 2001). These observations provide additional support for the importance of RNA as more than just the molecular switch, as the symmetry of the RNA within the core was shown to exert its own pressure on the protein structure. This is described as "reciprocal influence" and indirectly corroborating evidence has shown that when the size of the RNA to be packaged changes, so does the structure of the particle (Dong *et al.*, 1998; Marshall and Schneemann, 2001). Therefore, this line of research was one of the first to show that not only does RNA have an effect on initiating the assembly process but that there is also a dynamic relationship between the packaged RNA and the capsid proteins. Although, this does not necessarily imply packaging specificity as the

dodecahedral RNA cage was still detected when FHV and PaV VLPs were made containing exclusively cellular RNA (Johnson *et al*., 2004). Yet the similarities end here as the mechanism of packaging of nodavirus particles is remarkably different from that of their plant counterparts.
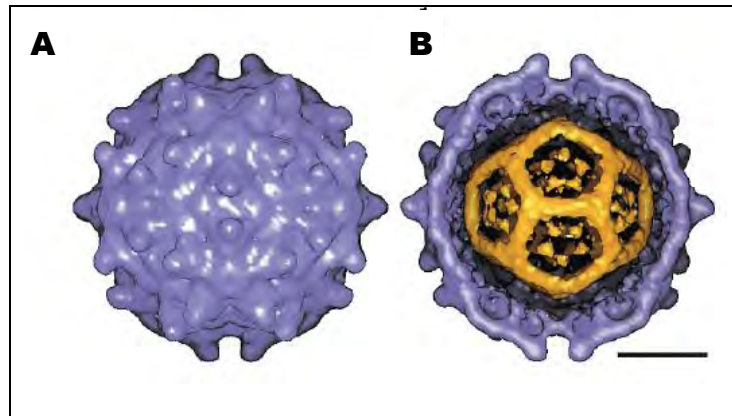
Figure 1.11: Cryo-EM three–dimensional reconstruction of both the protein and RNA components of PaV. (**A**) The protein component of the PaV particle was modelled via the crystal structure determined to 3.0 Å of resolution. (**B**) A difference map was generated by subtracting the signal responsible for protein with that of the RNA and was able to reveal the duplex RNA dodecahedral cage (gold) mimicking the symmetry of the *T*=3 protein capsid. Bar = 100 Å (Taken from Tang *et al.,* 2001).

Packaging

The story of nodaviral packaging starts with the observation by Schneemann and Marshall in 1998 that when the portion of the γ peptide (C-terminal region) not visible in the X-ray structure of FHV was deleted, particles similar to wild type particles resulted, but the VLPs packaged random cellular RNA. The same phenomenon was observed when a smaller N-terminal deletion was made instead of that of the C-terminal (Dong *et al.,* 1998). Therefore surprisingly, as was observed for bromoviruses, the nodavirus assembly mechanism is relatively promiscuous with regards to RNA-capsid binding. Once again, a specific mechanism must exist as two sets of RNA are consistently and specifically encapsidated by one particle in wild type infections (Schneemann *et al.,* 1994). This data led to the assumption that both the N and C termini of the capsid protein were not only crucial during the assembly pathway but that certain regions within each terminus played a role in selecting the RNA in the first place (Schneemann *et al.,* 1994; Dong *et al.,* 1998).

Subsequent studies showed that a key piece was missing from the nodavirus packaging puzzle. In the previous experiments only RNA 2 had been expressed in insect cells (Schneemann *et al.,* 1994; Dong *et al.,* 1998). In 2001 when Marshall and Schneemann repeated the same experiment with wild type RNA 1 and the N-terminal deletion mutant of RNA 2, the resulting VLPs efficiently packaged RNA 1 to wild type levels and RNA 2 less efficiently. Due to the fact that RNA 1 is able to kickstart replication of both itself and RNA 2 in insect cells, this led to the hypothesis that packaging and replication are linked in nodaviruses (Marshall and Schneemann, 2001). In the same study it was shown that instead of only RNA 2, smaller defective interfering (DI) RNAs were also being packaged, despite replication by RNA 1. This led to the additional conclusion that the N-terminus of the capsid protein is important in recognising RNA 2 and that the packaging pathways of RNA 1 and 2 must be distinct (Marshall and Schneemann, 2001). These results were substantiated by studies done later by the same group in which the construction of baculoviral vectors containing full length RNA 1 and 2 with C-terminal ribozyme sequences (to ensure the transcription of precise 3' ends) was reported. When both baculoviruses were infected into the *Spodoptera frugiperda* 21 (*Sf21*) insect cell line, replicating FHV particles resulted that packaged wild type RNA to almost identical wild type virus levels (Krishna *et al.,* 2003). Furthermore it was shown that when the RNA 1-expressing baculovirus was mutated so that replication was inhibited, the packaging of the VLPs reverted back to the heterologous cellular phenotype and, therefore, it is the activity of replication that is required for packaging and not RNA 1 alone (Krishna *et al.,* 2003).

Yet another interesting feature of nodaviral packaging was elucidated in this study, namely that the timing of expression is important for the packaging of genomic versus cellular RNA. When RNA 2 was transfected 24 hours after infecting with the RNA 1 baculovirus, VLP packaging was indistinguishable from wild type packaging, eliminating the small amounts of DI RNAs that were previously packaged in some particles (Krishna *et al.,* 2003). This experiment, which mimicked more closely the timing of transcription within FHV infected cells, showed that although packaging and

assembly can be directed by cellular RNA, there is some mechanism that maintains specificity.

A hypothesis on how nodaviral packaging specificity may come about has been proposed in recent years (Venter *et al.,* 2009). This hypothesis initially originated from the results of an experiment where the capsid protein was introduced into the FHV replicating tissue culture system in *cis* or in *trans*. When the capsid protein was provided in *trans* to non-replicating RNA, neither RNA 1 or RNA 2 was packaged but when the capsid protein was made from a replicating RNA 2 (and provided in *cis*) then its packaging became efficient, regardless of the replication state of RNA 1. Therefore, the capsid protein needed to be translated off a replicating RNA in order for it to initiate packaging and thus it was concluded that translation is also linked to the replication-packaging pathway (Venter *et al.,* 2005). The authors of this study proposed that the means by which RNA 2 translation-replication and packaging could be interlinked was via the environment which the RNAs take up in the cell. This therefore, gave rise to the new model for the spatial coordination of packaging in nodaviruses (Venter *et al.,* 2005).

It was proposed that FHV makes a specialised microenvironment within the cell where the replication of RNA 1 and 2 can be in close proximity to the translation of the capsid protein precursor. This means that the capsid protein can snatch RNAs as they are replicated and that the fact that they are being replicated ensures packaging specificity (Venter *et al.,* 2005). Thus the entire assembly and packaging process may hinge on the replication of RNA 2, as it is the location of its replication and thus translation that defines what it packages (Venter *et al.,* 2005). If assembly is initiated by the contact of RNA and protein then it followed that assembly too would be linked to the replication-translation-packaging pathway. This was elegantly proven by Venter and Schneemann in 2007 where they were able to show that two separate populations of particles could be produced in the same cell.   One population was made from replicated RNA and packaged viral RNA while the other was made from non-replicating RNA and consisted of mainly cellular RNA (Venter and Schneemann, 2007).

The site of FHV RNA replication has been well characterised and thus the current hypothesis is that RNA 1 and 2 are targeted to spherules formed by the invagination of the mitochondrial membrane (Miller *et al.,* 2001; Venter *et al.,* 2009). Subcellular localization of both the capsid and replicase proteins was used with mutational analysis to extend the proposed mechanism even further. In 2009 Venter and co-workers showed that initially the coat protein localizes with the endoplasmic reticulum (ER), where it is presumably translated from RNA 2, but that at some point during infection it is trafficked to the mitochondria where it co-localises with the replicase protein. The same study showed by mutational analysis that an ARM comprising residues 32 – 50 on the coat protein is critical in RNA 1 packaging. The mechanism of packaging was not sequence specific as both the substitution of each arginine residue with lysine or the HIV ARM sequence, rescued RNA 1 packaging (Venter *et al.,* 2009). Therefore, by combining these observations it was proposed that RNA 2 is translated at the ER and that the ARM or some other mechanism is involved in combining capsid protein and RNA 2 into a nucleoprotein complex that is trafficked to the site of replication near the mitochondria. This would then allow RNA 1 to be incorporated into the fledgling particle and the non-specific pathway of assembly to continue to complete the capsid (Venter *et al.,* 2009).

1.7   Comparison between tetravirus and nodavirus assembly mechanisms

The expression of the NωV capsid protein in insect cells provided the first line of evidence that tetraviruses behaved like nodaviruses, regarding the post-assembly autoproteolytic cleavage of a precursor protein. Using pulse-chase experiments, Agrawal and Johnson (1995) were able to show that NωV initially produced a 70 kDa precursor protein, which was cleaved post-assembly into a 62 kDa protein plus a 7 kDa peptide. Following on from this work, Munshi and co-workers (1996) proposed that there must be an evolutionary link between nodaviruses and tetraviruses. Not only was autoproteolytic cleavage conserved but cleavage also occurred between a similar pair of residues (Asn – Phe in tetraviruses and Asn – Ala in nodaviruses) and took place in the same region of the capsid protein precursor. The capsid proteins

themselves are also structurally conserved when two of the three tetraviral capsid domains are compared (Fig. 1.12). Therefore, it was no surprise that the assembly mechanism of nodavirus and tetravirus capsids is markedly similar.
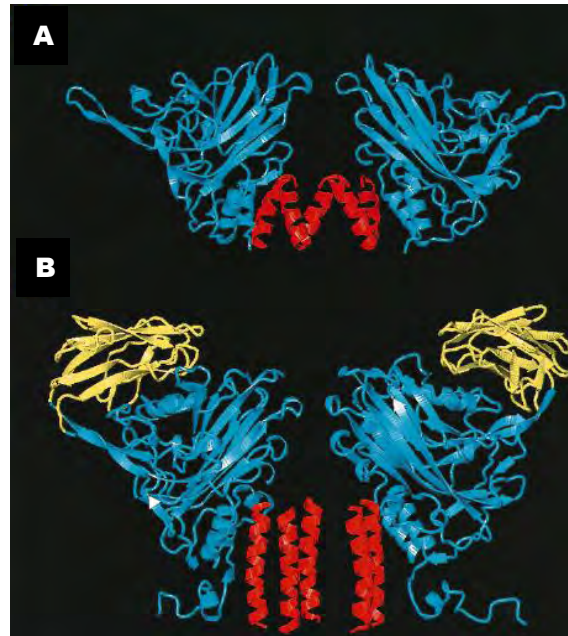
Figure 1.12: Comparison of the nodavirus (A) and tetravirus capsid precursor proteins. The nodaviruses are represented by BBV in **A** and NωV in **B**. The regions highlighted in blue represent the jelly-roll core while the regions highlighted in red represent the γ peptide. A high degree of similarity between (**A**) and (**B**) can be seen when comparing these two domains. One of the major differences between tetraviruses (**B**) and nodaviruses (**A**) is that tetravirus capsid proteins contain an additional immunoglobulin-like domain (gold) which is absent in nodaviruses (Munshi *et al*., 1996).

Despite these similarities, two distinct features separate tetraviruses from nodaviruses. Both nodavirus and tetravirus capsid proteins contain two distinctive domains, the jelly-roll core which is an important structural characteristic of many icosahedral viruses and the internal helical domains, which is made up of the N and C termini and are involved in molecular switching. Tetraviruses have evolved an additional immunoglobulin-like domain extending from the jelly-roll core facing extracellularly which is all together absent in the nodaviruses (Fig. 1.12). Secondly, and very importantly, tetraviruses have evolved a molecular switch that is distinct from that of the nodaviruses. Where nodaviruses utilise a combination of duplex RNA and N-terminal helices to act like a wedge between protein contacts,

tetraviruses have utilised a combination of the C-terminal regions of the C and D precursor protein subunits to effect the same function (Munshi *et al*., 1996; Thiéry *et al*., 2011).

Recently a second tetravirus was crystallized and analysed to a 3.8 Å resolution (Speir *et al*., 2010). PrV is the first betatetravirus for which a crystal structure is available and this work has revealed a very interesting feature of the evolution of this family. As mentioned above, there are many structural similarities between the tetravirus and nodavirus capsids, while perhaps the key difference is the identity of the molecular switch (Munshi *et al*., 1996). As has also been mentioned, PrV is a somewhat atypical tetravirus in that its genome does not share many of the characteristics typical of the tetraviruses (Walter *et al*., 2010). The crystal structure of the PrV capsid showed that instead of using C-terminal residues of the C and D subunits to form the molecular switch, PrV particles utilise N-terminal residues in combination with duplex RNA, in a similar manner to that of the nodaviruses (Speir *et al*., 2010). This observation prompted the hypothesis that PrV could be the evolutionary link between the nodaviruses and the tetraviruses and that evolution has acted on the molecular switch, reverting it to the opposite terminus, in order to maintain the same structure while accommodating another subunit into the capsid (Speir *et al*., 2010).

1.8 Tetravirus packaging and the *Helicoverpa armigera stunt virus* (HaSV)

The distinctive structural features of tetravirus particles have enjoyed much of the focus of research on tetraviruses to date; in contrast very little attention has been paid to how RNA is selected and encapsidated. A major reason behind the lack of research in this area is that tetraviruses do not form infectious particles in tissue cultured cells (like bromoviruses or nodaviruses), thus it is difficult to determine the packaging pathways. From the evidence above it would seem that equal arguments could be made for why packaging may be similar or very different from the structurally similar nodaviruses. Indeed it would appear that at least RNA 2 packaging is independent of replication as it was shown that NωV VLPs derived from

baculovirus vectors in insect cells, packaged viral mRNA 2 without being replicated in the cell (Agrawal and Johnson, 1995). VLPs constructed in plant protoplasts and derived from the simultaneous transfection of plasmids containing full length HaSV RNA 1, RNA 2 and the capsid precursor (*VCap*) ORF, showed no sign of RNA replication but were infectious when fed to larvae, insinuating the specific packaging of RNA (Gordon *et al*., 2001). This supports the hypothesis that assembly and packaging may be a replication-independent system in tetraviruses and thus differs from the mechanisms used by the nodaviruses and bromoviruses. When only the coat protein message was expressed by recombinant baculoviruses, mostly cellular RNA was packaged (Canady *et al*., 2000; Taylor, 2003).

One of the focuses of the tetravirus laboratory at Rhodes University is on using HaSV as a model tetravirus to study RNA packaging. HaSV was first isolated in a laboratory reared colony of *Helicoverpa armigera* (commonly known as the Cotton Bollworm) in Australia in 1993 (Hanzlik *et al*., 1993). As with most other tetraviruses, HaSV infects the midgut cells of *H. armigera* larvae, which in turn respond by sloughing virus infected cells, resulting in stunting of the larvae from the lack of nutrient uptake and eventual death (Brooks *et al*., 2002).

HaSV consists of two (+) ssRNA molecules housed within a single capsid particle (Fig. 1.13). Each RNA strand possesses a 5' cap but no polyadenylation signal, which is replaced by a tRNA-like structure terminating in a 3' hydroxyl residue (Hanzlik *et al*., 1995; Gordon *et al*., 1995). RNA 1 is 5.5 Kb in size and encodes one major and three minor ORFs. The major ORF (5.1 Kb) encodes a replicase protein of 1704 amino acids with a predicted molecular weight of 187 kDa (Gordon *et al*., 1995), with the three characteristic major domains (Gordon *et al*., 1995). When fused to the green fluorescent protein, the HaSV replicase has been shown to localise to membranes derived from the endocytic pathway, which have been proposed as the site of HaSV replication (Short *et al*., 2010). The three minor ORFs (*p11*, *p15* and *p8*) lie in a different reading frame from the *replicase* ORF (Gordon *et al*., 1995). The conservation of the position and amino acid sequence of these three ORFs on the RNA 1 of another omegatetravirus, DpTV, suggest that they are likely

to have a function in the life cycle of the virus, although this has yet to be determined (Yi *et al*., 2005; Dorrington and Short, 2010).
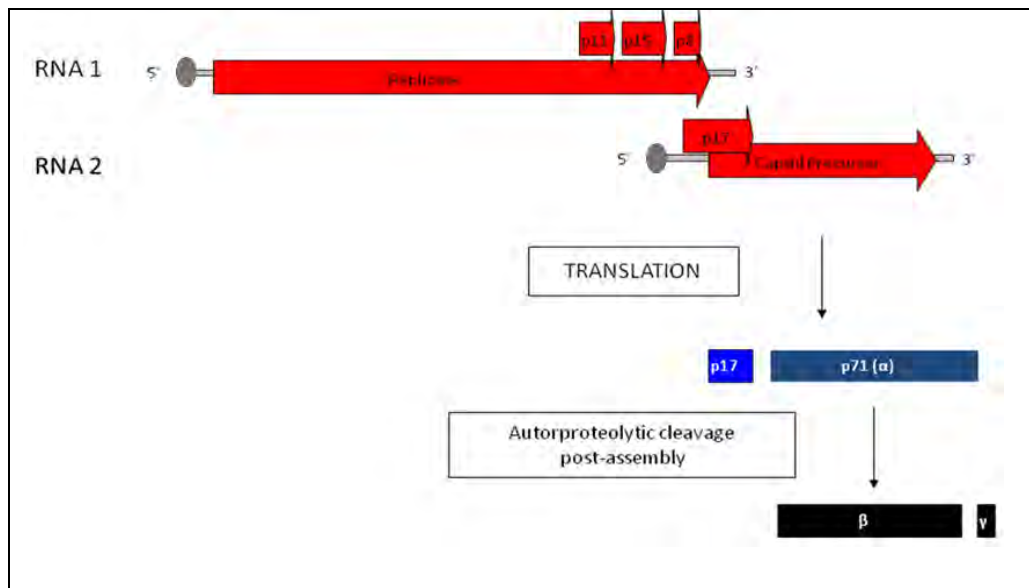
Figure 1.13: Genome organisation and translation products of HaSV. HaSV capsid particles package two sets of RNA molecules. Both sets are capped at the 5' end and contain terminal 3' hydroxyl molecules. RNA 1 encodes the non-structural proteins, namely the replicase (p187) and three smaller proteins; p11, p15 and p8. The existence as well as the function of these smaller proteins *in vivo* is under investigation. RNA 2 encodes the capsid precursor protein (p71) as well as p17. p71 otherwise known as protein α or VCap assembles spontaneously into a procapsid particle post-translation; each precursor protein then undergoes autoproteolytic cleavage during the phase of maturation to yield the major (p64 or β) and minor (p7 or γ) capsid proteins characteristic of a wild type capsid (adapted from Hanzlik *et al*., 1993).

The HaSV RNA 2 is 2.5 kb in size and encodes two ORFs. The larger of the two, codes for the capsid precursor protein (p71), this protein can also be referred to as protein α or the VCap protein (Hanzlik *et al*., 1995). As discussed earlier (section 4) 240 copies of the VCap protein assemble into a procapsid structure during the first phase of assembly and during maturation each capsid protein undergoes autoproteolytic cleavage at an Asn570 – Phe571 site to produce the major or β capsid protein of 64 kDa and the minor or γ protein of 7 kDa (Hanzlik *et al*., 1995). The presence of p64 is thus dependent on the assembly of a mature capsid particle and is, therefore, used as an assay for this process (Hanzlik *et al*., 1995; Bothner *et al*., 2005; Tomasicchio *et al*., 2007). The *p17* ORF precedes the *VCap* ORF, starting

at the first AUG start codon on HaSV RNA 2, is in the +2 frame and partially overlaps the *VCap* ORF. The predicted protein consists of 157 amino acids and has a predicted size of 17 kDa (Hanzlik *et al*., 1995).

Unpublished research has revealed that p17 is present in the midgut cells of *Helicoverpa armigera* larvae infected with HaSV and that the protein co-purifies with wild type HaSV particles at a ratio of approximately 1: 12 relative to the capsid protein (Vlok, 2008), suggesting that p17 might be packaged by the virus particles. The low p17 expression levels were shown to be due to the poor translational context of the AUG start codon of the *p17* ORF. These results warranted the establishment of a plasmid transfection system in which *Spodoptera frugiperda* 9 (*Sf9*) cells were transfected with various constructs expressing p17 in different contexts with the VCap protein. VLPs were then purified from the cells and the RNA content analysed. The results showed that expression of the RNA 2 constructs that contained the *p17* and the *VCap* ORFs resulted in the assembly of VLPs that contained viral mRNA, while VLPs assembled in cells expressing only VCap did not package the viral mRNA (Vlok, 2009). In addition, it was shown that deletion of the 5' and/or 3' UTR sequences of RNA 2 did not affect packaging of viral RNA (Vlok, 2009). These results have provided preliminary evidence that the omegatetravirus p17 might be involved in the packaging of viral RNA.

Support for this hypothesis comes from the studies of Agrawal and Johnson (1995) who reported the presence of viral RNA in NωV VLPs assembled via recombinant baculovirus expression of an RNA 2 construct which carried the *p17* ORF, while other studies in the Johnson laboratory have reported that VLPs assembled when only the omegatetravirus capsid protein precursor was expressed, packaged mostly cellular mRNAs and some viral mRNA. Furthermore, the results of a study by Zhou *et al.* (2008) have suggested that the DpTV p17 may be an RNA binding protein. However, there are still gaps in the p17-packaging hypothesis that remain a major challenge. Firstly, it was unclear from Vlok's data whether an RNA signal, present on the non-overlapping region of the *p17* ORF or the p17 protein itself was required for the specific packaging of viral RNA. Secondly, the previous study was unable to

demonstrate the presence of p17 in VLPs assembled in cells co-expressing p17 and VCap because of the low expression levels supported by the plasmid-based experimental system. Therefore, a more suitable expression system was required for the analysis of HaSV VLP packaging.

Hypothesis

A baculovirus-mediated system will be an effective expression system for the production of HaSV VLPs and thus the analysis of p17's role in RNA packaging.

Aim

The aim of this study was to develop a baculovirus expression system to determine whether p17 is required for the packaging of HaSV RNA 2.

Objectives

1. To confirm that the translation of p17 is required for the specificity of RNA 2 packaging in the plasmid mediated expression system.

2. To construct recombinant baculoviruses that co-express the HaSV capsid protein precursor (VCap/p71) together with p17.

3. To determine what effect the expression of p17 has on the packaging of HaSV RNA 2 into VLPs derived from recombinant baculoviral vectors.

Chapter 2
Materials and methods

2.1   Bacterial strains

All constructs were cloned in *E. coli* DH5α cells (*supE*44 Δ*lac*U1269 [ɸ80*lacZ*ΔM15] *hsd*R17 *rec*A1 *end*A1 *gyr*A96 *thi*-1 *rel*A1) (Hanahan, 1983) or in *E. coli* DH10Bac cells (F– *mcr*A Δ[*mrr-hsd*RMS-*mcr*BC] Φ80*lacZ*ΔM15 Δ*lac*X74 *rec*A1 *end*A1 *ara*D139 Δ[*ara leu*] 7697 *gal*U *gal*K λ– *rps*L *nup*G/ pMON14272/pMON7124) (Invitrogen).   The DH5α cells were maintained on Luria agar (LA) plates (1.0 % peptone, 0.5 % yeast extract, 0.5 % NaCl and 1.5 % bacterialogical agar) containing 100 µg/µl ampicillin (LA Amp) and frozen glycerol stocks (50 % bacterial culture and 50 % [1:1 Luria Bertani (LB) broth and glycerol mixture]) at -80 °C.   The DH10Bac cells were maintained in SOC medium (2 % tryptone, 0.5 % yeast extract, 0.24 % anhydrous magnesium sulphate, 0.05 % NaCl and 0.02 % KCl with 20 mM glucose added after autoclaving) pH 7.0 or on LA Bac plates containing 50 µg/ml kanamycin, 10 µg/ml tetracycline, 7 µg/ml gentamycin, 300 µg/ml 5-bromo-4-chloro-3-indolyl-β-d-galactopyranoside (X-Gal) and 50 µg/ml Isopropyl β-D-1 thiogalactopyranoside (IPTG).   *E. coli* BL21 cells (DE3) (*hsdS gal (λcIts857 ind1 Sam7 nin5 lacUV5-T7 gene 1)* (Studier and Moffatt, 1986) were used only once for the overexpression of His-p17.   These cells were maintained in the same manner as the DH5α cells.   The recipe for making all of the above strains competent as well as the transformation protocol was carried out according to Sambrook *et al*. (1989).

2.2 Recombinant plasmid construction

Table 2.1: Description of the plasmids used in this study

Plasmids	Genotype/description	Phenotype	Reference
pGEM-T Easy	Cloning vector (*T7 SP6* promoter)	amp^R	Promega
pCW56	Insect expression vector containing the *eGFP* CDS flanked by 5'*BamH1* and 3'*NotI* restriction sites (*hr:AcMNPV* promoter)	amp^R, kan^R	Walter, 2008
pMV2	Vector containing N-terminal 6x His HaSV *p17* CDS	amp^R	Vlok, 2009
pMV18	Insect expression vector (pCW56 backbone) with HaSV RNA 2 cDNA sequence inserted using 5'*BamH1* and 3'*SexA1* (*hr:AcMNPV* promoter)	amp^R, kan^R	Vlok, 2009
pAM8	pGEM-T Easy containing 5'UTR of HaSV RNA 2 and *p17* CDS flanked by 5'*HindIII* and 3'*BglII* sites (*T7* promoter)	amp^R	This study
pAM9	pAM8 sequence with a mutation to the start codon of the *p17* CDS to an *EcoRV* site, silencing the gene (ATG AGC – GAT ATC)	amp^R	This study
pAM10	Insect expression vector (pMV18 backbone) with mutated HaSV RNA 2 cDNA sequence from pAM9 in which the *p17* CDS has been silenced (*hr:AcMNPV* promoter)	amp^R, kan^R	This study
pFastBac Dual	Baculovirus donor plasmid (AcMNPV bacmid with both *polH* and *p10* promoters)	amp^R, gent^R	Invitrogen
pAM20	Baculovirus donor plasmid (pFastBac Dual backbone) with HaSV RNA 2 sequence (from pMV18) inserted into the *p10* cloning cassette between 5' *SmaI* and 3' *NsiI* sites	amp^R, gent^R	This study

Plasmids	Genotype/description	Phenotype	Reference
pAM21	Baculovirus donor plasmid (pFasBac Dual backbone) with mutated HaSV RNA 2 sequence (from pAM10) inserted into the p10 cloning cassette between 5' *SmaI* and 3' *NsiI* sites	amp^R, gent^R	This study
pAM12	pGEM-T Easy containing the *p17* CDS PCR amplified from pMV18 (using primers AM13F and AM14R)	amp^R	This study
pAM22	Baculovirus donor plasmid (pFasBac Dual backbone) with *p17* CDS (from pAM12) inserted into the *polH* cloning cassette between 5'*BamHI* and 3'*PstI* sites	amp^R, gent^R	This study
pAM23	Baculovirus donor plasmid (pFasBac Dual backbone) with HaSV RNA 2 sequence (from pAM20) in the *p10* cassette and the *p17* CDS (from pAM22) in the *polH* cassette	amp^R, gent^R	This study
pAM24	Baculovirus donor plasmid (pFasBac Dual backbone) with mutated HaSV RNA 2 sequence (from pAM21) in the *p10* cassette and the *p17* CDS (from pAM22) in the *polH* cassette	amp^R, gent^R	This study
pMT20F	pGEM-T Easy containing HaSV *VCap* (*p71*) CDS (*T7* and *SP6* promoter)	LEU2, amp^R	Tomasicchio *et al.* 2007
pAM26 polHF	pGEM-T Easy containing a fragment of the *polH* promoter and cloning cassette from pFastBac Dual (cloned via PCR amplification using primers AM18polH and JRS 61)	amp^R	This study

eGFP – enhanced green fluorescence protein; *hrAcMNPV* – hybrid insect promoter from the *Autographica californica multicapsid nuclear polyhedrosis virus*; UTR – untranslated region; CDS – coding sequence; amp^R – ampicillin resistance (100 µg/µl); kan^R – kanamycin resistance (50 µg/µl); gent^R – gentamycin resistance (7 µg/µl).

Construction of pAM10

A schematic representation of the cloning strategy used for the construction of the plasmid pAM10, in which the AUG start codon of the *p17* ORF is mutated to an *EcoRV* restriction site, is shown in Fig. 2.1. pAM10 was derived from pMV18, a construct developed by M. Vlok (Vlok, 2009). This construct contains the wild type HaSV RNA 2 cDNA sequence under the control of the hybrid promoter from the *Autographa californica multicapsid nuclear polyhedrosis virus* (*hr:AcMNPV*, which is transcriptionally active in *S. frugiperda Sf9* cells). In this construct, HaSV RNA 2 is flanked precisely at its 3' end by the hairpin cassette (HC) ribozyme followed by the *Simian Virus 40* (SV40) origin of replication and an ampicillin resistance selectable marker (amp^R). A 719bp fragment from *HindIII* to *BglII* of pMV18, which included the full *p17* coding sequence, was amplified using primers AM7F (AACAACCAAGCTTAATCGAATTCCG) and AM8R (AGATCTCTCTTATCTCT GCGTCGACGGA). The PCR was carried out using the Expand High Fidelity PCR system (Roche), the amplification product gel-purified using the Zymoclean Gel DNA Recovery kit (Zymo Research) and then ligated into the pGEM-T Easy vector. The resulting plasmid, pAM8, was transformed into competent DH5α cells using the methods of Sambrook *et al.* (1989). MacConkey agar plates containing ampicillin (100 µg/µl) were used to screen for recombinant clones. Colonies potentially containing the plasmid of interest were picked and inoculated into LB broth containing ampicillin (100 µg/µl) and allowed to grow at 37 °C overnight. Plasmid DNA was then extracted using the "Easyprep" method developed by Berghammer and Auer, (1993), and digested with *EcoRI* as a diagnostic test since this enzyme releases inserts from the vector DNA. pAM8 DNA was isolated using the High Pure Plasmid Isolation Kit (Roche) and digested with relevant endonucleases to confirm the identity of the new plasmid. The fidelity of the sequence was further confirmed by Sanger sequencing.
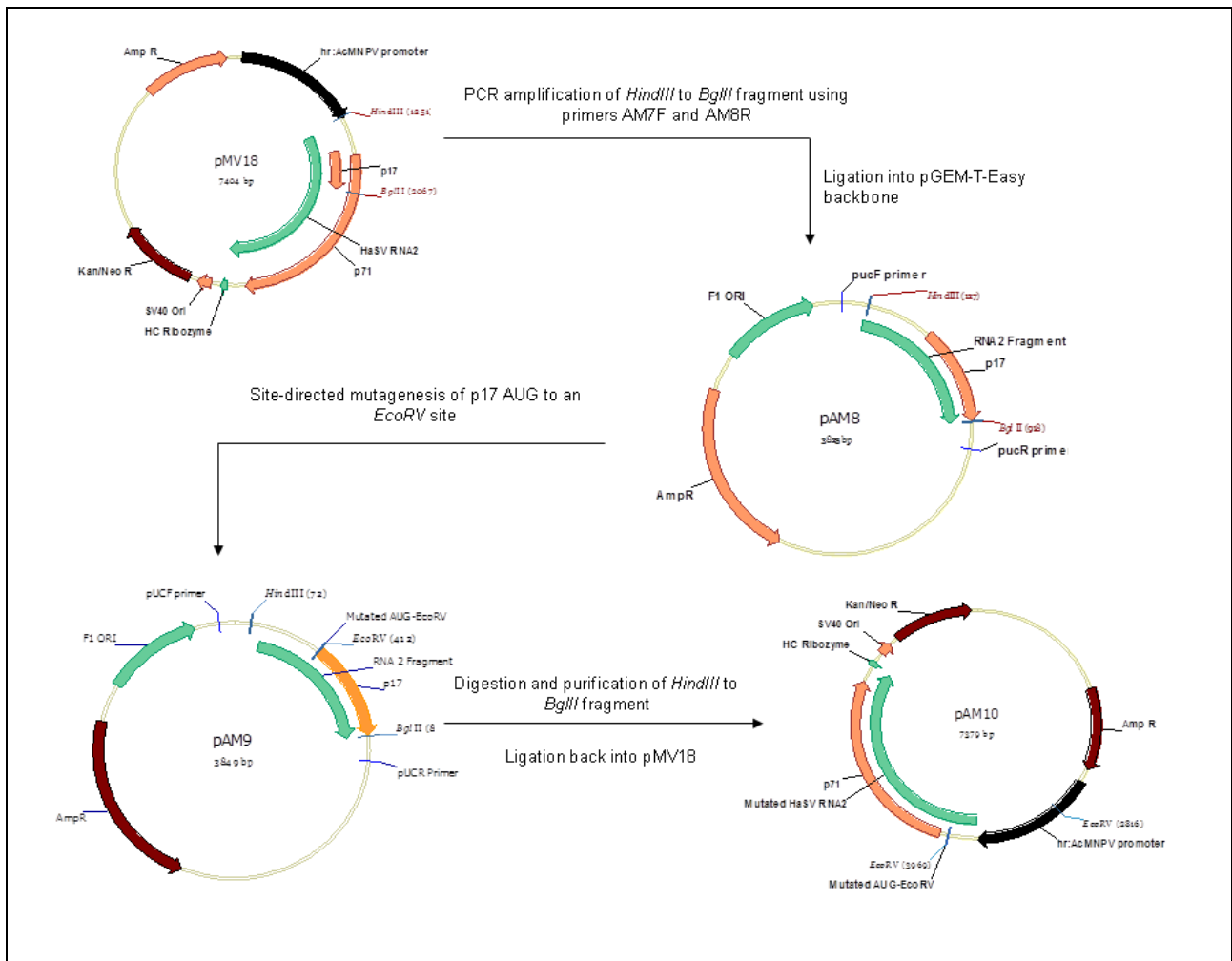
Figure 2.1: Cloning strategy for the construction of pAM10. pAM10 contains an exact full length HaSV RNA 2 cDNA sequence (as in pMV18) but for a mutation to the *p17* start codon and thus will not express p17. A precise 3'UTR is ensured due to the HC ribozyme sequence. A more detailed explanation of the process as well as the characteristics of each vector is outlined in the paragraph above.

Plasmid pAM8 was subjected to site-directed mutagenesis (SDM) using *pfu* DNA polymerase (Promega) and primers AM9SDM (CAGCGTTGATAGCG CCGATTGATATCGAGCACACCATCGCCCAC) and AM10SDM (GTGGGCGAT GGTGTGCTCGATATCAAATCCGCGCTATCAACGCTG) such that the first and second codons of the *p17* ORF (ATG AGC) were mutated to an *EcoRV* restriction endonuclease site (GAT ATC), which served as a diagnostic test for the mutant plasmid, pAM9. Following digestion with *DpnI* to remove template DNA, a *HindIII* to *BglII* fragment carrying the mutated *p17* ORF was excised from pAM9 and inserted into pMV18 to create pAM10, which carries the full HaSV RNA2 sequence with the AUG start codon of *p17* mutated to GAT to prevent expression of p17.

42

Construction of recombinant pFastBac Dual transfer vectors

pFastBac Dual was used as the transfer/donor vector for the development of recombinant baculoviruses according to the Bac-to-Bac Baculovirus Expression System (Invitrogen). The transfer plasmids pAM20 (Fig. 2.2 A) and pAM23 (Fig. 2.2 B), derived from pMV18 carry the wild type HaSV RNA 2 cDNA sequence expressing p17 and VCap (p71), the virus capsid protein precursor, while pAM21 (Fig. 2.2 C) and pAM24 (Fig. 2.2 D) are derived from pAM10, in which the *p17* start has been mutated and thus express only VCap off RNA 2. Both pAM23 and pAM24 contain a functional *p17* ORF on a separate promoter (*polH*) and thus will express p17 regardless of the mutation state of RNA 2.

To construct pAM20 and pAM21, plasmids pMV18 and pAM10 were digested with *SmaI* and *NsiI* and the resulting fragment of 2628 bp, which encompasses the full length HaSV RNA2 cDNA sequence (wild type or mutated) with the HC ribozyme at its 3' end, was gel-purified and cloned into the same sites on the pFastBac Dual vector, downstream the *p10* promoter. pAM20 is thus analogous to pMV18 and pAM21 to pAM10.

Constructs pAM23 and pAM24 are derivatives of pAM20 and pAM21 respectively, and carry the *p17* ORF downstream of the *polH* promoter on pFastBac Dual (Fig. 2.2). The plasmid pAM12 contains the *p17* ORF, generated by cloning a PCR product from pMV18 using primers AM13F (AGATCTATGAGCGA GCACACCATCGCC) and AM14R (CTGCAGTT ATCTCTGCGTCGACGGAGAACT). The *p17* ORF was subcloned into pFastBac Dual (Invitrogen) using the restriction sites liberated by *PstI* and *BglII*. The resulting intermediate vector, pAM22, was screened using *SphI* and represents a baculoviral transfer vector containing only the *p17* ORF under the control of the *polH* promoter. pAM23 and pAM24 were constructed by digesting pAM20 (producing the insert for pAM23) and pAM21 (producing the insert for pAM24) with *SmaI* and *NsiI* and each fragment was ligated into the corresponding sites on pAM22.
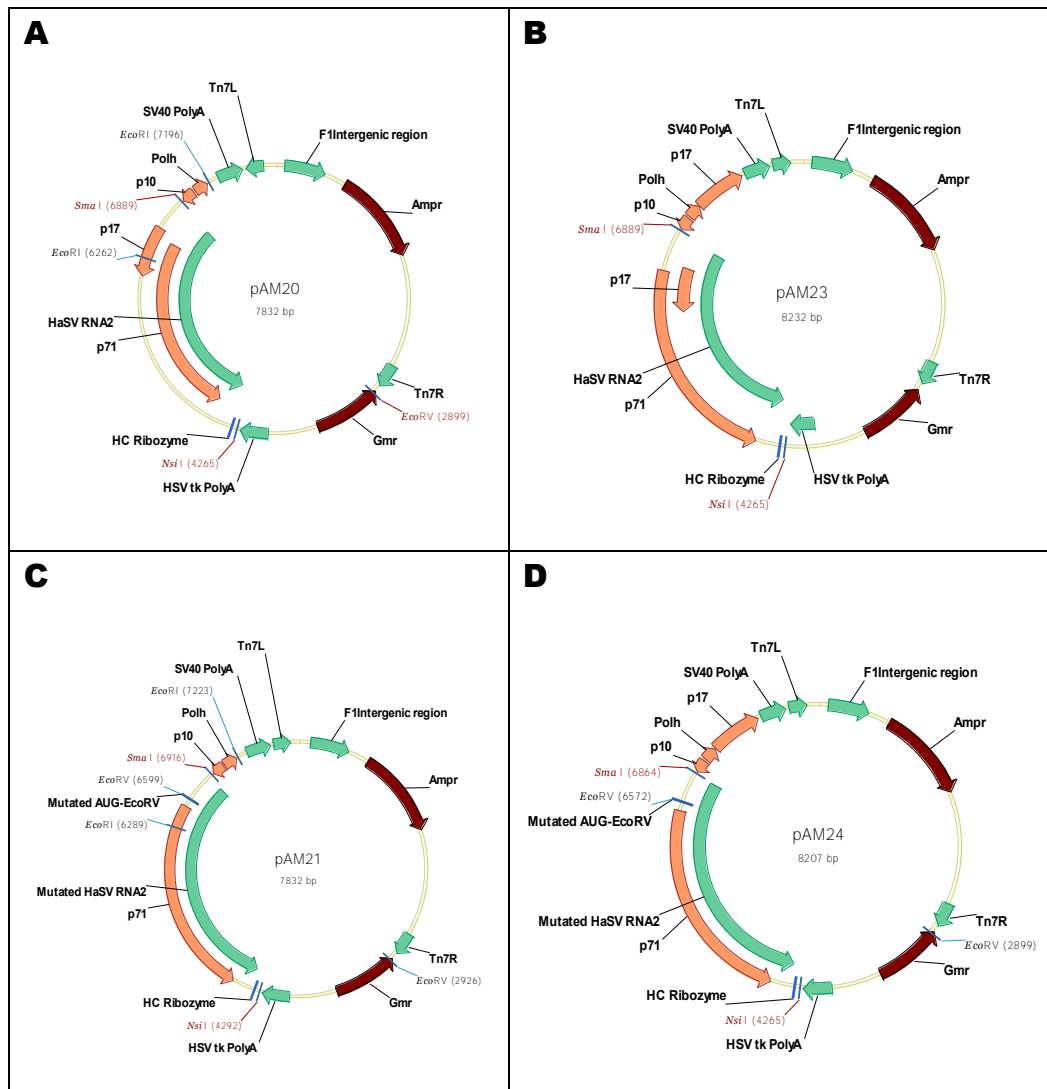
Figure 2.2: Recombinant baculovirus transfer/donor vectors used in this study. The vectors in this diagram were constructed by cloning into the pFastBac Dual backbone and consequentially contain all the essential features for the development of a recombinant baculovirus, i.e. Tn7L and Tn7R transpositional elements and two selectable markers the gentamycin (Gmr) and ampicillin (Ampr) resistance genes. The pFast-Bac Dual system allows for the expression of two sets of genes by one virus via the dual promoters, *p10* and *polH*. pAM20 (**A**) and pAM21 (**C**) contain HaSV RNA 2 cDNA under the transcriptional control of the *p10* promoter flanked precisely by the HC ribozyme (3' end). Both p17 and VCap (p71) will be expressed from pAM20, while only VCap (p71) will be expressed from pAM21. pAM23 (**B**) was derived from pAM20 but will express another copy of p17 from the *polH* promoter as well. pAM24 (**D**) was derived from pAM21 and will only express p17 from *polH*.

The plasmids pAM23 and pAM24 contain HaSV RNA2 cDNA under the control of the *p10* promoter in one direction and the *p17* ORF under the control of the *polH* promoter in the other direction (Fig. 2.2). pAM24 differs from pAM23 in the same manner as pAM21 differs from pAM20, in that the *p17* ORF is silenced on the RNA 2

cDNA sequence. The integrity of the viral cDNA in each of the constructs used for generating recombinant baculoviruses was confirmed by Sanger sequencing.

2.3   Construction of recombinant baculoviruses (Bac20, Bac21, Bac23 and Bac24)

Construction of recombinant bacmids

Plasmid transfer constructs pAM20, pAM21, pAM23 and pAM24 were transformed into DH10Bac cells according to the methods described in the Bac-to-Bac Baculovirus Expression System manual (Invitrogen).   Blue white screening (facilitated by adding X-Gal and IPTG to the LA Bac plates) was carried out by spreading each transformation reaction onto LA Bac plates and allowing the cells to grow at 37 °C for 24 – 48 hours. White colonies, which represented the successful transposition of the recombinant DNA from the transfer vector into the genomic baculoviral DNA, were picked and incubated into LA containing the relevant antibiotics and allowed to grow overnight at 37 °C. In order to confirm that the colonies where "true whites" the liquid culture was re-streaked using the 3-way streak technique. After confirmation of the phenotype, the ZR Bac DNA Miniprep kit (Zymo Research) was used to isolate the recombinant baculoviral genome, referred to as a bacmid. The bacmids and thus the subsequent recombinant baculovirus that would be generated from each bacmid were designated Bac20, Bac21, Bac23 and Bac24; after the plasmid transfer vectors from which they were derived.

PCR analysis was carried out using KAPA Taq ReadyMix DNA polymerase (KAPA Biosystems) to verify the recombinant bacmid DNA.   Due to the size of the recombinant sequence inserted into the bacmids, five separate reactions with different primer pairs were used to verify the fidelity of each bacmid. The primer pairs used were as follows: (1) M13F (CCCAGTCACGACGTTGTAAAACG) and M13R (AGCGGATAACAATTTCACACAGG); (2) M13F and 60F (CCCCGCC ACTGACAACTTC); (3) AM14R (CTGCAGTTATCTCTGCGTCGACGGAGAACT) and M13R; (4) AM18polH (ATTCATACCGTCCCACCATCGGG) and AM14R; (5) JRS56   (GTCGTTGGGAGTTTCGTCCG)   and   JRS57

(CGGTTCTGAACATCGGAAAGG) (the binding sites for each primer are represented schematically in Fig. 2.3). A more detailed description of these as well as the other primers used in this study is provided in Appendix 1. The conditions for the PCR reactions are presented in Appendix 2. Each amplicon that resulted from the amplification between JRS56 and JRS57 was also subjected to digestion with *EcoRV* to verify the presence of the mutation in Bac21 and Bac24.
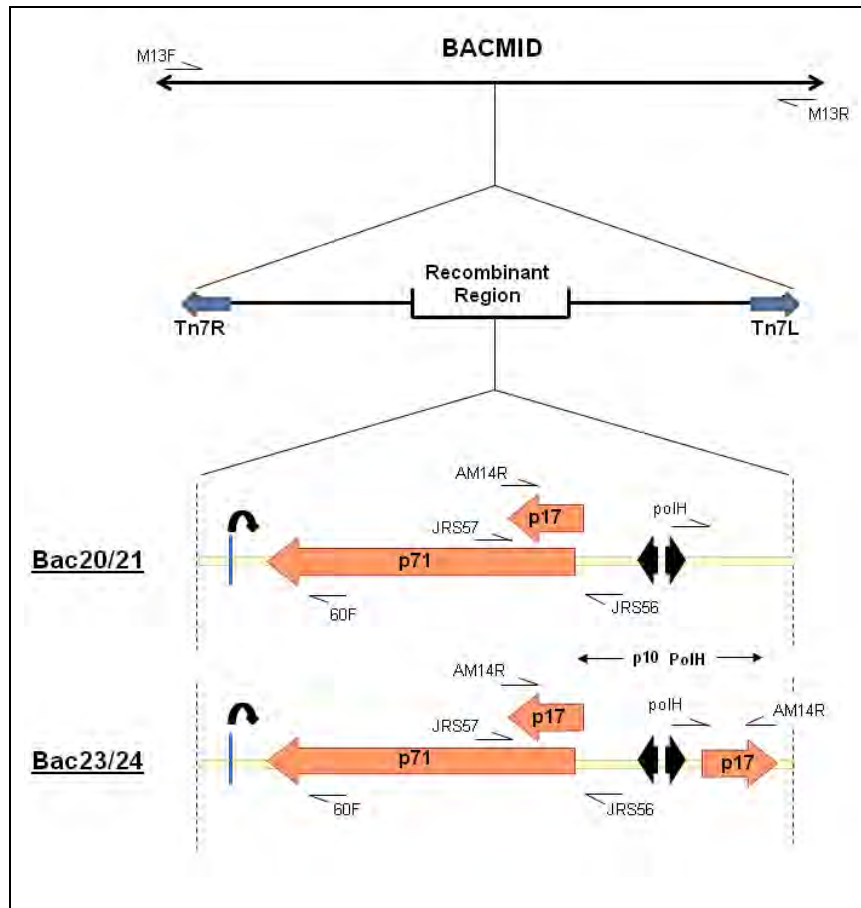
Figure 2.3: Schematic representation of primer binding sites on the recombinant bacmids. The recombinant region between the Tn7R and Tn7L (blue arrows) transposons was transferred into the bacmid and PCR used to verify the recombinant genes. Different primer pairs were used to span the length of the HaSV RNA 2 cDNA. The sequence of each primer and which primers were used together are mentioned in the paragraph above. The approximate region of each binding site is represented in the figure. Black arrows – promoters *p10* and *polH*, orange arrows – recombinant HaSV genes (VCap [p71] and *p17*) and the curved arrow above the blue line – HC ribozyme.

Transfection of *Sf9* cells with recombinant bacmid DNA

The *Sf9* cell line was maintained in TC100 complete insect growth medium (Cambrex) containing 10 % foetal bovine serum (v/v), and 1 % penicillin/streptomycin (v/v) at 28 °C. For bacmid transfections, approximately 8 x10^5 cells were seeded into each well of a six-well plate, in 2 ml TC100 complete insect medium. The cells were evenly dispersed across the surface of the well by gentle agitation and left to settle. Approximately 0.8 μg of recombinant Bac20, Bac21, Bac23 and Bac24 bacmid DNA was added to 12 μl of Fugene HD (Roche) transfection reagent made up to 200 μl with serum-free TC100 medium and incubated at room temperature for 30 minutes. The Fugene:DNA complex was then added dropwise to the cells which were left at 28 °C for 15 minutes. Next, 200 μl of serum-free medium was added and the cells incubated at 28 °C for 45 minutes, followed by the addition of a further 600 μl of medium and a further 2 hours' incubation. Finally 1.5 ml medium was added and the cells incubated for 3 days at 28 °C. Recombinant baculoviruses were harvested from the cells by removing the spent medium after the 3 days. This represented the primary baculovirus stock for each virus (designated Passage #1).

Infection of *Sf9* cells with recombinant baculovirus and plaque purification.

Approximately 8 x10^5 *Sf9* cells was seeded into each well of a six-well plate and after the cells had settled the medium was removed. Next 500 μl of Passage #1 baculovirus was added to each well. The cells were then incubated at 28 °C with very gentle agitation (55 rpm) for 1 hour and 2.6 ml of fresh TC100 complete medium subsequently added. The cells were then incubated at 28 °C for 4 days.

The supernatant extracted from each well (Passage #2) was used in to purify recombinant baculovirus from potential wild type contamination. A six well plate was prepared containing 8.5 x10^5 cells per well. A ten-fold dilution series was prepared for each virus from 10^{-1} to 10^{-6}, to a final volume of 500 μl in Grace's complete insect medium (Gibco). Each dilution was dispensed per well of the plate and the cells incubated with gentle agitation (55 rpm) for 1 hour at 28 °C. After incubation, the medium containing the baculovirus was removed from the wells and 2 ml of a 1:1

mixture of molten agarose (2 % v/v) and Graces's complete medium (2 x v/v), warmed to 40 °C in order to maintain the agarose as a liquid, was carefully added to each well. Once the agarose had set, the cells were incubated at 28 °C for 6 days after which 500 µl thiazolyl blue tetrazolium bromide stain (Sigma) (0.1 % v/v in phosphate buffered saline solution) was added to each well and left overnight to visualize viable vs lysed cells.

Plaques were identified as circular zones where cell death had occurred and thus appeared lighter in colour compared to the healthy stained cells. Virus present in plaques that were well distanced from any others and distinctive in size was removed using a 1 ml pipette tip and mixed into 500 µl TC100 complete medium. At least 3 plaques were picked per baculovirus and 8×10^5 cells subsequently infected with each plaque virus suspension, in the same manner as before. After 3 days, the cells were examined for the presence of recombinant protein using SDS-PAGE and western blot analysis. The resulting supernatant was set aside and represented Passage #3 of each baculovirus.

Determination of viral titre and optimization of protein expression

A single baculovirus was selected from those purified by plaque purification and a T25 flask of *Sf9* cells was infected with 500 ul of the Passage #3 virus stock in order to increase the volume of recombinant virus. The passaging procedure involved the same infection procedure as was carried out before, except that 4.5×10^5 cells was infected and the total volume of virus added to the cells was increased to 2 ml. After 4 days incubation at 28 °C, a total of 5 ml supernatant (Passage #4) baculovirus stock was removed and the titre of each recombinant baculovirus stock determined using the agarose overlay protocol described above with a ten-fold dilution series from 10^{-3} to 10^{-8}. The titre was defined as the number of plaque forming units (pfu) per milliliter of inoculum used per well (pfu/ml) and was calculated according to the following formula:

- Pfu/ml = [1/dilution factor of virus infecting the well] x [number of plaques counted in the well] x [1/ml of baculovirus stock used per well]

The virus titre was then used to calculate the optimal ratio of infectious virus particles to cells being infected, otherwise known as the multiplicity of infection (MOI):

- MOI = pfu/ml divided by the number of cells to be infected.

Titres of between 5×10^7 and 1×10^8 were routinely obtained.

Protein expression was optimized using expression of VCap (p71) as an indication to the potential of the baculovirus to produce HaSV VLPs. Two parameters affecting protein expression were optimized, namely the MOI of the recombinant virus and the time of incubation. In the first instance, 2×10^6 cells per well of a six well plate were infected at a MOI of either: 0.1, 1.0, 2.0, 5.0 or 10.0 and incubated for 3 days at 28 °C. The cells were harvested and subjected to SDS-PAGE and western blot analysis using anti-VCap antibodies. The lowest MOI that produced the highest amount of VCap was chosen and used to infect cells, which were then incubated for either 2 – 5 days. These cells were also harvested and subjected to SDS-PAGE and western blot analysis to determine the optimum time of incubation for maximum expression levels.

2.4 SDS-PAGE and western blot analysis

Total cellular protein from baculovirus-infected cells was analysed by harvesting the cells in the following manner. First the cells were resuspended in the spent medium and pelleted by centrifugation at 4000 xg for 5 mins. After each point at which baculovirus had been passage through cells, the supernatant was set aside as a new baculovirus stock. The pelleted cells were washed with 100 µl 50 mM sodium acetate, 250 mM NaCl, 5 mM Na_2EDTA (pH 5.0) buffer and pelleted again at 5500 xg for 5 minutes. The final pellet was then resuspended in 100 µl of the sodium acetate buffer mentioned above with 100 µl 2 x SDS-PAGE sample buffer (12.5 % 1M Tris pH 7.6, 0.04 % SDS, 10 % β-merchaptoethanol, 10 % glycerol and 0.01 % bromophenol blue). Purified VLPs were mixed directly with an equivalent volume of 2 x sample buffer. All the samples were boiled for 5 minutes prior to loading and

SDS-PAGE carried out as per the protocol of Laemmli, (1970), using either 10 % (for the detection of VCap) or 15 % (for the detection of p17) resolving gels. Proteins were either stained with Coomassie Briliant Blue (Sigma) or subjected to western blot analysis using the BM Chemiluminescence western blotting kit (Mouse/Rabbit) (Roche). VCap was detected with rabbit polyclonal anti-VCap antibodies at a dilution of 1:10000 (diluted in 1 % bovine serum albumin (BSA) in TBS Tween buffer [10 % 1 M Tris pH 7.6, 3 % 5 M NaCl and 0.1 % TBS Tween-20)] or rabbit polyclonal anti-p17 antibodies at a dilution 1:25000 (also diluted in the 1 % BSA TBS Tween solution). The procedure was carried out according to the methods of Towbin *et al.* (1979).

2.5   Infection of *Sf9* cells and VLP purification

Approximately 1.4 x10^7 *Sf9* cells were placed in each of two T75 flasks which were infected with either of the recombinant baculoviruses Bac20, Bac21, Bac23 and Bac24 at a MOI of 5. An additional virus, designated VCAP, was also included in this experiment. This baculovirus was developed and optimized in the laboratory of Prof. Jack Johnson at the Scripps Research Institute and was kindly supplied for experimentation (Taylor, 2003).   After 4 days, a modified protocol adapted from Taylor *et al.* (2002) and Bothner *et al.* (2005) was used to purify VLPs from the baculovirus-infected insect cells. Zero point five percent NP-40 (v/v) was added directly to each flask and left to shake on ice for 15 minutes. After shaking, cellular debris was pelleted by centrifugation at 10000 x*g* for 20 minutes at 4 °C. The VLPs were pelleted through a 30 % sucrose cushion (w/v) prepared in 50 mM sodium acetate, 250 mM NaCl, 5 mM EDTA (pH 5) by ultracentrifugation at 100 000 x*g* for 4 hours at 4 °C. The resulting VLP pellets were resuspended overnight at 4 °C in approximately 100 µl of the sodium acetate buffer. The following day VLPs were subjected to sucrose gradient ultracentrifugation (10 – 40 % w/v) for 1 hour and 30 minutes at 140 000 x*g*. The gradient was prepared using a Biocomp gradient maker 107 ip. The VLP band was subsequently extracted using a syringe and needle. The VLPs were then concentrated by a final ultracentrifugation step at 140 000 x*g* for 4 hours at 4 °C, ensuring that the tubes were filled to the brim (11 ml) by the addition of the sodium acetate buffer. The resulting pellets were resuspended in 100 µl of the

sodium acetate buffer and either subjected to SDS-PAGE and western blot analysis or used for RNA extractions.

2.6 Purification of wild type HaSV from infected _Helicoverpa armigera_ insects

Wild type HaSV was purified from infected _Helicoverpa armigera_ insects according to the protocol described in the masters thesis of Vlok, (2009). Essentially the only difference between extracting the wild type virus from the insects and extracting VLPs from the cells (described above) is the homogenization of the infected _Helicoverpa armigera_ larvae. _H. armigera_ larvae previously infected with HaSV and stored at -80 °C were allowed to thaw on ice and then homogenized in approximately 200 ml of 50 mM Tris-Cl (pH 7.4) per 100 g of infected larvae using a hand held blender. The homogenization was then filtered through cheesecloth. The wild type virus suspension was then subjected to the same series of centrifugation and ultracentrifugation steps as has been described for the extraction of VLPs. The resulting pellets were resuspended in 100 µl of 50 mM sodium acetate, 250 mM NaCl, 5 mM EDTA (pH 5) buffer and either subjected to SDS-PAGE and western blot analysis or used for RNA extractions.

2.7 Overexpression and affinity purification of 6x His-p17 in _E. coli_

The vector pMV2 (Vlok, 2009) was used to express p17 with an N-terminal 6x His tag, in _E. coli_ BL21 (DE3) cells. _E. coli_ BL21 (DE3) cells were transformed with the plasmid and single colonies inoculated into 5 ml of LB broth with ampicillin (100µg/µl). The cells were left to grow overnight with agitation (200 rpm) at 37 °C. Two sets of 5 ml overnight cultures were inoculated into 100 ml LB broth with ampicillin (100 µg/µl) in 500 ml Erlenmeyer flasks. The flasks were incubated at 37 °C with agitation (200 rpm) until the $OD_{600 \ nm}$ reading reached 0.4 – 0.6 nm. Expression of p17 was induced in one of the two flasks by the addition of 1 mM Isopropyl β-D-1 thiogalactopyranoside (IPTG) while the other was left uninduced as a control. One milliliter samples were taken at time zero and every 2 hours for a total

4 hours. Both induced and uninduced samples were analysed via SDS-PAGE and western blot to detect expression of p17.

In order to produce larger quantities of p17, 500 ml of the LB-Amp broth was inoculated with 50 ml pMV2 transformed BL21 culture. After 4 hours the cells were harvested from the broth via centrifugation at 2500 xg for 10 mins. The pellets were stored at -80 °C or resuspended in 200 µl sonication buffer.

His-p17 purification involved the sonication of the cells on ice for 10 second intervals for 5 mins at 45 Hertz. The cellular debris was then pelleted at 10000 xg for 20 mins at 4 °C. The His-Spin Protein Miniprep (Zymo Research) kit was used to purify the His-p17 from the supernatant according to the manufacturers' instructions. The protein was resuspended in 150 µl of the His-elution buffer and 5 µl tested via SDS-PAGE. To the rest of the sample 150 µl 2 x SDS-PAGE sample buffer was added and split into three 50 µl aliquots. Aliquots were stored at -20 °C until used.

2.8   Analysis of RNA packaged into VLPs

RNA extraction and denaturing gel electrophoresis

Where possible, all materials used during RNA experimentation were double-baked at 200 °C or in the case of autopipettes, tips and other disposables, treated with a combination of household bleach and RNAse Away (Molecular Bioproducts). Total cellular RNA was extracted from 2 x10^6 Bac20, Bac21, Bac23, Bac24 and VCAP infected and uninfected *Sf9* cells using the Quick-RNA MiniPrep kit (Zymo Research) according to the manufacturers' instructions. The RNA was resuspended in 40 µl RNAse-free tripled distilled water (dddwater). The total 100 µl of the VLP preparation extracted from the *Sf9* cells as well as an equivalent concentration of wild type HaSV was used for RNA extraction. The RNA contained in the VLPs as well as the wild type virus was extracted using the phenol/chloroform method of Walter, (2008). The RNA pellet from each VLP or wild type virus isolation was also resuspended in 40 µl RNAse-free dddwater and left to resuspend for approximately 1 hour at 4 °C.

Prior to northern blotting, RNA was analysed using formaldehyde denaturing agarose gel electrophoresis in 4-Morpholine-propane sulfonic acid (MOPS) buffer (200 mM MOPS, 50 mM sodium acetate, 10 mM EDTA, pH 7.0 with sodium hydroxide) according to the methods described in Sambrook *et al*. (1989). Prior to loading, 2 x RNA loading dye which also contained ethidium bromide (Fermentas) was added to each RNA sample and heated at 70 °C for 10 minutes. Two microlitres of the RiboRuler High Range Ladder (Fermentas) was treated in the same manner and electrophoresed beside the samples. RNA was visualised on a UV transilluminator and imaged using the Uviprochemi (Uvitech) program.

In vitro transcription labeling of RNA probes

Two probes were generated for northern blot analysis. The first was used to detect HaSV RNA 2 transcripts and was synthesized *in vitro* from pMT20F, a plasmid constructed by M. Tomassicchio (Tomasicchio *et al*., 2007). This plasmid contains the *VCap* ORF flanked by *SP6* and *T7* promoters. The second probe was designed to detect baculoviral RNA transcripts expressed from the *polH* promoter using the vector pAM26 polHF. This construct was derived by PCR amplification of the cloning cassette down-stream the *polH* promoter on the native pFastBac Dual vector using primers AM18polH (ATTCATACCGTCCCACCATCGGG) and JRS61 (CTCTAGTACTTCTCGACAAGCTTGTCGAG). The resulting fragment was cloned into pGEM-T Easy resulting in pAM26 polHF.

For *in vitro* transcription reactions, both plasmids were digested with *NcoI* and the linearised DNA purified using the Zymo DNA Clean and Concentrator Kit (Zymo research). The probes were synthesized by transcription with *SP6* RNA polymerase (Roche) and labeled *in vitro* using the DIG High Prime DNA labeling and Detection Starter Kit (Roche). The reaction was incubated at 42 °C for 1 hour after which 2 µl RNAse-free DNAse (Roche) was added and the mixture placed at 37 °C. After allowing 15 minutes for DNA digestion, the reaction was stopped by the addition of 2 µl 0.2 M Na_2EDTA (pH 8.0). The quality of the probes was determined by analysis

on a 1 % non-denaturing agarose gel and the RNA visualized in the same manner as before. If not used immediately, the probes were stored in aliquots at -80 °C.

Northern blot analysis

Northern blots were carried out by transferring the RNA from a denaturing agarose gel onto a nitrocellulose membrane (Amersham Biosciences) according to Schneider *et al.* (1994) and fixed to the membrane by UV-irradiation for 5 minutes. Following the transfer and fixing of the RNA to the membrane, it was pre-hybridised in 15 ml DIG Easy Hyb Buffer (Roche) at 68 °C for 30 minutes.   During this time, one microgram of either of the probes was added to 50 µl of RNAse-free dddwater and heated to 65 °C for 5 minutes, after which the probe was placed on ice. The RNA probe was then further diluted by adding the full volume (55 µl) to approximately 10 ml pre-warmed (68 °C) DIG Easy Hyb Buffer (Roche).   After the 30 min pre-hybridisatioin period had elapsed, the DIG-labeled probe/hybridisation buffer solution replaced the buffer that was washing over the membrane and the probe was left to hybridise to the RNA for approximately 16 hours with rotation. After hybridisation, the membrane was washed twice with 50 ml low stringency buffer (2 x SSC, 0.1 % SDS) at room temperature with gentle rocking for 5 minutes. These washes were followed by two 15 minute washes with 50 ml pre-warmed high stringency buffer (0.1 x SSC, 0.1 % SDS) at 68 °C in the oven. DIG-labeled RNA targets were visualised using the CSPD Chemiluminescent assay as per the instructions of the DIG High Prime DNA labeling and Detection Starter Kit (Roche).

Chapter 3
Results

3.1   Introduction

The plasmid expression system improved the understanding of tetravirus packaging by elucidating some of the features that were essential for the specific packaging of RNA 2 by VLPs (Vlok, 2009). Using the plasmids depicted in Fig. 3.1. the Vlok study showed that neither deletions of the 5' UTR preceding the *p17* ORF (pMV20), the 3' UTR after the *VCap* ORF (pMV27) or the deletion of both regions together (pMV28) had any effect on the packaging of RNA 2 by VLPs assembled in the plasmid transfected *Sf9* cells.
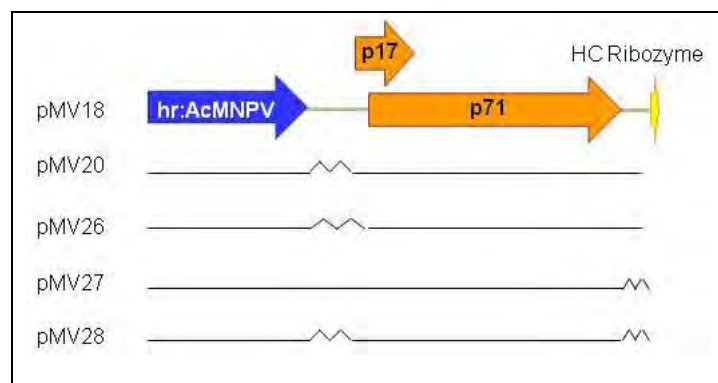
Figure 3.1: Schematic representation of the plasmids used in the study by Vlok (2009). The construct pMV18 represents the wild type HaSV RNA 2 plasmid as both the 5'UTR (semi-precise) and 3'UTR (precise) are intact and p17 and p71 (VCap) are expresssed from the baculoviral insect promoter *hr:AcMNPV*. Each plasmid represented by lines below pMV18 contains a deletion of the RNA 2 sequence depicted as a line-break: pMV20 (5'UTR deleted), pMV26 (5'UTR and the first 80 nucleotides of *p17* deleted), pMV27 (3'UTR deleted) and pMV28 (both 5'and 3'UTR's deleted). A precise 3'UTR is maintained by an HC ribozyme on each construct.

The only plasmid that changed the RNA 2 packaging phenotype in the experiment was pMV26. HaSV RNA 2 could not be detected in VLPs derived from the transfection of pMV26. In this plasmid the first 80 base pairs of the *p17* ORF (which do not overlap *VCap*) as well as the 5'UTR region had been deleted. Therefore, pMV26 was the only plasmid depicted above in which p17 would not be expressed when transfected into the *Sf9*'s. Since the 5'UTR deletion alone did not effect

packaging, it was concluded that either p17 itself was required for packaging or that the packaging signal was present in the sequence between the start of the *p17* and *VCap* ORFs. Unfortunately Marli's experiments were not able to delineate between the requirement for an RNA signal alone or the requirement for the protein as well as a potential signal. For this reason this experiment was repeated with a new construct in which the RNA sequence would be maintained but p17 expression abolished (pAM10).

3.2 The effect of silencing p17 on the packaging of RNA 2 into VLPs using the plasmid expression system

In order to determine whether translation of the *p17* ORF is required for the packaging of HaSV RNA 2 by VLPs, SDM was employed to mutate the AUG start codon of the *p17* ORF to GAU, which encodes aspartic acid and thus abrogates initiation of translation. Therefore, by mutating the *p17* AUG cDNA sequence, p17 translation could be abolished with only two codons being affected in the corresponding RNA sequence (AUG AGC to GAU AUC). This would also serve to introduce a diagnostic *Eco*RV site while maintaining most of the RNA sequence but abolishing p17 translation. The construct pAM10 was thus an exact copy of pMV18 but for the mutation of the first two codons of the *p17* ORF. Both pAM10 and pMV18 were transfected into each of 4 T75 flasks (approximately 5 x10^7 cells) and the VLPs purified using the methods described in chapter 2.
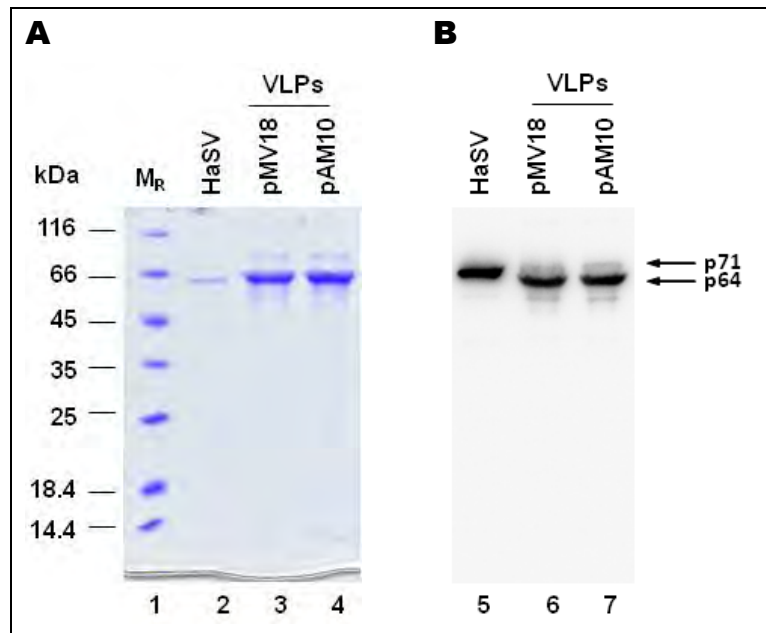
Figure 3.2: Analysis of VLPs purified from pMV18 and pAM10 transfected *Sf9* cells. After transfection of each plasmid into *Sf9* cells, VLPs were purified according to the protocol mentioned in chapter 2 and subjected to SDS PAGE (**A**) and western blot (**B**). Lane 1 – Unstained protein molecular weight marker, lanes 2 and 5 – wild type HaSV, lanes 3 and 6 – pMV18 derived VLPs and lanes 4 and 7 – pAM10 derived VLPs. The molecular weight standards are indicated in kDa next to the SDS-PAGE gel. The arrows next to the blot indicate the position of p71 (VCap) – the capsid protein precursor and p64 - the major capsid protein. The presence of p64 is indicative of VLP formation. Western analysis was carried out using anti-VCap antibodies at a 1 in 10 000 dilution.

VLPs were prepared from *Sf9* cells transfected with pMV18 (wild type HaSV RNA 2) and pAM10 (p17 AUG start mutated) by resuspending the pellets obtained after ultracentrifugation and then sending them through a sucrose cushion and subjecting them to SDS-PAGE and western analysis. Two protein products migrating at approximately 64 kDa and 71 kDa, were observed on polyacrylamide gels stained with Coomassie brilliant blue (Fig. 3.2 A, lanes 3 and 4). The 64 kDa band, which co-migrates with the wild type HaSV capsid protein, is likely the mature β capsid subunit, while the 71 kDa band, observed only in VLP samples, corresponds to the uncleaved, capsid protein precursor. Western analysis with anti-VCap antibodies confirmed that the 64 kDa and 71 kDa proteins corresponded to viral p64 and VCap (Fig. 3.2 B, lanes 6 and 7). The presence of p64 as the major band in the VLP samples indicated the presence of mature VLPs. The p7/(γ) capsid protein was not detected.
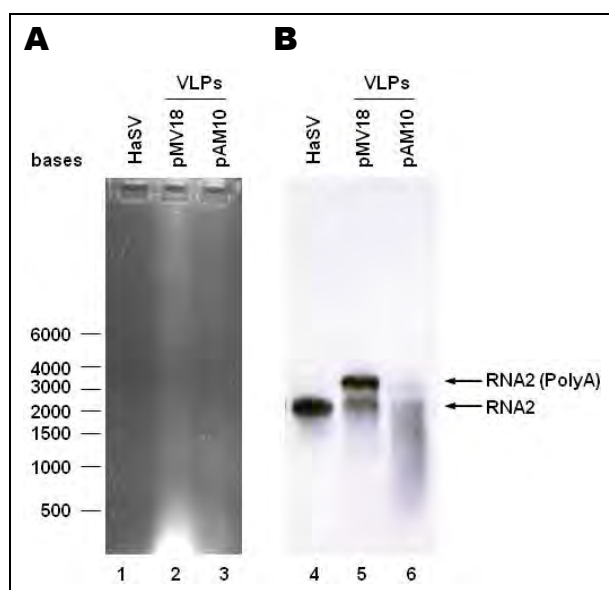
Figure 3.3: RNA 2 packaging by VLPs assembled in cells expressing HaSV VCap and/or p17. (**A**). Denaturing agarose gel stained with ethidium bromide. Lane 1 – wild type HaSV RNA ; lane 2 – RNA extracted from pMV18-derived VLPs and lane 3 – RNA extracted from pAM10-derived VLPs. The sizes of the RNA marker are indicated to the left of the image. (**B**) Northern analysis of RNA extracted from VLPs assembled in *Sf9* cells transfected with pMV18 (Lane 5) and pAM10 (Lane 6) compared with RNA extracted from the wild type virus (Lane 4). Arrows to the right indicate the position of transcripts detected with a probe for HaSV RNA 2.

RNA was extracted from the purified VLPs as well an equivalent amount of wild type HaSV, via a phenol/chloroform protocol described in chapter 2. Analysis of the extracted RNA by denaturing agarose gel electrophoresis showed no significant RNA bands corresponding to the expected size of an RNA 2 transcript (2500 bases) for pMV18 VLPs (Fig. 3.3 A, lane 2) or pAM10 VLPs (Fig. 3.3 A, lane 3), nor were the genomic RNAs from the wild type virus detected (Fig. 3.3 A, lane 1). Northern analysis using a probe for HaSV RNA 2, detected the viral RNA 2 migrating at approximately 2300 bases (Fig. 3.3 B, lane 4). Two RNA species were detected in VLPs derived from pMV18, one migrating at approximately the same size as wild type HaSV RNA 2 and a larger species migrating at approximately 3500 bases consistent with the size of mRNA 2 uncleaved by the HC ribozyme (Fig. 3.3 B, lane 5). The result is consistent with previous observations (Vlok, 2009). The same packaging phenotype was not observed in VLPs that assembled in cells transfected with pAM10. A very faint signal for both RNA species was detected as well as a large amount of degraded RNA (Fig. 3.3 B, lane 6). Since equivalent quantities of

VLPs were used for extraction of RNA (Fig. 3.2 A, compare lanes 3 and 4 and Fig. 3.2 B, compare lanes 6 and 7), the decrease in the amount of viral RNA detected in VLPs assembled from cells transfected with pAM10 may indicate that p17 expression is required for RNA 2 packaging.

The major problem with the plasmid-based experimental system was the inefficient expression of both p17 and VCap and the inability to purify sufficient quantities of VLPs to for example, reliably quantify the amount of RNA extracted from the VLPs used for northern analysis. In addition, the low levels of expression prevented the detection of p17 in cell-free extracts, so the veracity of the mutation in pAM10 could not be confirmed. Thus it was decided to develop an alternative expression system that would result in more efficient expression of p17 and VCap.

3.3   Development of a recombinant baculovirus expression system for the expression of VCap (p71) and p17

The high levels of protein expression traditionally ascribed to a baculovirus system are primarily achieved due to the fact that the researcher is taking advantage of the natural infectious cycle of the virus to express a heterologous protein (Van Oers, 2011). It was decided that baculoviral expression would be the best system upon which to improve the analysis of HaSV RNA packaging.   The baculovirus *Autographica californica multicapsid nucleopolyhedrosis virus* (AcMNPV) is the most widely used and commercially available baculovirus and it was decided that the Bac-to-Bac baculovirus expression system (Invitrogen), which uses AcMNPV, would be the best way to utilise baculoviruses for the expression of HaSV proteins. Not only has the Bac-to-Bac system been widely used but it provides the additional advantage that each baculovirus can be made to produce two sets of recombinant proteins. This is because the transfer/transplacement vector upon which the entire set-up relies, pFastBac Dual, contains bi-direction cloning cassettes under the control of the *p10* and *polH* (polyhedrin) promoters.   These promoters are transcriptionally highly active during late phase infection of the baculovirus and cloning into either cassette does not limit protein expression from the other. Thus a

recombinant baculovirus developed with the Bac-to-Bac system can produce more than one foreign protein in an insect cell. Flanking the cloning cassettes on this plasmid are Tn7 transposon sites which have also been engineered into the cloned baculoviral genome housed in specific DH10Bac *E. coli* cells, known as a bacmid. After transformation of the recombinant plasmid into the *E. coli* cells and the application of selection pressure, transposition of the region between the transposon sites of the plasmid into the bacmid occurs via homologous recombination. This then represents a recombinant baculovirus genome which is infectious and able to produce recombinant baculovirus able to produce foreign proteins.

Once recombinant baculoviruses have been developed, two more steps need to be completed before the large scale expression of heterologous proteins is ensured. Firstly, the recombinant nature of the viruses has to be validated which involves PCR and baculoviral plaque purification. Secondly, once pure recombinant baculoviruses have been isolated, the optimum conditions for protein expression in the insect cells need to be determined. From the point at which the recombinant pFastBac Dual clones have been developed to the point at which optimal expression of recombinant protein occurs, takes several months and this is one of the few drawbacks of using baculoviral expression systems.

The main reason to utilise baculoviruses was, as has been mentioned, because of their reputed high levels of protein expression. It was reasoned that the best way to take advantage of this, in terms of studying HaSV RNA 2 packaging, would be to repeat the VLP packaging protocol developed by Vlok (2009) and carried out in section 2 of this chapter, but with baculoviruses instead of plasmids.

Construction and validation of recombinant bacmids

The first two baculoviruses developed were Bac20, a baculovirus representative of pMV18 and Bac21, a baculovirus representative of pAM10 (Fig. 3.4 A and C). The primary objective for repeating the packaging experiments with Bac20 and Bac21 was that the baculoviruses would produce higher levels of HaSV mRNA and

therefore more protein, consequently more VLPs could be produced meaning more RNA for analysis. Clearly the expectation was that packaging by the Bac20 and Bac21-VLPs would be consistent with the packaging by the pMV18 and pAM10-VLPs.
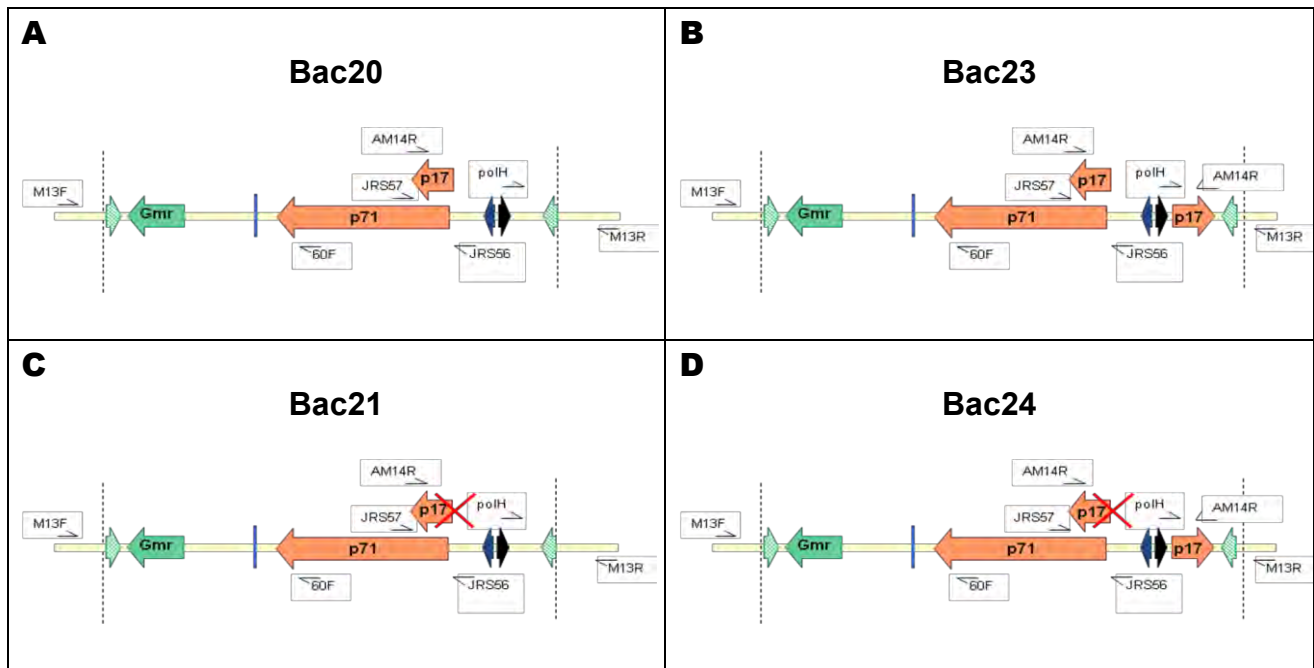
Figure 3.4: Schematic maps of the recombinant regions of the Bac20, Bac21, Bac23 and Bac24 bacmids developed in this study. In each panel the HaSV recombinant ORF's *p71* (*VCap*) and *p17* are depicted in orange arrows (5' to 3'). The solitary blue line 3' to the *p71* ORF depicts the end of HaSV RNA 2 and the point at which cleavage occurs via the HC ribozyme. Each of the baculoviruses contains a copy of wild type HaSV RNA 2 cDNA (**A** and **B**) or the mutated RNA 2 cDNA (**C** and **D**) opposite the *p10* promoter (blue arrow). The mutation on the *p17* ORF is depicted as a red cross. In addition Bac23 and Bac24 (**B** and **D**) house a second functional *p17* ORF opposite the *polH* promoter (black arrow). Arrows in green stripes represent the Tn7R and Tn7L transposon sites which are responsible for the transposition of the portion between the black dashed arrows from the pFastBac Dual vector into the bacmid. The primer binding sites used to confirm the viability of the recombinant bacmids by PCR are depicted by arrows above the map and correspond to the primer pairs shown in Table 3.1. Gmr – gentamycin resistance gene.

As mentioned previously, the Bac-to-Bac system carries the advantage of being able to produce more than one foreign protein from one recombinant baculovirus. This therefore, made it possible to ask another question of the p17-RNA packaging system. If a functional *p17* ORF was expressed side-by-side the RNA 2 of pMV18

and pAM10, what would the packaging of the VLPs look like? This was the motivation behind the development of the third and fourth baculoviruses; Bac23 (pMV18 plus p17) and Bac24 (pAM10 plus p17) (Fig. 3.4 B and D). As the data in section 2 suggested that the expression of p17 may mediate the packaging of RNA 2, it would be interesting to see whether or not the protein could still mediate packaging if expressed from another RNA strand (*trans* packaging) and if it could mediate the packaging of its own mRNA as well.

Following construction of the relevant recombinant plasmids, transposition of the expression cassette and isolation of bacmid DNA, it was important to verify that each bacmid contained the correct HaSV RNA 2 sequences. In order to do this, PCR analysis was employed with a combination of primers, which would be able to distinguish between the wild type AcMNPV bacmid and Bac20 and Bac21 on the one hand and Bac23 and Bac24 on the other. A description of the strategy used for the verification of the baculoviruses by PCR is presented in Table 3.1. and the results of the corresponding PCRs in Fig. 3.5.

According to the Bac-to-Bac system manual (Invitrogen), the primers M13F (pucF) and M13R (pucR), which correspond to regions on the AcMNPV bacmid approximately 128 (M13F) and 145 (M13R) bp from the site of transposition should be used to determine whether the insert has been transposed into the bacmid. This primer set would produce a PCR product of 276 bp from the empty AcMNPV bacmid, while recombinant bacmids would produce a larger amplicon consisting of the 5298 bp of vector sequence plus the sequence of the insert (Table 3.1). Unfortunately, despite repeated attempts at optimisation of this reaction, no conclusive results were obtained when using the recombinant bacmids as template DNA. For this reason no result for this primer pair is reported in Fig. 3.5. It was believed that the problem in this regard was that the desired product was too big to be amplified using this protocol.

Table 3.1: Strategy for the validation of the recombinant bacmids by PCR

PCR primer pair	Primer binding sites	Expected PCR product size (bp)				
		AcMNPV	Bac20	Bac21	Bac23	Bac24
M13F and M13R	M13F – AcMNPV bacmid M13R - AcMNPV bacmid	273	5298	5298	5298	5298
M13F and 60F	M13F – AcMNPV bacmid 60F – 3' end *p71* (Nt 2075 – 2094)	0	2327	2327	2327	2327
AM14R and M13R	AM14R – 3'end of *p17* (Nt 757 – 733) M13R - AcMNPV bacmid	0	1328	1328	1328	1328
polH and AM14R	polH – *polH* promoter (Nt 103 – 125) M13R - AcMNPV bacmid	0	0	0	600	600
JRS56 and JRS57	JRS 56 – 5' HaSV UTR (Nt 144 – 164) JRS57 – *p71* (862 – 841)	0	719	719	719	719

AcMNPV – Bac-to-Bac *Autographica californica multicapsid nucleopolyhedrosis virus* bacmid isolated and used in parallel with the recombinant bacmids; Nt – nucleotide; UTR – untranslated region; ORF – open reading frame.
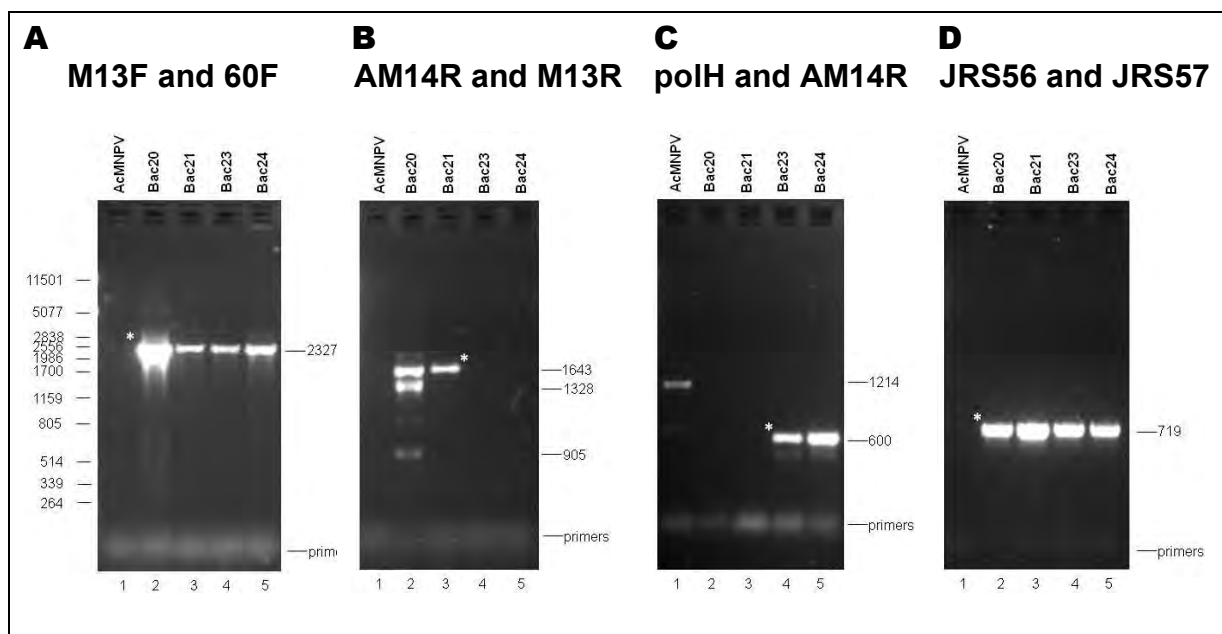
Figure 3.5: PCR analysis of the four recombinant bacmids constructed for the expression of HaSV proteins. Table 3.1 indicates the five sets of PCR reactions used to verify that Bac20 (lane 2), Bac21 (lane 3), Bac23 (lane 4) and Bac24 (lane 5) contained recombinant HaSV cDNA sequence. Agarose gel analysis of the resulting PCR products is presented above with each primer pair indicated above each image. A non-recombinant AcMNPV bacmid was also included in the analysis (lane 1). The size of the molecular weight marker is indicated to the left of (**A**) and the size of each amplicon indicated to the right of each picture in base pairs. Predicted amplicons from each reaction are indicated by a white asterix.

To overcome this problem a further set of PCR reactions involving the M13 primers in conjunction with HaSV RNA 2 specific primers, which would produce shorter PCR products, was employed (Table 3.1). As expected, PCR amplification with the AcMNPV bacmid as a template, using primers M13F and 60F, which binds in *VCap*, produced no amplicon (Fig. 3.5 A, lane 1). In contrast a PCR product of 2327 bp was detected in the four recombinant bacmids, which is consistent with the presence of the RNA 2 sequence downstream of the *p10* promoter (Fig. 3.5 A, lanes 2 – 5). In the next PCR reaction, primers AM13R (which binds in p17) and M13R produced the expected amplicon of 1328 bp when only Bac20 was used as a template (Fig. 3.5 B, lane 2). This reaction also resulted in other non-specific products of 1643 and 905 bp. When Bac21 was used as a template, using the same primers, only the 1643 bp band was visualised (Fig. 3.5 B, lane 3). No amplicons for Bac23 and Bac24 were produced using the same reaction (Fig. 3.5 B, lanes 4 and 5). There was no definitive reason why the Bac21 reaction did not produce the anticipated results, although it is interesting that a consistent non-specific product of 1643 bp was also observed. With regards to the Bac23 and Bac24 reaction, it was postulated that the fact that there were two binding sites for the AM13R primer (two *p17* ORFs in Bac23 and Bac24) may have had an effect on the fidelity of the reaction. This conclusion though remains to be proven. The optimisation of this reaction will be required if it is going to be used for the validation of recombinant HaSV RNA 2 bacmids in the future, although it is was not necessary for this experiment, given the results of the remaining PCRs.

To confirm that the *p17* ORF was present downstream of the *polH* promoter on Bac23 and Bac24, a primer designed to bind in the *polH* promoter region (labelled polH) as well as a p17 specific primer, AM14R, was used (Fig. 3.5 C). An expected PCR product of 600 bp was detected in the reactions with Bac23 and Bac24, while there was no corresponding PCR product in the reactions with Bac20 and Bac21 (Fig. 3.5 C, lanes 4 and 5 vs. lanes 2 and 3). A non-specific product of 1214 bp was observed in the AcMNPV lane (Fig. 3.5 C, lane 1). Finally, a PCR using two RNA 2 specific primers (JRS56 and JRS57) produced an expected 719 bp amplicon in reactions containing all four recombinant bacmids, which was absent in the wild type bacmid (Fig. 3.5 D, lanes 2 – 5). Taken together the PCR analysis confirmed the

integrity of the recombinant bacmids and that they contained the correct HaSV RNA 2 sequence. One final element of verification was required to be absolutely sure of the nature of the four recombinant bacmids and that was the fidelity of the mutation on Bac21 and Bac24 carrying the mutant *p17* ORF derived from pAM10.

To confirm that Bac21 and Bac24 carried the mutant RNA2 sequence with the mutated start codon of *p17*, PCR products were generated using primers JRS56 and JRS57 (the product of which includes the *p17* start site). The PCR products were then digested with *Eco*RV and resolved by agarose gel electrophoresis.
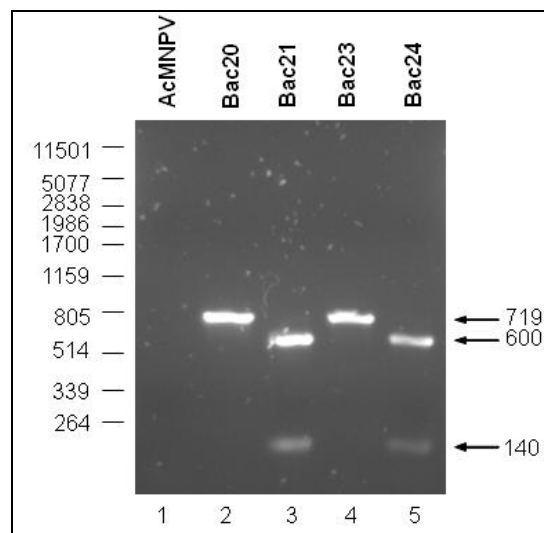
Figure 3.6: Restriction analysis of PCR products from JRS56 to JRS57 with *Eco*RV. The agarose gel depicts the results of the *Eco*RV digestion of the amplicons produced by PCR of the recombinant bacmids with JRS56 and JRS57. Lane 1: AcMNPV bacmid DNA; lanes 2 – 5: Bac20 – 24 DNA.

In contrast to Bac20 and Bac23, which remained undigested, *Eco*RV digestion of the PCR products derived from Bac21 and Bac24 produced restriction fragments of approximately 600 and 140 bp (Fig. 3.6, lanes 2 and 4 vs. Lanes 3 and 5). In combination with the results from PCR analysis, this result confirms the presence of the correct HaSV RNA 2 sequences in the recombinant bacmids.

Production of recombinant baculovirus stocks

Having confirmed the isolation and identity of each recombinant bacmid generated, the next step in the process was to generate recombinant virions. Accordingly, *Sf9* cells were transfected with each recombinant bacmid and the supernatant used for a plaque assay to enable the isolation of individual recombinant baculovirus clones. For each virus, three plaques that were well defined and well separated from one another was purified. Each plaque suspension was then used in one further round of infection to increase the virus titre (Passage #3). Western blot analysis of whole cell extracts was used to confirm expression of VCap and thereafter one recombinant virus (from one of three plaques) was selected for each of the four baculoviruses for further studies.
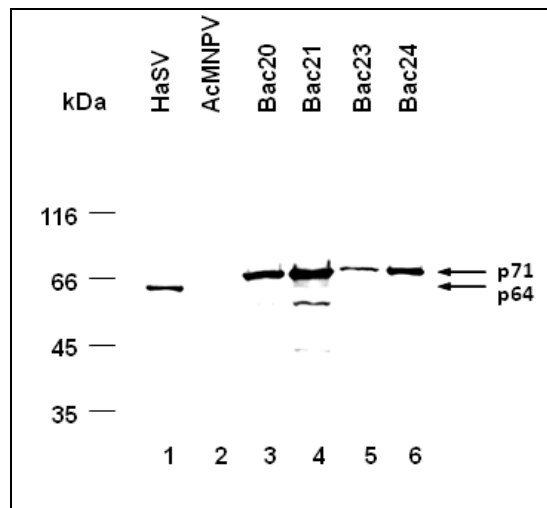
Figure 3.7: Western analysis of protein extracts from cells infected with purified recombinant baculoviruses, Bac20, Bac21, Bac23 and Bac24. Whole cell extracts from the cells infected with purified recombinant plaqued viruses were resolved by SDS-PAGE and western analysis conducted with anti-VCap antibodies (1: 10000 dilution). Lane 1 marked HaSV represents a wild type HaSV sample isolated from infected *H. armigera* larvae. Lane 2 marked AcMNPV represents the whole cell extracts from a non-recombinant baculovirus vector that was isolated and infected in parallel with the recombinant baculoviruses.

A protein migrating at approximately 71 kDa was detected in cell free extracts derived from *Sf9* cells infected with recombinant viruses Bac20, Bac21, Bac23 and Bac24 (Fig. 3.7, lanes 3 – 6). This protein was not expressed in *Sf9* cells infected with the AcMNPV vector (Fig. 3.7, Lane 2). The level of expression supported by

each of the baculoviruses was not equivalent, probably due to each virus stock having a different titre. It is also important to note that protein expression by each virus was not yet optimised at this juncture. In addition, the presence of p71 and little p64 as represented by the wild type HaSV particles (Fig. 3.7, lane 1) indicated that the VLPs had not matured at the time of protein analysis. The selected recombinant virus isolates were used to seed fresh tissue culture cells and passaged to increase the virus titre.

3.4 <u>Optimisation of VCap (p71) and p17 expression by the recombinant baculoviruses</u>

There are three conditions that are directly responsible for the amount of protein a recombinant baculovirus will produce. The first is the number of cells which are infected by the virus and the aim here is to have every cell infected. According to the Bac-to-Bac system manual (Invitrogen) the optimal number of cells tends to range consistently between $8 - 9 \times 10^5$ cells per well in a six well plate. The second factor is the multiplicity of infection (MOI), which refers to the number of virions per cell. The aim is to determine at what MOI one would achieve the most efficient rate of infection given both the cell density and the titre of the inoculum being used. This is therefore, determined by the number of cells in the dish and the concentration of the virus used in the infection. The third factor that needs to be optimised is the time of expression. In order to achieve optimal expression of a heterologous protein, the correct balance between the MOI and the time of expression needs to be determined and thus each of these two elements was independently optimised for the four recombinant baculoviruses.

The determination of the titre of each of the recombinant virus stocks was calculated by using plaque assays and a formula described in chapter 2. The titre for each stock varied from 6×10^7 to 1.2×10^8. The specific titre of each of the recombinant baculoviruses was used to calculate the MOI for each virus to infect one well of a six well plate. An MOI optimisation assay was carried out separately with each virus at

a MOI of 0.1, 1.0, 2.0, 5.0 and 10 in order to determine the most effective infection strategy. The time of expression was kept constant at 3 days.
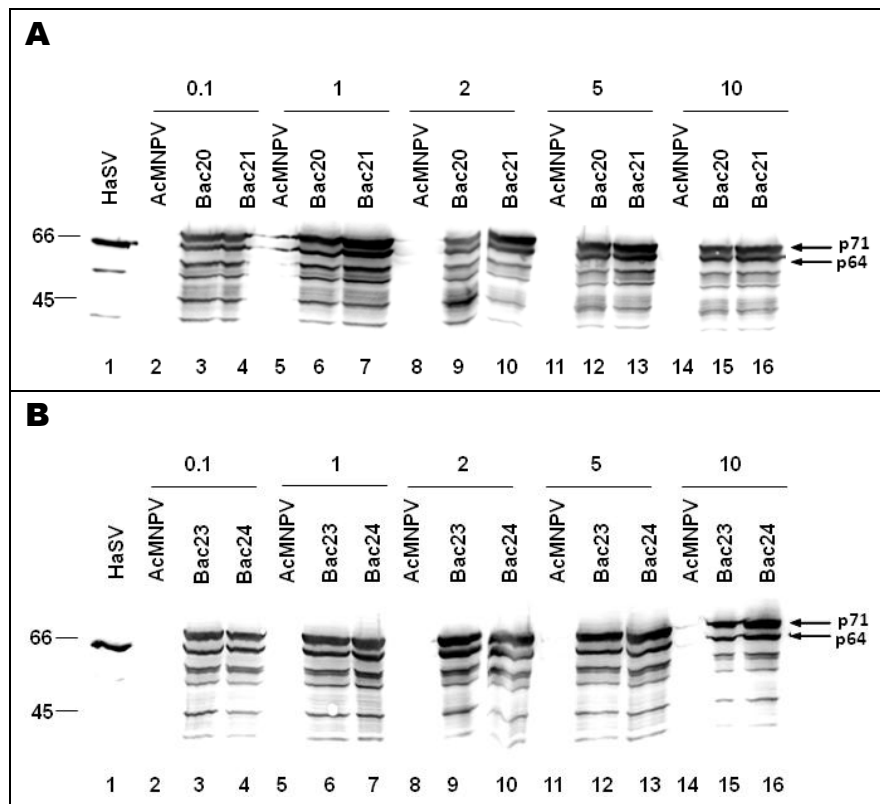
Figure 3.8: MOI optimisation assay of VCap expression by recombinant baculoviruses. Western analysis was carried out on cell free extracts after the cells were infected for 3 days with Bac20 and Bac21 (**A**) and Bac23 and Bac24 (**B**) at a MOI of between 0.1 and 10 using anti-VCap antibodies (1 in 10 000 dilution). Lanes 1 labelled HaSV signify a sample of wild type HaSV isolated from *H. armigera* larvae. The lanes labelled AcMNPV signify protein derived from cells infected with the baculovirus vector AcMNPV. The size markers are presented to the left of each figure (in kDa) and bands believed to represent p71 (VCap) and p64 (β) by arrows to the right.

Two major bands, migrating at 71 kDa and 64 kDa, were detected at each MOI used for infection in cell free extracts derived from *Sf9* cells infected with Bac20, Bac21, Bac23 and Bac24 (Fig. 3.8, A and B). The presence of p64 suggested the presence of mature virions despite the fact that the extracts were only briefly exposed to the low pH buffer which favours assembly. Several additional smaller proteins were also detected in the extracts, which were attributed to VCap degradation products since they were not present in the cell-free extracts derived from cells infected with the wild type AcMNPV baculovirus (Fig. 3.8 Lanes 2, 5, 8, 11 and 14). It could be argued

that given the over-expression by the baculoviruses, not all the VCap is assembled into provirions and, therefore, is degraded by cellular proteases. Although p71 and p64 were present at each MOI tested, judging by the strength of the signal, western analysis revealed that a MOI of 5 or 10 was the most consistent MOI at which to infect all four recombinant viruses to produce high levels of p71. Due to the limited quantities of baculovirus stock available, it was decided to work with a MOI of 5 to make VLPs.

As mentioned before, the amount of time allowed for recombinant baculoviruses to infect the cells and subsequently express recombinant protein is also an important factor determining a high level expression strategy. Accordingly, a time course assay was carried out with all four recombinant baculoviruses. Since it had been concluded that a MOI of 5 was the most optimal level of infection for each virus, this element was kept constant while the time at which the protein extracts were collected was varied between 2 to 5 days. Whole cell extracts from infected cells were resolved by SDS-PAGE and the presence of VCap detected by western blot using anti-VCap antibodies (Fig 3.9).

Only a very slight and gradual increase in protein production was observed between 2 – 5 days of expression as a function of the strength of the signals from the protein bands (Fig. 3.9, A and B). The VCap degradation products observed during the MOI optimisation assay were also observed in this experiment. Given the results of this assay, one could argue that the VLPs could be produced from each of the baculoviruses at a MOI of 5 following 2, 3, 4 or 5 days of expression. An analysis of the literature illustrated that at a MOI of 5, the production of NωV VLPs was favoured at 4 days post-infection (Agrawal and Johnson, 1995; Taylor *et al*., 2002; Maree *et al*., 2005). Thus it was decided to allow 4 days for maximum expression of VCap.
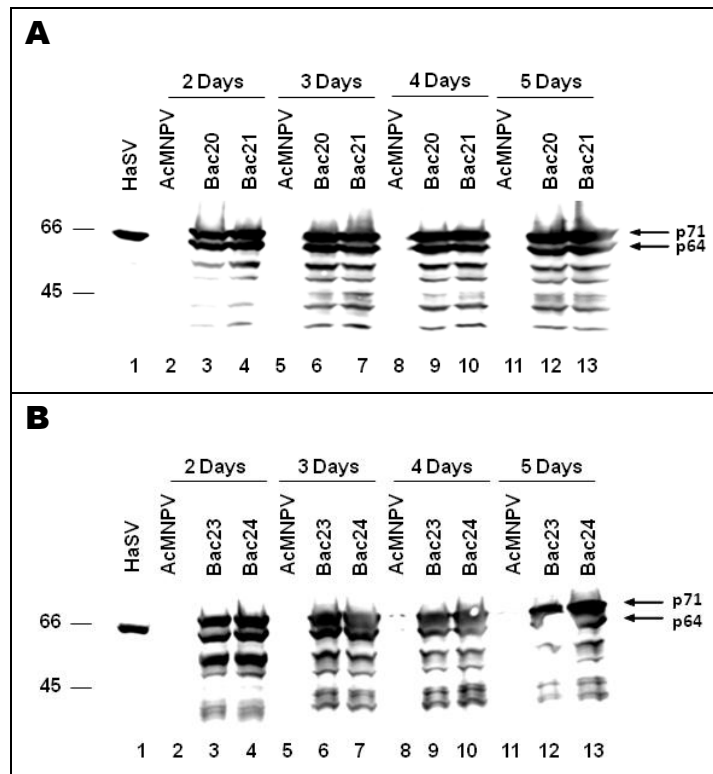
Figure 3.9: Time course assay of VCap expression by recombinant baculoviruses. Western analysis to detect VCap in cells infected with (**A**) Bac20 and Bac21 and (**B**) Bac23 and Bac24 at a MOI of 5 for 2 – 5 days. Lanes 1 labelled HaSV signify a sample of wild type HaSV isolated from *H. armigera* larvae. The lanes labelled AcMNPV signify protein derived from cells infected with the baculovirus vector AcMNPV. The size markers are presented to the left of each figure (in kDa) and bands believed to represent p71 (VCap) and p64 (β) by arrows to the right. Anti-VCap antibodies were used at a 1 in 10 000 dilution.

Having optimised VCap expression, it was important to determine whether p17 could be detected in the baculovirus infected *Sf9* cells under the same conditions. For this reason the same whole cell extracts used above were further analysed for the presence of p17 by SDS-PAGE and western blot. A protein cross-reacting with p17-specific antibodies, migrating at approximately 24 kDa, was detected in cell free extracts derived from Bac20, Bac23 and Bac24 infected cells (Fig. 3.10, lanes 3, 5 and 6) but not in Bac21-infected cells (Fig. 3.10, lane 4) or in cells infected with the control baculovirus (Fig. 3.10, lane 2). This protein migrated slightly lower than purified, recombinant His-tagged p17 (Fig. 3.10, lanes 1 vs. 3). The slight difference in size is to be expected due to the presence of the 6x His tag adding to the weight of the control p17.
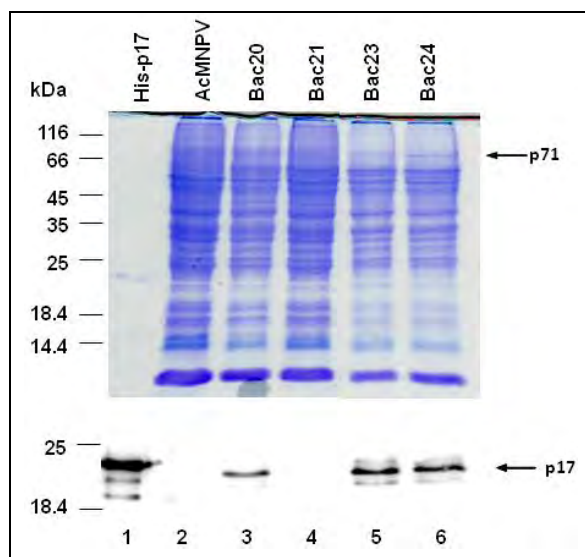
Figure 3.10: Detection of p17 in baculovirus-infected *Sf9* cells. Whole cell extracts were resolved by SDS-PAGE (top) and western analysis (below) with anti-p17 antibodies used to detect p17 expression. His-p17: 6x His-tagged p17 expressed in *E. coli* BL21 cells and purified by nickel affinity chromatography. AcMNPV: protein derived from cells infected with the baculovirus vector AcMNPV. The anti-p17 antibodies were used at a dilution of 1: 25000. The position of the molecular weight marker proteins is indicated on the left of the images. The position of p71 (VCap) and p17 are indicated to the right of the figure.

It was concluded from this data that three of the four recombinant baculoviruses were expressing p17. This represents an important improvement over the plasmid-based expression system, in which no p17 could be detected in cell free extracts. In addition it is important to note that the *p17* ORF has a poor Kozak sequence and that despite this, p17 could be detected in baculovirus infected cells via western blot. P17 expression was still down-regulated relative to VCap, given that VCap could still be detected via Coomassie staining alone and p17 could not. The expression of VCap also resulted in a stronger signal from the same samples using western analysis (Fig. 3.9, lanes 9 and 10 vs. Fig. 3.10 lanes 3, 5 and 6). The mutation on the start codon of the *p17* ORF on Bac21 prevented its expression as predicted from its design (Fig. 3.10, lane 4). Importantly, the ability of Bac21 to express VCap (to the same level as the other baculoviruses) was maintained (Fig. 3.9, lane 10). The final conclusion one can make from the data presented, is that Bac23 and Bac24 are responsible for slightly higher levels of p17 expression than Bac20. This is based on the fact that the signal from the western blot is stronger in lanes 5 and 6 in Fig. 3.10 than in lane 2, despite equivalent amounts of protein being loaded (Fig. 3.10, top

71

panel). This is an interesting observation given that p17 is expressed off the *polH* promoter from Bac23 and Bac24 while it is expressed off *p10* in Bac20.

3.5   RNA packaging by bac-VLPs assembled in the presence and absence of p17

A total of 2.8 x10^7 *Sf9* cells (two T75 flasks) were infected with each of the baculoviruses Bac20, Bac21, Bac23 and Bac24 at a MOI of 5. Following 4 days of incubation at 28 °C, the cells were subjected to a VLP purification protocol adapted from Taylor *et al.* (2002) and Bothner *et al.* (2005). This method employs an acidic (pH 5.0) sodium acetate buffer in order to favour the maturation of the VLPs, and stabilisation of the particles. Absorbance readings at 280 nm were used to determine the concentration of the VLPs purified and approximately 50 µg was purified on average from each preparation. Fewer VLPs were obtained using the plasmid expression system even though double the amount of cells was used (four T75 flasks vs. two T75 flasks), making the baculovirus expression system a more efficient method for producing VLPs. SDS-PAGE analysis revealed a small amount of p71 with the majority being p64, which co-migrated with wild type HaSV (Fig. 3.11, lanes 3 – 6). The predominance of p64 relative to p71 in all the VLP samples confirmed that the majority of the particles were fully matured.
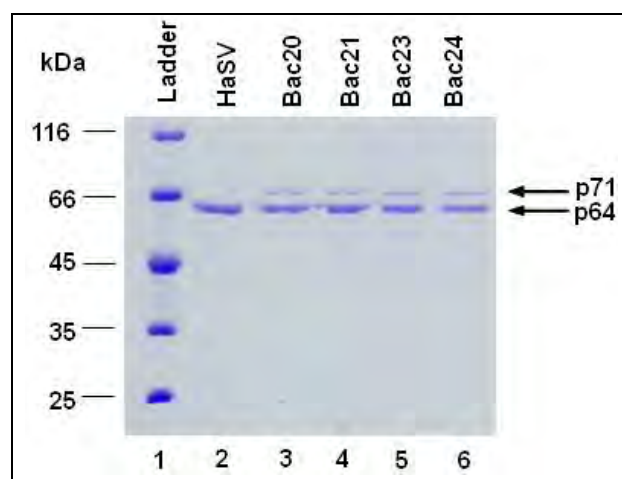
Figure 3.11: SDS-PAGE analysis of HaSV VLPs from recombinant baculovirus-infected cells. The molecular weight marker is indicated to the left and the presence of p64, indicative of mature VLPs and p71 (VCap) to the right.

The data presented in section 2 of this chapter suggested that when utilising the plasmid expression system for the co-expression of p17 and p71, there was a requirement for the expression of p17 for RNA 2 to be packaged effectively into VLPs. The first question that the baculoviruses would aide in answering was whether or not the expression of p17 still mediated packaging when the same experiment was duplicated using recombinant baculoviruses Bac20 and Bac21 to make the VLPs. Due to the fact that HaSV RNA could be transcribed off a separate RNA strand using Bac23 and Bac24, the second question that could be asked was whether or not the VLPs were able to package viral RNA that is not RNA 2 (*cis* vs. *trans* packaging). Finally, taking into account the answers to these questions, a conclusion could be made as to whether RNA 2 packaging into bac-VLPs is specific or non-specific and whether or not p17 expression has any effect on this.

In order to answer the questions raised above it was important to confirm that both the HaSV RNA 2 and p17 mRNA transcripts were present in baculovirus-infected *Sf9* cells. Accordingly, total cellular RNA including baculoviral transcripts was extracted from *Sf9* cells infected with recombinant baculoviruses Bac20, Bac21, Bac23, Bac24 and VCAP. The VCAP recombinant baculovirus contains only the *p71* ORF with an optimised Kozak, and expresses p71 under the control of the *polH* promoter. This baculovirus is representative of pMV26, a plasmid developed in the Vlok (2009) study and mentioned in section 1. The RNA was resolved by denaturing agarose gel electrophoresis and subjected to northern analysis to probe for the presence of HaSV RNA 2-derived transcripts.
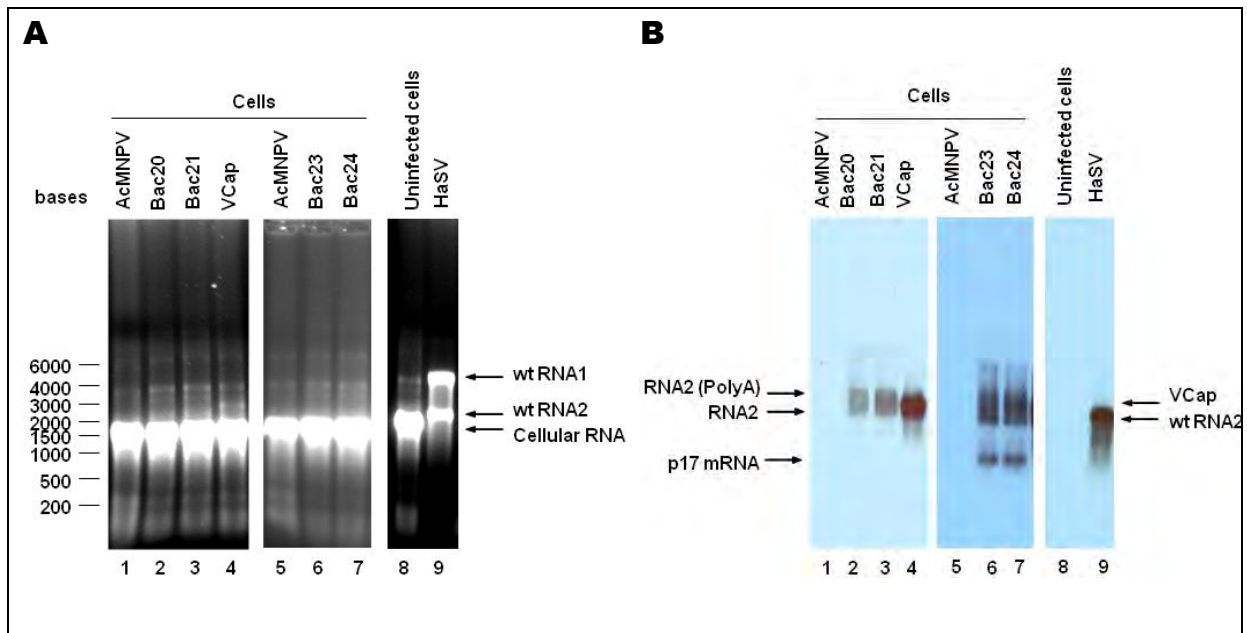
Figure 3.12: Northern analysis of cellular RNA from uninfected and baculovirus infected *Sf9* cells. (**A**) Analysis of total cellular RNAs by denaturing agarose gel electrophoresis; **(B)** Northern analysis probing for the presence of HaSV RNA2. Cellular RNA from AcMNPV (lanes 1 and 5), Bac20 (lane 2), Bac21 (lane 3), VCAP (lane 4), Bac23 (lane 6) and Bac24 (lane 7) infected cells was used in this experiment. In addition uninfected *Sf9* cellular RNA (lane 8) and RNA extracted from wild type HaSV (lane 9) was also analysed. The molecular weight standards are indicated to the left of the gel, while the arrows next to each image indicate the positions of cellular RNA, wild type (wt) HaSV RNA1 and RNA 2, RNA 2 derived from the *p10* promoter (RNA 2), un-cleaved RNA 2 derived from the *p10* promoter (RNA-PolyA) and *p17* mRNA derived from the *polH* promoter.

Ethidium bromide staining of cellular RNAs resolved by denaturing agarose gel electrophoresis did not reveal any dominant bands corresponding to the HaSV RNA transcripts expressed by the recombinant baculoviruses (Fig. 3.12 A). However the RNA 2-derived transcripts were detected by northern analysis using a probe directed against HaSV RNA 2. Two transcripts of approximately 3600 bases and 2500 bases, respectively, were detected in Bac20, Bac21, Bac23 and Bac24 infected cells, as observed previously using the plasmid derived expression system (Fig. 3.3, B lane 5 and Fig. 3.12 B). The second of the two (labelled RNA 2) migrated to approximately the same position as viral RNA 2 (Fig. 3.12 B, lanes 2, 3, 6 and 7 vs. 9), while the larger fragment was attributed to the uncleaved mRNA. The mRNA transcribed from the VCAP baculovirus migrated at a relative size of approximately 3000 bases, which is slightly bigger than viral RNA 2 (Fig. 3.12 B, lane 4 vs. 9). The size of this band can be explained by the fact that no ribozyme is present

74

downstream of the *VCap* ORF on the VCAP baculovirus. A polyA tail is thus added to the *p71* ORF making it bigger than RNA 2 but smaller than RNA 2(PolyA). Interestingly, there was a stronger signal for the VCap transcript from the same relative concentration of total RNA. This suggested that more VCap RNA is being transcribed from this baculovirus, when compared to the recombinant baculoviruses developed in this study, probably as a result of the optimised Kozak sequence on the *p71* ORF.

An approximately 900 base size RNA band was also detected in the Bac23 and Bac24-infected cells but absent in Bac20, Bac21 and VCap-infected cells (Fig. 3.14 B, lanes 6 and 7 vs. lanes 2, 3 and 4). It was concluded that this band represented the *p17* mRNA expressed under the control of the *polH* promoter in Bac23 and Bac24. Taken together, this data confirmed the expression of the full length RNA 2-derived transcript under the control of the *p10* promoter in Bac20, Bac21, Bac23 and Bac24 and the *p17* mRNA from the *polH* promoter in Bac23 and Bac24.
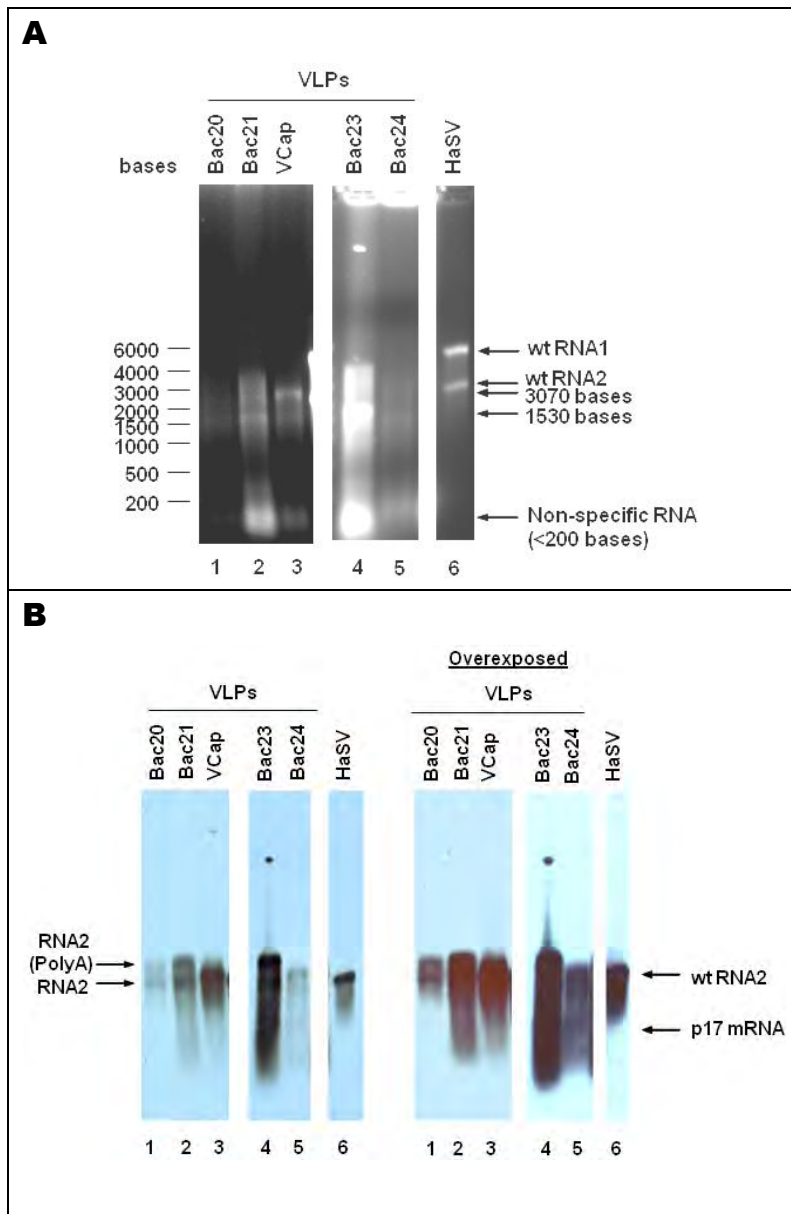
Figure 3.13: Northern analysis of RNA extracted from bac-VLPs. (**A**) Analysis of VLP RNAs by denaturing agarose gel electrophoresis and (**B**) Northern analysis probing for the presence of HaSV RNA2. RNA extracted from VLPs derived from the infection of Bac20 (lane 1), Bac21 (lane 2), VCAP (lane 3), Bac23 (lane 4) and Bac24 (lane 5) was analysed by denaturing gel electrophoresis and northern analysis. RNA extracted from wild type HaSV (lane 6) was also analysed. The northern blot was also overexposed in order to clarify fainter signals. The molecular weight standards are indicated to the left of the gel, while the arrows next to each image indicate the positions of wild type (wt) HaSV RNA1 and RNA 2, RNA 2 derived from the *p10* promoter (RNA 2), un-cleaved RNA 2 derived from the *p10* promoter (RNA-PolyA), *p17* mRNA derived from the *polH* promoter as well as the size of RNA molecules of unknown origin.

The denaturing gel stained with ethidium bromide revealed three consistently sized bands of RNA extracted from VLPs derived from Bac21, Bac23 and Bac24 infections. The size of these RNAs is approximately 3070 bases, 1530 bases and less than 200 bases respectively. It was difficult to determine whether the two larger RNAs represented viral RNA as neither of the 3070 or 1530 base bands is consistent to the size of RNA 2 or the RNA 2(PolyA) species (Fig. 3.13 A, lanes 2, 4 and 5). This raised the possibility that each of the bac-VLPs may have packaged random cellular RNA. Not enough RNA was extracted from Bac20-VLPs to be effectively defined on the gel (Fig. 3.13 A, lane 1). Repeated attempts were made to equilibrate the amount of RNA analysed so that it was approximately equal for each set of VLPs but these were unsuccessful due to the poor integrity of the extracted RNA. Therefore, less Bac20 and Bac24-VLP RNA was analysed compared to the other VLPs. Northern analysis using an HaSV RNA 2-specific probe, detected two transcripts in each set of VLPs corresponding in size to the RNA 2 and RNA 2 (PolyA) RNAs detected in the infected cells (Fig. 3.12 B, lanes 2, 3, 6 and 7 vs. Fig. 3.13 B, lanes 1, 2, 4 and 5). Both RNA 2 and RNA 2(PolyA) were observed from RNA extracted from Bac20 and Bac24 derived VLPs by overexposing the northern blot (Fig. 3.13 B right hand blot, lanes 1 and 5). VLPs isolated from VCAP infected cells also packaged the VCap mRNA detected in the cells (Fig. 3.12 B, lane 4 vs. Fig. 3.13 B, lane 3).

VLPs purified from cells infected with Bac23 and Bac24 also packaged an additional RNA of 900 bases, corresponding in size to the p17-encoding transcript expressed by the *polH* promoter and detected in the Bac23 and Bac24 infected cells (Fig. 3.12 B, lanes 6 and 7 vs. Fig. 3.13 B, lanes 4 and 5). This suggested that RNA other than the RNA 2 encoding VCap was also packaged by the VLPs. However, this RNA encoded the *p17* ORF and potentially a packaging signal, which could promote the packaging of p17 mRNA.

By analysing the RNA extracted from the bac-VLPs it was concluded that the expression of p17 had no effect on the encapsidation of RNA 2. Furthermore, the bac-VLPs were also able to package HaSV RNA not derived from RNA 2. Two

interpretations could be made from this data: (1) HaSV RNA packaging is specific for any HaSV-derived RNA sequence or (2) bac-VLPs package non-specifically any RNA that is produced in abundance in the cell (i.e. baculovirus derived RNA). In order to differentiate between specific and non-specific HaSV RNA packaging another experiment was devised.

The next set of northern blots aimed at deciphering whether the HaSV VLPs were preferentially packaging HaSV RNA transcripts over other baculoviral transcripts, and, therefore, specific vs non-specific packaging. This was done using Bac20 and Bac21, which encode the viral RNA 2 transcript in the *p10* direction and have no HaSV-derived sequence downstream of the *polH* promoter (Fig. 3.4, A and C). If packaging was non-specific, then one would expect VLPs produced by these two baculoviruses to also contain the other, abundant mRNAs, such as that expressed by the baculoviral *polH* promoter. A polH specific probe was thus designed to detect the 91 bases of the *polH* cloning cassette.
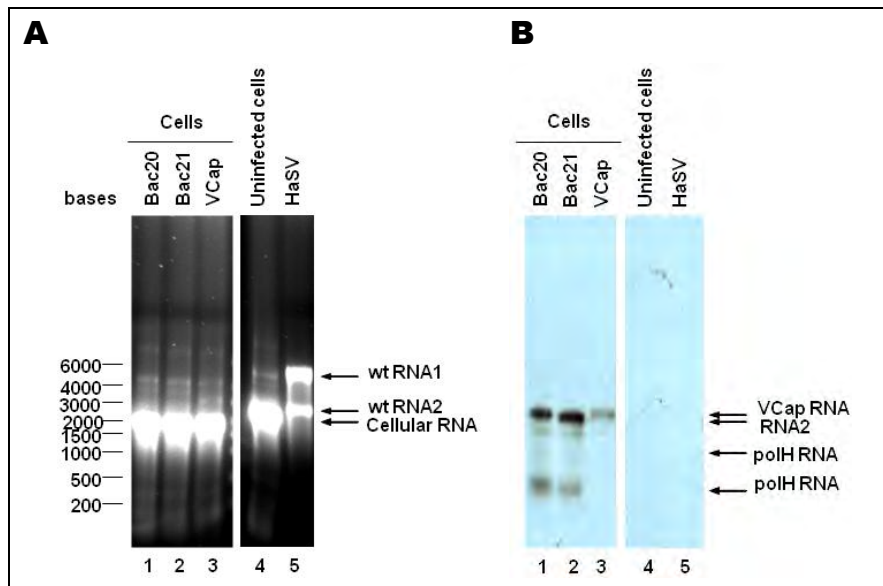
Figure 3.14: Detection of small RNAs derived from the expression of the _polH_ cloning cassette in cells infected with Bac20, Bac21 and VCAP. (**A**) Analysis of cellular RNAs by denaturing agarose gel electrophoresis; (**B**) Northern analysis probing for transcripts derived from the empty _polH_ cloning cassette. In this experiment only Bac20 (lane 1), Bac21 (lane 2) and VCAP (lane 3) recombinant baculoviruses were analysed alongside uninfected _Sf9_ cells (lane 4) and wild type HaSV RNA (lane 5). The molecular weight standards are indicated to the left of the gel while RNAs derived from the baculoviruses are indicated with arrows to the right.

Northern analysis of total RNA extracted from cells infected with Bac20 and Bac21 showed the presence of polH-derived transcripts of approximately 480 bases (Fig. (Fig. 3.14 B, lanes 1 and 2). This band was not present in cells infected with the VCAP baculovirus or in uninfected cells (Fig. 3.14 B, lanes 3 and 4). In addition, the polH probe detected a second, larger band in Bac20, Bac21 and VCAP-infected cells (Fig. 3.14 B, lanes 1, 2 and 3), but not in uninfected cells (Fig. 3.14 B, lane 4). The largest RNA band detected in the Bac20 and Bac21 infected cells was approximately the same size as RNA 2 detected by the RNA 2-specific probe in the previous two blots (Fig. 3.12 B and Fig. 3.13 B). Although the polH probe was not designed to detect RNA 2, it appeared that due to a small degree of overlap in the sequence of the _p10_ and _polH_ cloning cassettes, the probe was able to bind both baculovirus-expressed RNAs. This is supported by the fact that baculoviral VCap mRNA, which is fused downstream of the polH promoter, was detected but wild type HaSV RNA 2 was not (Fig. 3.14 B, lanes 3 vs. 5).

79
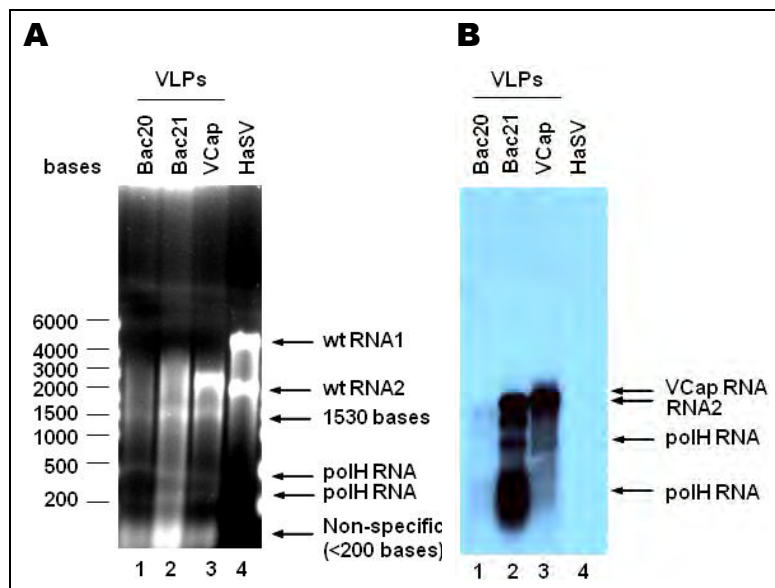
Figure 3.15: Packaging of non-viral RNA by bac-VLPs. (**A**) Denaturing agarose gel electrophoresis and (**B**) Northern blot analysis of RNA extracted from Bac20 (lane 1), Bac21 (lane 2) and VCAP (lane 3) HaSV VLPs, probed for RNAs containing polH non-coding sequence. RNA extracted from wild type HaSV was also analysed (lane 4). The molecular weight standards are indicated to the left of the gel while RNA's derived from the baculoviruses are indicated with arrows to the right.

The packaged RNA was resolved by denaturing agarose gel electrophoresis and visualised by staining with ethidium bromide. This revealed a similar band pattern of packaged RNA as the previous denaturing gel analysis of the VLPs (Fig. 3.13 A vs. Fig. 3.15 A). Two bands originating from the *polH* cloning cassette of 488 and 208 bases respectively were observed towards the bottom of the gel (Fig. 3.15 A, lanes 1, 2 and 3). Over and above these RNAs, there were less defined RNA species larger than 4000 bases that were also resolved on the gel (Fig. 3.15 A, lanes 1, 2 and 3). None of these RNAs were present in wild type HaSV particles (Fig. 3.15 A, lane 4 vs. 1, 2 and 3). Less RNA from Bac20-VLPs was analysed when compared to the Bac21 and VCAP-VLPs (Fig. 3.15 A, lane 1 vs. 2 and 3).

Northern analysis using the polH probe revealed that, as observed before (Fig. 3.13 B, lanes 2 and 3), Bac21 and VCAP-VLPs packaged RNA 2 and VCap mRNA (Fig. 3.15 B, lanes 2 and 3). However, the signal for RNA from Bac20-VLPs was much lower, as was observed previously with the RNA 2 probe (Fig. 3.13 B, lane 1 vs. Fig.

80

3.15 B, lane 1). The two polH RNAs of 488 and 208 bases were also detected by northern analysis as a smear towards the bottom of the blot. Due to the size of these RNAs and the binding to the probe it was concluded that the Bac21-VLPs packaged non-coding *polH* RNA.

The VCAP-VLPs appeared to package predominantly VCap mRNA, although in this instance the probe was not able to detect non-coding RNA, proven by the fact that only VCap RNA was detected previously in VCAP infected cells (Fig. 3.14 B, lane 3 and Fig. 3.15 B, lane 3). Therefore, no additional inferences on VCAP-VLP packaging can be made. Bands corresponding to the *polH* transcript were not detected in Bac20 VLPs, which is likely to be due to the uneven loading of the RNA samples. However, when one compares the strength of the *polH* signal relative to the signal from the RNA 2 band in the Bac21-VLP sample, it is possible that the Bac20-VLPs may be packaging significantly less or no *polH* RNA. No RNA was detected by northern blot even when the membrane was over-exposed (Fig. 3.15 B, lane 1 vs. 2).

The results of this experiment are thus inconclusive because not as much packaged Bac20 RNA was analysed compared to Bac21 RNA. It therefore, remains uncertain whether bac-VLPs package HaSV RNA specifically or non-specifically the most abundant RNA proximal to the assembling particle.

Chapter 4
Discussion

4.1 Introduction

Tetraviruses provide a unique insight into the assembly and packaging biology involved in the production of small insect RNA viruses. They were the first T=4 symmetry icosahedral viruses to be discovered and many studies have been dedicated to identifying how these particles assemble (Canady *et al*., 2000 and 2001; Taylor *et al*., 2002; Matsui *et al*., 2009). A major challenge in doing so is the fact that these viruses cannot replicate in tissue cultured cells and thus the assembly of structurally indistinguishable, yet non-infectious VLPs has provided a useful alternative to a replicating system (Agrawal and Johnson, 1995; Tomasicchio *et al*., 2007; Gordon *et al*., 2001). The packaging of RNA into a capsid particle is an important process during assembly and in many instances the combination of the RNA and protein components of a virus need to combine in a specific manner in order to produce a viable particle (Schneemann, 2006). Despite this fact, very few studies have focused on the packaging element of tetravirus assembly.

Prior to this study, a plasmid transfection system was developed to study the assembly and packaging of HaSV VLPs (Vlok, 2009). This system was used to assemble VLPs in *Sf9* cells via the co-expression of the two proteins coded for by HaSV RNA 2, p17 and VCap (p71), in different contexts. The VLPs were then purified from the cells and their packaging phenotype determined by the content of the RNA within (Vlok, 2009). This system was advantageous in that it was a relatively simple way of testing a variety of elements that were potentially important to HaSV VLP packaging and it did not require a large amount of time to carry out each experiment. Data developed in this study aided in the formulation of the hypothesis that p17 or a signal present on the first 28 codons of the *p17* ORF are essential for the specific packaging of HaSV RNA 2 into plasmid-VLPs. This hypothesis was based on the observation that no HaSV RNA 2 was packaged by VLPs made from the transfection and expression of a plasmid only coding for VCap (pMV26 – Fig. 3.1) whereas RNA 2 was packaged by the VLPs made from a wild

type RNA 2 plasmid (pMV18 – Fig. 3.1) as well as plasmids in which the UTRs were removed but the *p17* ORF maintained (pMV20, 26 and 27 – Fig. 3.1).

However, despite its advantages there were certain drawbacks to the plasmid-based system. Firstly, expression levels were not high enough to detect the expression of p17 from the plasmids in the insect cells. Secondly, the yield of VLPs purified from the plasmid-transfected cells was not substantial enough to purify large amounts of RNA. It was for this reason that the recombinant baculovirus expression system was developed and one of the major aims of this study was to utilise this new system to elucidate the specific events involved in the packaging of RNA by tetravirus particles. The reasoning behind this study was to develop recombinant bacoluviruses that would essentially express the same RNA 2 sequences as the plasmids used in the transfection system. Another major reason to convert to baculoviruses was that two proteins could be efficiently expressed from one recombinant virus. This afforded the opportunity to refine the p17-packaging hypothesis by testing whether or not p17 could direct the packaging of sequences other than RNA 2 (*trans* packaging), by including the *p17* ORF on a different cloning cassette. This would have been more challenging using plasmids.

4.2 <u>Comparison of plasmid and baculovirus-mediated expression systems</u>

The data reported by Marli Vlok, (2009) as well the results of this study (section 3.2), indicated that plasmid-transfection was a moderately efficient method of producing VLPs. The low level expression of the plasmids resulted in fewer VLPs and thus less RNA to analyse. Expression of p17 could not be detected in the plasmid-transfected cells by western analysis and, therefore, it was not possible to confirm that p17 was required for RNA 2 packaging. The baculovirus system developed in this study was more efficient in terms of protein expression. Firstly, half the amount of cells (two T75 flasks) produced a two-fold increase in purified VLPs. Secondly, p17 was detected in cells infected with the recombinant baculoviruses, which thus

provided reliable data confirming which VLPs were assembled in the presence or absence of the protein.

Over and above improving the expression levels of HaSV proteins, baculoviruses have the potential to provide further advantages over plasmids. By utilising the Bac-to-Bac system it was demonstrated in this study that it was relatively easy to reliably produce two or more sets of proteins from one baculovirus, therefore, cutting out the need for sometimes complicated plasmid co-transfections. This made it possible to analyse packaging from another angle, in that it allowed for the analysis of the effect of p17 on *cis* or *trans* packaging. HaSV is a bi-partite virus and utilises both RNA 1 and RNA 2 during its infectious cycle (Hanzlik *et al.*, 1993). Therefore, by taking advantage of the bi-directionality of the baculoviruses, a more comprehensive approach to the analysis of packaging could be undertaken by including RNA 1 opposite RNA 2 on a single baculovirus. Finally, the large scale production of VLPs would be extremely useful, regardless of whether the aim is fundamental research or biotechnological application. In this regard, the infection of colonies of insect larvae by the recombinant viruses could provide an effective means of large scale VLP production. This approach has been more widely adopted in asian countries but its potential to both efficiently and effectively produce large amounts of recombinant protein have been documented elsewhere and thus this remains a somewhat interesting avenue for the production of VLPs (Kost *et al.*, 2005).

The disadvantage of using recombinant baculoviruses is the time required to develop and optimise a functional system. Compared to cloning plasmids and then carrying out a transfection, the development of baculoviruses can take between 2 to 8 months after which there is still the optimisation of protein expression. Despite this, the baculovirus system proved an effective means of study the packaging of HaSV VLPs. This system provided additional insights into the packaging biology of HaSV that were not necessarily clear from the plasmid-based system.

4.3 The packaging of RNA 2 by HaSV VLPs derived from plasmid transfection

As mentioned above, a previous study using a plasmid-transfection system was able to show that either the expression of p17 or a signal sequence between the *p17* and *VCap* start codons was responsible for the specific packaging of RNA 2 into HaSV VLPs (Vlok, 2009). Further analysis in this study, using the same system, has shown that when two codons of the p17 RNA sequence are mutated so that p17 is not translated (AUG AGC to GAU AUC), VLPs fail to effectively package RNA 2 mRNA when compared to a wild type RNA 2-plasmid control (Fig. 3.3). This data in combination with the Vlok, (2009) study suggested that it is p17 expression that was required for RNA 2 packaging, although the presence or absence of p17 in the cells transfected with wild type (pMV18) or mutated (pAM10) plasmids could not be confirmed. However, since western analysis of the same sequences expressed by recombinant baculoviruses confirmed that the mutation had abolished translation of p17, it is likely that the protein was not present in the pAM10-transfected cells. An alternative possibility is that p17 is not required for packaging, but rather that there is a packaging signal that includes the six mutated nucleotides in pAM10 and that the disruption of these, is in fact the reason for the lack of RNA 2 packaging.

4.4 The packaging of RNA 2 by HaSV VLPs derived from the baculovirus expression system

The shortfalls in terms of protein expression meant that the packaging data developed using the plasmid expression system could not conclusively implicate p17 as a requirement for RNA packaging. An alternative test of the p17 hypothesis was constructed by developing recombinant baculoviruses based on the plasmids used by Vlok, (2009). First, two recombinant baculoviruses, namely Bac20 (analogous to pMV18) and Bac21 (analogous to pAM10), were constructed. These baculoviruses were constructed in such a way that the mRNA that resulted from transcription from the *p10* promoter would be precise at the 3'end (via the HC ribozyme) while containing approximately 125 bp of baculoviral RNA at the 5'end. Short regions of non-viral RNA have been reported to effect viral processes such as assembly and replication and thus the precise fusion of RNA 2 to the 5'end of the promoter remains a goal for future experiments (Kay *et al*., 2001). Western analysis confirmed that

VLPs derived from Bac20, assembled in the presence of p17 while Bac21-VLPs assembled without the protein (Fig. 3.10 and Fig. 3.11). In terms of the packaging of the bac-VLPs, northern blot analysis (Fig. 3.13) showed that the VLPs derived from Bac20, Bac21 and VCAP (a baculovirus analogous to pMV26) infections all packaged both RNA 2 mRNA (representing baculovirus mRNA cleaved by the ribozyme) as well as RNA 2(PolyA) mRNA (resulting from the lack of ribozyme activity and the addition of a polyA tail to RNA 2). It was thus concluded that Bac20 and Bac21 do not require the expression of p17 or a signal sequence between the two start codons to package RNA 2 mRNA. Thus the data obtained from this set of bac-VLPs contradicts the results obtained from the plasmid expression system.

As mentioned previously, an advantage of using baculoviruses is that two sets of ORFs can be incorporated into one recombinant virus and that this element would allow for the analysis of p17-mediated *cis*/*trans* RNA packaging. In order to achieve this, two further recombinant baculoviruses were constructed in this study; Bac23 (pMV18 plus an additional *p17* ORF) and Bac24 (pAM10 plus an additional *p17* ORF). The question posed by making VLPs from these two baculoviruses was whether or not the additional *p17* mRNA would be packaged by the VLPs. The presence of p17 as well as the purification of VLPs was confirmed by western analysis after the infection of both of these viruses (Fig. 3.10 and Fig. 3.11). It was also confirmed that both sets of VLPs were able to package both sets of RNA 2-derived RNAs (RNA 2 and RNA 2-PolyA) in a similar manner to Bac20 and Bac21 (Fig. 3.13). In addition to the RNA 2 species, Bac23 and Bac24-VLPs also packaged the *p17* mRNA. This result as well as the result from the analysis of Bac20 and Bac21-VLP packaging indicated that the bac-VLPs were either specifically packaging any HaSV-derived RNA sequence or simply packaging any RNA that was in abundance in the cell, which would include baculovirus derived HaSV-RNA.

Ethidium bromide staining of purified RNA packaged by the bac-VLPs and resolved by denaturing agarose gel electrophoresis showed additional RNAs that were not detected by northern analysis using the RNA 2-probe (Fig. 3.13 A and Fig. 3.15 A). This was interpreted as evidence of the non-specific nature of bac-VLP packaging and thus an experiment was designed to test the specificity of HaSV bac-VLP RNA

packaging. This experiment was based on the assumption that a large degree of non-coding RNA, derived from the *polH* promoter, would be transcribed from Bac20 and Bac21. This RNA corresponds to the cloning cassette of the Bac20 and Bac21 viruses and thus if these VLPs were packaging non-specifically (the most abundant RNA) then it was reasoned that this RNA should be present in the particles. The northern analysis indicated that Bac21 packaged a variety of non-HaSV RNAs that were detected by the polH probe. No corresponding signals were detected in RNA purified from Bac20 derived VLPs (Fig. 3.15 B) suggesting the exclusion of non-viral RNA in the presence of p17. However, this result could also be due to the uneven loading of RNA samples because the amount of RNA from the Bac20-VLPs was less than that extracted from the Bac21-VLPs. Thus the data is inconclusive. It was very tempting to formulate the hypothesis that p17 may still have an effect on packaging by excluding non-HaSV RNAs but then RNA 2 should still have been detected on the blot. Therefore, RNA packaging in the baculovirus system appeared to be less selective than in the plasmid system but whether or not bac-VLPs package RNA non-specifically cannot conclusively be stated.

4.5   Bac-VLPs versus plasmid-VLPs, how does HaSV package its genome?

The data in this study presents two very different pictures of HaSV RNA packaging. On the one hand it was concluded that p17 is very important in the selective packaging of RNA 2 (plasmid system) whereas on the other hand VLP packaging is non-selective and p17 plays no role (baculovirus system). The key difference between the data from the two systems is the significantly increased levels of transcription by baculoviruses compared to plasmids. Therefore, VLP assembly can be described as taking place in an RNA-limiting environment in the plasmid-transfected cells versus an RNA-excess environment in the baculovirus-infected cells.

The question one is therefore, forced to ask is which system is more representative of a wild type HaSV infection? Meaning essentially which system is better for studying packaging? These questions are difficult to answer because like packaging

literature, there are also relatively few studies that have focused on the pathogenicity of tetravirus infections. A quantitative study of the pathogenicity of HaSV was carried out by Christian and colleagues in 2001 and this revealed that HaSV varied in virulence depending on which larval stage the virus infected. In some instances low-level infection was required for the stunting of early instar larvae whereas in other instances higher doses could not effect stunting on more developed larvae (Christian *et al*., 2001). A more in depth analysis was carried out by Brooks *et al*. (2002) who were able to show that the infection of HaSV to early instar *H. armigera* larvae was initiated at multiple points in the midgut and developed into widespread foci of infection that covered virtually all the cells. Furthermore it was proposed that due to the immune response of the insects, which results in sloughing of infected cells, the virus relies on the speed of RNA replication and assembly to accumulate virions before apoptosis (Brooks *et al*., 2002). This data suggests that at least initially wild type HaSV infection is like the baculovirus system, in that viral RNA is produced in excess and many virions are produced rapidly. Conversely, it also suggests that the infected insects do gain a level of immunity of infection relatively quickly and thus the RNA-limiting environment may be more representative of larvae infected after early instar development. Exactly where the *Sf9* tissue cultured cells fit in, in terms of at what stage of development they are being forced to make HaSV VLPs, is unclear. Therefore, it is unclear whether an RNA-limiting or an RNA-excess environment is better suited for studying packaging.

An explanation that takes both data sets into account is that p17 plays an important role in promoting the selective packaging of viral RNA when RNA is limiting but plays a minor role when RNA is in excess. Even though this hypothesis takes into account both sets of data, it fails to explain the RNA packaging observed by tetraviruses in the literature. In contradiction to the bac-VLP packaging data, a specific replication-independent RNA packaging system has been implied by two groups prior to this study. Agrawal and Johnson (1995) used baculoviruses to express the NωV VCap protein (p70) and inadvertently the NωV equivalent of p17 in *Sf9* cells. It was shown via northern blots that the resulting VLPs packaged RNA 2, although the specificity of this packaging was implied but not necessarily depicted.
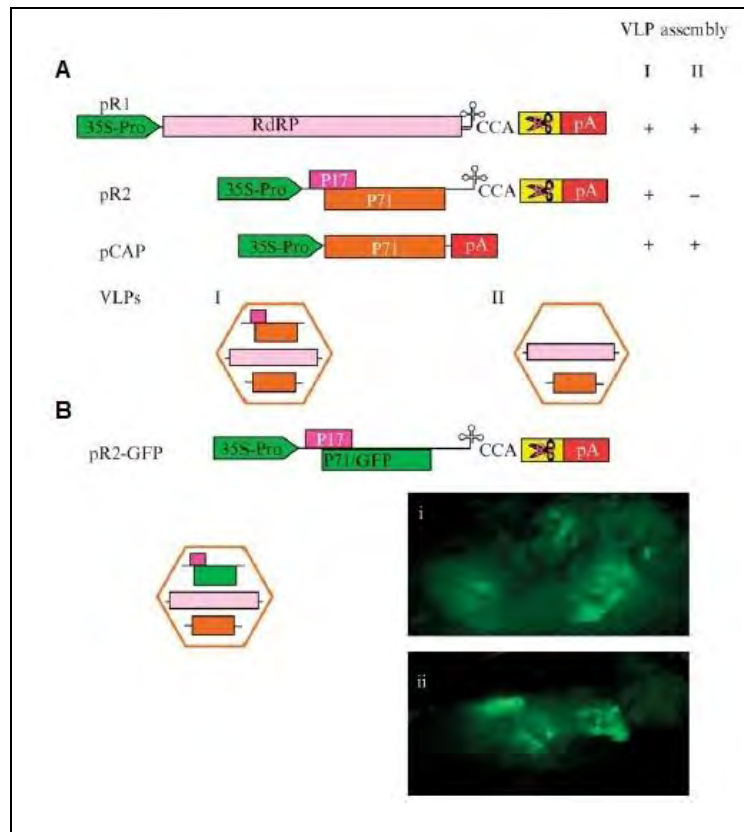
Figure 4.1: System for the assembly of HaSV VLPs in plant protoplasts. Gordon *et al*. (2001) used the plasmids depicted in (**A**) to produce VLPs in plant protoplasts that would eventually be fed to live larvae. pR1 and pR2 contain HaSV RNA 1 and RNA 2 cDNA while pCAP contains only the *VCap* ORF. The HaSV genes were inserted into plasmids containing the *Cauliflower mosaic virus* (CaMV) 35S promoter (35S-Pro) and poly-adenylation signal (pA) as well as a *cis*-acting ribozyme sequence (depicted by scissors). Depicted below the plasmids are the two sets of VLPs that were hypothesised to be constructed from the transfection of all three plasmids (I) or just pR1 and pCAP (II). (**B**) Gordon and Waterhouse, (2006) reported the results of unpublished data in which pR2 was modified to include a p71-GFP fusion ORF (pR2-GFP). Also reported was the analysis the anterior midgut regions of larvae infected with the VLP depicted in (**B**) by fluorescence microscopy (figure reproduced from Gordon and Waterhouse, 2006).

In a different study on HaSV (cited in Gordon and Waterhouse, 2005), a plasmid-based system was developed in which plant protoplasts were transfected with constructs containing either HaSV RNA 1, RNA 2 or *VCap* cDNA (Fig. 4.1 A). The transfected-protoplasts were then fed to healthy *H. armigera* larvae and the assembly of infectious particles was confirmed by electron microscopy and bioassays. Despite the lack of replication in the protoplasts and the lack of any northern analysis of RNA extracted from the VLPs purified from the protoplasts, it was implied that the VLPs specifically packaged RNA 1, RNA 2 and the *VCap*

mRNAs because the insects showed symptoms of stunting. The same system was modified to introduce a p71-green fluorescence protein (GFP) fusion into the protoplasts (Fig. 4.1 B). The fusion plasmid was introduced together with the VCap and RNA 1 plasmids into the protoplasts and when fed to larvae resulted in fluorescence when the anterior midgut of the larvae was analysed (Gordon and Waterhouse, 2006).

Neither of the two studies set out with the aim of studying HaSV RNA packaging and thus the results were not necessarily conclusive. Despite reporting the packaging of RNA 2 in NωV VLPs, Agrawal and Johnson (1995) provided no additional data on the packaging of the VLPs or why the VLPs would package only RNA 2, when NωV is also a bipartite virus. In terms of the HaSV VLPs assembled in the protoplasts, no data has been provided similar to this study, in which the resulting VLPs were analysed by denaturing agarose gel electrophoresis and northern analysis. This therefore, begs the question as to whether or not the plasmids themselves were the infecting agent from the protoplasts or the VLPs.

The literature mentioned above as well as both systems described in this study all have one fundamental flaw when it comes to analysing the events involved in tetraviral RNA packaging. Using both plasmids and baculoviruses, the proteins coded for by RNA 2 have been expressed predominantly in isolation in *Sf9* cells. Yet this is not in keeping with the natural infectious cycle of an omegatetravirus which requires the translation of RNA 1 and RNA 2 and consequentially replication, assembly and then packaging to be infectious. The problem faced by using these systems is that they are artificial assembly systems where not all the natural components are available.

The next question is thus, what effect does this have on the analysis of tetraviral packaging? The literature indicates that RNA plays an essential role in the assembly of tetraviruses and other structurally similar viruses (Fox *et al.*, 1994). In broad terms, the model for assembly of these viruses relies on RNA binding to capsid oligomers early on in assembly and in some cases acting as part of a molecular switch (nodaviruses, bromoviruses and PrV) while in other cases it does the

fundamental job of neutralising positively charged capsid protein terminals so that they can fuse together to form a cohesive particle (Fisher and Johnson, 1993; Speir *et al*., 2010). Thus if RNA is in fact required for assembly, then one can logically assume that RNA will be packaged in any system producing VLPs. An artificial assembly system may force the VLPs to package RNAs in order to assemble a particle even if it would not normally do so, essentially requiring a head-full of RNA for assembly.

Support for this theory is present in the packaging data provided in this as well as the plasmid-based study (Vlok, 2009). Both studies illustrate that when HaSV RNA 2 is packaged, it is accompanied by a larger RNA 2 derived strand (RNA 2-polyA). In both sets of studies the relative abundance of RNA 2 to RNA 2(PolyA) in the VLPs has been shown to be approximately equivalent (if not favoured slightly towards RNA 2-polyA). This packaging pattern thus looks similar to that of the wild type particles where RNA 2 is consistently packaged and RNA 2(PolyA) takes up the space normally left for RNA 1 in the VLPs. Therefore, by assembling the VLPs in an artificial system they are forced to package mRNA 2 with the polyA extension. It would be interesting to test whether or not this is the reason why the ribozyme is so inefficient. This also may provide the reason why extraneous RNA is observed by denaturing gel analysis of bac-VLP packaging. In order to create a head-full of RNA, the VLPs would potentially be forced to fill the space not taken by the two RNA 2 species and thus extraneous RNA would be packaged. Overall this suggests that a major challenge in interpreting any data on tetraviral RNA packaging is how to align an artificial assembly system with what may occur naturally.

The assembly and packaging of nodaviruses has been studied in a baculovirus system that mimics closely the natural conditions of viral infection. When nodaviral RNA 1 and RNA 2 were expressed off baculoviruses, both sets of RNAs were replicated and the particles packaged both RNAs to near wild type specificity (Krishna, Marshall and Schneemann, 2003). A very different picture of packaging was depicted when only the RNA 2 baculovirus was used (Schneemann *et al.,* 1994; Dong *et al.,* 1998). Subsequent studies employing the replicating system showed that nodaviruses utilise trafficking of the assembling virion to replication

microdomains as a means of ensuring packaging specificity (Venter *et al*., 2005 and 2009). This illustrates another problem with the artificial system employed in this study. Tetraviruses are structurally related to nodaviruses and may share the requirement of replication to ensure effective packaging and thus without replication in the baculovirus or plasmid systems, the VLPs may be packaging whatever RNA may happen to be proximal to the assembling particle. Using fluorescence microscopy, Short *et al*. (2010) proposed that endosomes created from membranes of the endocytic pathway may represent the site of tetravirus replication. It will be very interesting to see whether or not bac-VLPs or plasmid-VLPs assemble near these endosomes regardless of their state of replication. This would provide a handy clue as to whether or not nodaviral and tetraviral packaging is similar.

Fortunately, there is the potential to move away from artificial tetravirus assembly. As has been alluded to already, there is evidence that the baculoviruses produced in this study can express a different set of proteins from each of the two promoters (*p10* and *polH*). The next step in the research project will thus be to introduce RNA 1 into the *polH* cloning cassette of Bac20 and Bac21, effectively introducing all the components of HaSV cDNA into a single cell. This would allow us to ask some interesting questions; 1) will both RNA 1 and RNA 2 be able to replicate and what effect will the lack of p17 have on this; 2) will assembly take place and 3) if VLPs/viable HaSV particles form what effect will p17 have on packaging.

4.6   Alternative hypotheses for HaSV packaging

The literature review introduced two structurally similar insect virus families (the bromoviruses and nodaviruses) in which there is more information regarding RNA packaging. Although the conclusions can only remain speculative until correctly tested, it may be useful to contrast bromovirus and nodavirus packaging mechanisms with what is known about tetraviruses.

It has been hypothesised that bromoviruses utilise a "C1-model" of RNA packaging in which the concentration of VCap upon initial infection is utilised to allow the protein to bind only high affinity RNA binding sites on the viral RNA. VCap thus acts as a "structural identifier" for the RNA 1 molecule and as the VCap concentration

increases more copies bind to the ribonucleoprotein complex forming a capsid particle (Johnson *et al*., 2003). It is tempting to hypothesise that p17 may be some sort of "structural identifier".   Perhaps in an RNA-limiting environment (plasmid-system) the concentrations of RNA, VCap and p17 are balanced so that p17 is able to identify RNA 2 effectively, whereas in an RNA-excess environment (baculovirus-system) VCap and RNA are able find each other more easily and thus there is no need for p17. Furthermore, the "C1 model" predicted that other sets of RNA could also be packaged but that given its identification by VCap, viral RNA is favoured. The results of this study indicate that HaSV VLPs have the ability to do the same, as RNA derived from polH was packaged by Bac21-derived VLPs but so was RNA 2 (Fig. 3.15).   Choi and Rao (2003) speculated that BMV utilises both nucleating signals which are hypothesised to be 3' tRNA-like structures as well as packaging elements specific to each RNA to ensure VCap binding. Interestingly, tetraviruses also have 3' tRNA-like structures and this presents one further line of speculative evidence towards a bromovirus-like model of packaging.

Nodaviruses utilise an entirely different mechanism of packaging and one that is dependent on a variety of interlinked processes in order to function.   It is hypothesised that nodaviruses are able to package two sets of RNAs by ensuring that the initial ribonucleoprotein complex is shipped to the site of replication where the other copy of RNA will be present (Venter *et al*., 2009). Therefore, by ensuring that all the components of a nodavirus are present in close vicinity, the natural affinity of VCap to combine RNA and protein to create a capsid is used to form a nodavirus particle. It is difficult to provide any evidence for a similar process in tetraviruses, given that no one has yet been able to set up a replicating system. Although given the large degree of structural similarity between the two families it may not be very surprising if their packaging mechanisms turn out to be similar.

4.7   Future prospects

The development of a replicating system for tetraviruses remains the ultimate goal as this will provide the means to improve on a variety of aspects of tetravirus research. It is believed that this may be possible utilising the baculovirus mediated system. Over and above setting up a replicating system, our laboratory has begun

to develop a direct quantitative PCR (qPCR) system to provide a quantitative figure behind the amount of each RNA species being packaged by the particles. This could provide an indication as to the efficiency of RNA 2 packaging by each set of bac-VLPs. In addition, it is believed that novel approaches such as deep sequencing of a population of VLPs may be very useful in providing data as to exactly what is being packaged by the particles. By comparing the homo or heterogeneity of the RNAs packaged by each set of VLPs to that of wild type packaging one could get a very good idea if what is being observed represents a natural packaging phenomenon.

Despite the fact that there is now little novelty in the T=4 structure of a tetravirus particle, there remains many reasons to still conduct tetravirus research. Firstly, it has been shown in this study that tetraviral RNA packaging may be unique and this information can only serve to add to the volume of the relatively small size of RNA packaging literature. Besides the fundamental question of RNA packaging, there is also the potential for viruses such as tetraviruses to be small molecule delivery vehicles. It is thus hoped that tetraviruses will one day, not only be relatively interesting viruses to study but also a clinically important element of the future.

Appendices

Appendix 1 – Primers

Table A1.1: List of Primers used in this study

Primer	Location	Direct/ complimentary	Sequence (5'- 3')
AM7F	Nt 1198 – 1223 of hr:AcMNPV promoter	D	AACAACCAAGCTTAATCGAATTCCG
AM8R	Nt 766 - 738 p17 - RNA 2	C	AGATCTCTCTTATCTCTGCGTCGACGGA
AM9 SDM	Nt 262 – 307 RNA 2	D	CAGCGTTGATAGCGCCGATTGATATCGAGCACACCATCGCCCAC
AM10 SDM	Nt 307 - 262 RNA 2	C	GTGGGCGATGGTGTGCTCGATATCAAATCCGCGCTATCAACGCTG
AM13F	Nt 283 – 304 p17 RNA 2	D	AGATCTATGAGCGAGCACCATCGCC
AM14R	Nt 757 - 733 p17 pMV18	C	CTGCAGTTATCTCTGCGTCGACGGAGAACT
M13F	AcMNPV bacmid	D	CCCAGTCACGACGTTGTAAAACG
M13R	AcMNPV bacmid	C	AGCGGATAACAATTTCACACAGG
60F	Nt 2075 - 2094 p71 – RNA 2	D	CCCCGCCACTGACAACTTC
AM18 polH	Nt 103 – 125 *polH* promoter AcMNPV bacmid	D	ATTCATACCGTCCCACCATCGGG
JRS56	Nt 144 – 164 5'UTR – RNA 2	D	GTCGTTGGGAGTTTCGTCCG
JRS57	Nt 862 – 841 p71 – RNA 2	C	CGGTTCTGAACATCGGAAAGG
JRS61	Nt 115 – 87 polH cloning cassette AcMNPV bacmid	C	CTCTAGTACTTCTCGACAAGCTTGTCGAG

Nt - nucleotide

Appendix 2 – Thermal cycling parameters used in this study

Table A2.1: The cycling parameters for PCR amplification of *p17* prior to SDM (AM7F to AM8R).

Stage	Temperature (°C)	Time	No. of cycles
1	94	2min	1
2	94	15sec	25
	53	30sec	
	72	50sec – 1min	
3	72	7min	1
4	4		∞

Table A2.2: The cycling parameters used for SDM

Stage	Temperature (°C)	Time	No. of cycles
1	95	30sec	1
2	95	30sec	18
	55	1min	
	78	4min	
3	4		∞

Table A2.3: The cycling parameters used for the analysis of the recombinant bacmids

Stage	Temperature (°C)	Time	No. of cycles
1	95	2min	1
2	95	30sec	25
	55	30sec	
	78	4min	
3	72	10min	1
4	4		∞

Table A2.4: The cycling parameters used for the amplification of the *polH* sequence for the development of an RNA probe

Stage	Temperature (°C)	Time	No. of cycles
1	94	2min	1
2	94	15sec	20
	57	30sec	
	72	30sec	
3	72	2min	1
4	4		∞

Appendix 3 – Plasmid construction
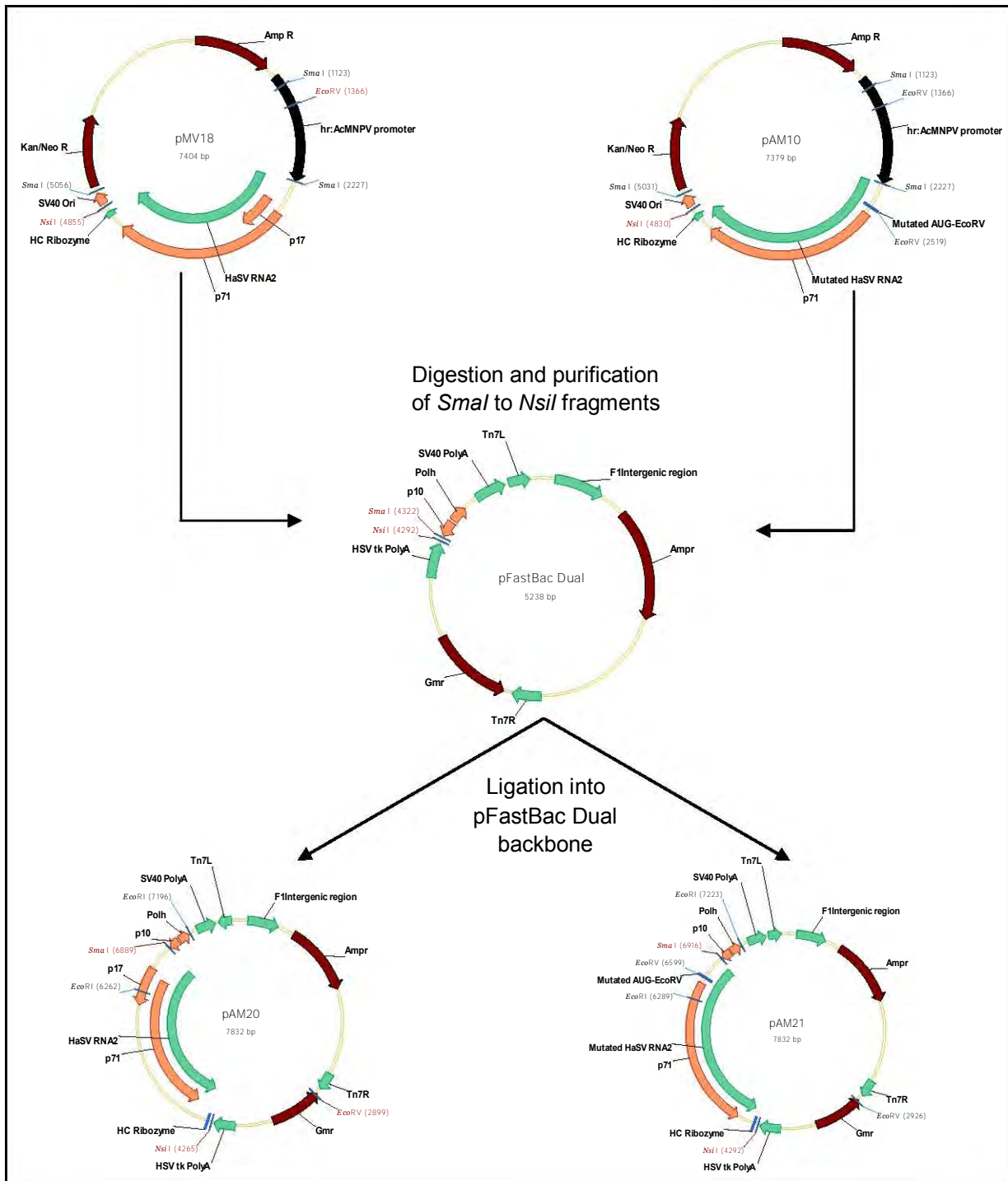
Figure A3.1: Construction of pAM20 and pAM21 transfer vectors. AmpR – ampicillin resistance gene; Kan/NeoR – kanamycin/neomycin resistance gene; Gmr – gentamycin resistance gene; hrAcMNPV - hybrid promoter from the *Autographa californica nuclear polyhedrosis virus*; SV40 ori – *Simian virus 40* origin of replication; SV40 polyA - *Simian virus 40* polyadenylation signal; p17 – HaSV p17; p71 – HaSV VCap/p71; Tn7L and Tn7R – transposon sites.

Figure A3.2: Construction of pAM23. The construction of pAM24 followed the same protocol except pAM21 was used instead of pAM20 to yield pAM24. AmpR – ampicillin resistance gene; Kan/NeoR – kanamycin/neomycin resistance gene; Gmr – gentamycin resistance gene; hrAcMNPV - hybrid promoter from the *Autographa californica nuclear polyhedrosis virus*; SV40 ori – *Simian virus 40* origin of replication; SV40 polyA - *Simian virus 40* polyadenylation signal; p17 – HaSV p17; p71 – HaSV VCap/p71; Tn7L and Tn7R – transposon sites.
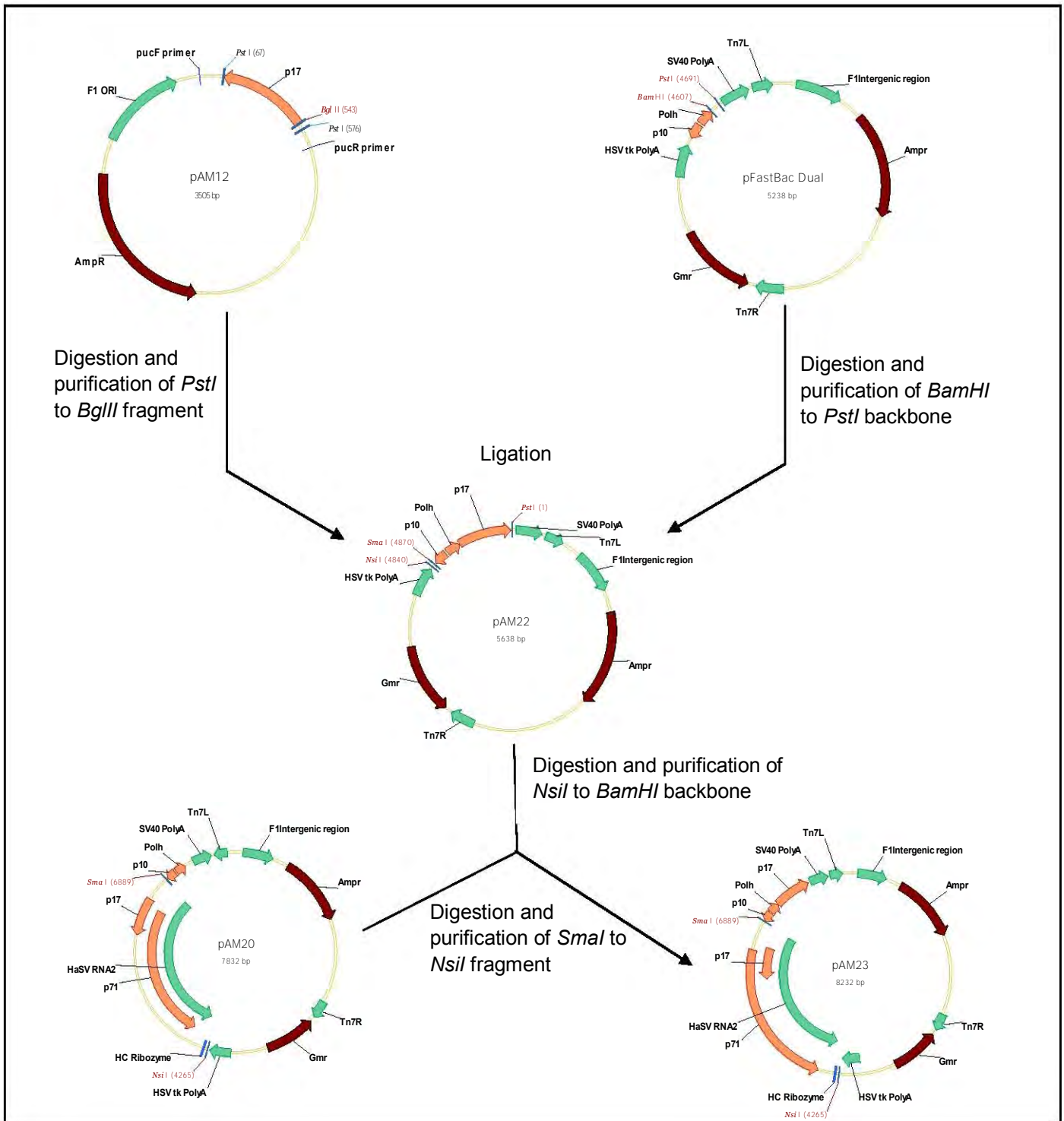
References

1. Agrawal, D.K. and Johnson, J.E. 1995. Assembly of the *T*=4 *Nudaurelia capensis omega virus* capsid protein, post-translational cleavage and specific encapsidation of its mRNA in a baculovirus expression system. *Virol.* **207,** 89 – 97.

2. Alquist, P. 1994. Bromoviruses, In: *Encyclopaedia of Virology.* (Webster, R.G. and Granoff, A., eds) pp. 181 – 185. Academic Press, San Diego.

3. Annamalai, P., Swapna, A., Wilkens, S. and Rao, A.L.N. 2005. Deletion of highly conserved arginine-rich RNA binding motif in *Cowpea chlorotic mottle virus* capsid protein results in virion structural alterations and RNA packaging constraints. *J. Virol.* **79,** 3277 – 3288.

4. Bancroft, J.B., Hills, G.J. and Markham, R. 1967. A study of the self-assembly process in a small spherical virus formation of organised structures from protein subunits *in vitro*. *Virol.* **31,** 354 – 379.

5. Bawden, A.L., Gordon, K.H.J. and Hanzlik, T.N. 1999. The specificity of *Helicoverpa armigera stunt virus* infectivity. *J. Invertbr. Pathol.* **74,** 156 – 163.

6. Berghammer, H. and Auer, B. 1993. "Easypreps": Fast and easy plasmid minipreparation for analysis of recombinant clones in *E. coli. Biotechniques.* **14,** 527 – 528.

7. Bloomer, A.C., Champness, J.N., Bricogne, G., Staden, R. and Klug, A. 1978. Protein disk of *Tobacco Mosaic* virus at 2.8 Å resolution showing the interactions within and between subunits. *Nature.* **276,** 362 – 368.

8. Bothner, B., Taylor, D., Jun, B., Lee, K.K., Siuzdak, G., Schlutz, C.P. and Johnson, J.E. 2005. Maturation of a tetravirus capsid alters the dynamic properties and creates a metastable complex. *Virol.* **334,** 17 – 27.

9. Brooks, E.M., Gordon, K.H.J., Dorrian, S.J., Hines, E.R. and Hanzlik, T.N. 2002. Infection of its lepidopteran host by the *Helicoverpa armigera stunt virus* (*Tetraviridae*). *J. Invertebr. Pathol.* **80,** 97 – 111.

10. Bujarski, J., Figlerowicz, M., Gallitelli, D., Roossinck, M.J. and Scott, S.W. 2011. *Bromoviridae.* In: *Virus taxonomy: classification and nomenclature of viruses: Ninth Report of the International Committee on Taxonomy of Viruses.* (King, A.M.Q., Adams, M.J., Carstens, E.B. and Lefkowitz, E.J., eds). pp 964 – 976. Elsevier Academic Press, London.

11. Canady, M.A., Tihava, M., Hanzlik, T.N., Johnson, J.E. and Yeager, M. 2000. Large conformational changes in the maturation of a simple RNA virus, *Nudaurelia capensis ω virus* (NωV). *J. Mol. Biol.* **299,** 573 – 584.

12. Canady, M.A., Tsuruta, H. and Johnson, J.E. 2001. Analysis of rapid, large-scale protein quaternary structural changes: Time-resolved X-ray solution scattering of *Nudaurelia capensis ω virus* (NωV) maturation. *J. Mol. Biol.* **311,** 803 – 814.

13. Carrillo-Tripp, M., Shepherd, C.M., Borelli, I.A., Venkataraman, S., Lander, G., Natarajan, P., Johnson, J.E., Brooks, C.L. and Reddy, V.S. 2009. VIPERdb2: an enhanced and web API enabled relational database for structural virology. *Nucleic Acids Res.* **37**: D436 – D442, doi: 10.1093/nar/gkn840.

14. Casjens, S. and King, J. 1975. Virus Assembly. *Annu. Rev. Biochem.* **44,** 555 – 611.

15. Casper, D.L.D. and Klug, A. 1962. Physical principles in the construction of regular viruses. Cold Spring Harbour Symp. *Quant. Biol.* **72,** 1 – 24.

16. Cavarelli, J., Bomu, W., Liljas, L., Kim, S., Minor, W., Munshi, S., Muchmore, S., Schmidt, T., Hendry, D.A. and Johnson, J.E. 1991. Crystallization and preliminary structure analysis of an insect virus with *T*=4 quasi-symmetry: *Nudaurelia capensis ω virus.* *Acta. Crystollographica.* **B47,** 23 – 29.

17. Chen, Y.P., Nakashima, N., Christian, P.D., Bakonyi, T., Bonning, B.C., Valles, S.M. and Lightner, D. 2011. *Dicistroviridae.* In: *Virus taxonomy: classification and nomenclature of viruses: Ninth Report of the International Committee on Taxonomy of Viruses.* (King, A.M.Q., Adams, M.J., Carstens, E.B. and Lefkowitz, E.J., eds). pp 840 – 845. Elsevier Academic Press, London.

18. Chen, Z.G., Stauffacher, C., Li, Y., Schmidt, T., Bomu, W., Kamer, G., Shanks, M., Lomonosoff, G. and Johnson, J.E. 1989. Protein-RNA interactions in an icosahedral virus at 3.0 Å resolution. *Science.* **245,** 154 – 159.

19. Choi, Y.G. and Rao, A.L.N. 2000a. Molecular studies on bromovirus capsid protein. VII Selective packaging of BMV RNA 4 by specific N-terminal arginine residues. *Virol.* **275,** 207 – 217.

20. Choi, Y.G. and Rao, A.L.N. 2000b. Packaging of *Tobacco Mosaic virus* subgenomic RNAs by *brome mosaic virus* coat protein exhibits RNA controlled polymorphism. *Virol.* **275,** 249 – 257.

21. Choi, Y.G. and Rao, A.L.N. 2003. Packaging of *Brome mosaic virus* RNA 3 is mediated through a bipartite signal. *J. Virol.* **77,** 9750 – 9757.

22. Christian, P.D. and Scotti, P.D. 1998. Picornalike Viruses of Insects, In: *The Insect Viruses.* (Miller L.K. and Ball, L.A., eds). pp 301 – 336. Academic Press, New York.

23. Christian, P.D., Dorrian, S.J., Gordon, K.H.J. and Hanzlik, T.N. 2001. Pathology and properties of the tetravirus *Helicoverpa armigera stunt virus*. *Biological Control.* **20,** 65 – 75.

24. Crick, F.H.C. and Watson, J.D. 1956. Structure of small viruses. *Nature.* **177,** 473 – 475.

25. Cuillel, M., Herzog, M. and Hirth, L. 1979. Specificity of *in vitro* reconstitutiuon of *brome grass virus*. *Virol.* **95,** 153 – 156.

26. D' Souza, V. and Summers, M.F. 2005. How retroviruses select their genomes. *Nat. Reviews.* **3,** 643 – 655.

27. Dong, X.F., Natarajan, P., Tohova, M., Johnson, J.E. and Schneemann, A. 1998. Particle polymorphism caused by deletion of a peptide molecular switch in a quasiequivilent icosahedral virus. *J. Virol.* **72,** 6024 – 6033.

28. Dorrington, R.A. and Short, J.R. 2010. Tetraviruses, In: *Insect Virology.* (Asgari, S. and Johnson, K., eds). pp 283 – 305. Caister Academic Press, Norfolk, U.K.

29. Dorrington, R.A., Gorbalenya, A.E., Gordon, K.H.J., Lauber, C. and Ward, V.K. 2011. *Tetraviridae*. In: *Virus taxonomy: classification and nomenclature of viruses: Ninth Report of the International Committee on Taxonomy of Viruses*. (King, A.M.Q., Adams, M.J., Carstens, E.B. and Lefkowitz, E.J., eds). pp 1091 – 1102. Elsevier Academic Press, London.

30. Draper, D.E. 1995. Protein-RNA recognition. *Annu. Rev. Biochem.* **64,** 593 – 620.

31. Du Plessis, L., Hendry, D.A., Dorrington, R.A., Hanzlik, T.N., Johnson, J.E. and Appel, M. 2005. Revised RNA 2 sequence of the tetravirus, *Nudaurelia capensis ω virus* (NωV). *Arch. Virol.* **150,** 2397 – 2402.

32. Eckerle, L.D. and Ball, L.A. 2002. Replication of RNA segments of a bipartite viral genome by a transactivating subgenomic RNA. *Virol.* **296,** 165 – 176.

33. Fallows, D.A. and Goff, S.P. 1995. Mutations in the epsilon sequences of *Human Hepatits B virus* affect both RNA encapsidation and reverse transcription. *J. Virol.* **69,** 3067 – 3073.

34. Finch, J.T., Crowther, R.A., Hendry, D.A. and Struthers, J.K. 1974. The structure of *Nudaurelia capensis β virus*: the first example of a capsid with icosahedral surface symmetry *T*=4. *J. Gen. Virol.* **24,** 191 – 200.

35. Fisher, A.J. and Johnson, J.E. 1993. Ordered duplex RNA controls capsid architecture in an icosahedral animal virus. *Nature.* **361,** 176 – 179.

36. Fox, J.M., Johnson, J.E. and Young, M.J. 1994. RNA/protein interactions in icosahedral virus assembly. *Seminars in Virology.* **5,** 51 – 60.

37. Friesen, P.D. and Rueckert, R.R. 1981. Synthesis of *Black Beetle virus* proteins in cultured *Drosophila* cells: differential expression of RNAs 1 and 2. *J. Virol.* **37,** 876 – 886.

38. Frolova, E., Frolov, I. and Schlesinger, S. 1997. Packaging signals in Alphaviruses. *J. Virol.* **71,** 248 – 258.

39. Gallagher, T.M. and Rueckert, R.R. 1988. Assembly-dependant maturation cleavage in provirions of a small icosahedral insect ribovirus. *J. Virol.* **62,** 3399 – 3406.

40. Gordon, K.H.J. and Waterhouse, P.M. 2006. Small RNA viruses of insects: Expression in plants and RNA silencing. *Adv. Virus Res.* **68,** 459 – 502.

41. Gordon, K.H.J., Johnson, K.N. and Hanzlik, T.N. 1995. The larger genomic RNA of *Helicoverpa armigera stunt virus* encodes the viral RNA polymerase and has a novel 3'- terminal tRNA-like structure. *Virol.* **208,** 84 – 98.

42. Gordon, K.H.J., Williams, M.R., Baker, J.S., Bawden, A.L., Millgate, A.G., Larkin, J. and Hanzlik, T.N. 2001. Replication-independent assembly of an insect virus (*Tetraviridae*) in plant cells. *Virol.* **288,** 36 – 50.

43. Gordon, K.H.J., Williams, M.R., Hendry, D.A. and Hanzlik, T.N. 1999. Sequence of the genomic RNA of *Nudaurelai β virus (Tetraviridae)* defines a novel genome organisation. *Virol.* **258,** 42 – 53.

44. Hanahan, D. 1983. Studies on the transformation of *Eschericia coli* with plasmids. *J. Mol. Biol.* **166,** 557 – 580.

45. Hanzlik, T.N., Dorrian, S.J., Gordon, K.H.J and Christian, P.D. 1993. A novel small RNA virus isolated from the cotton bollworm, *Helicoverpa armigera*. *J. Gen. Virol.* **74,** 1805 – 1810.

46. Hanzlik, T.N., Dorrian, S.J., Johnson, K.N., Brooks, E.M. and Gordon, K.H.J. 1995. Sequence of RNA 2 of the *Helicoverpa armigera stunt virus* (*Tetraviridae*) and bacterial expression of its genes. *J. Gen. Virol.* **76,** 799 – 811.

47. Harrison, S.C. 2001. The familiar and the unexpected in the structures of isosahedral viruses. *Curr. Opin. Struct. Biol.* **2,** 195 – 199.

48. Harrison, S.C., Olson, A.J. Schutt, C.E., Winkler, F.K. and Bricogne, G. 1978. *Tomoto Bushy stunt virus* at 2.9 Å resolution. *Nature.* **276,** 368 – 373.

49. Hohn, T. and Hohn, B. 1970. Structure and assembly of simple RNA bacteriophages. *Adv. Virus Res.* **16,** 43 – 98.

50. Hosur, M.V., Schmidt, T., Tucker, R.C., Johnson, J.E., Gallagher, T.M., Selling, B.H. and Rueckert, R.R. 1987. Structure of an insect virus at 3.0 Å resolution. *Proteins: Structure, Function and Bioinformatics.* **2,** 167 – 176.

51. Johnson, J.M., Wilits, D.A., Young, M.J. and Zlotnick, A. 2003. Interaction with the capsid protein alters RNA structure and the pathway for *in vitro* assembly of *Cowpea chlorotic mottle virus*. *J. Mol. Biol.* **335,** 455 – 464.

52. Johnson, K.N., Tang, L., Johnson, J.E. and Ball, L.A. 2004. Heterologous RNA encapsidated in *Pariacoto virus*-like particles forms a dodecahedral cage similar to genomic RNA in wild type virions. *J. Virol.* **78,** 11371 – 11378.

53. Kao, C.C., Ni, P., Hema, M., Huang, X. and Dragnea, B. 2011. The coat protein leads the way: an update on basic and applied studies with the *Brome mosaic virus* coat protein. *Mol. Plant Pathol.* **12,** 403 – 412.

54. Kay, M.A., Glorioso, J.C. and Naldini, L. 2001. Vectors for gene therapy: the art of turning infectious agents into vehicles for therapeutics. *Nature.* **7,** 33 – 40.

55. Knowles, N.J., Hovi, T., Hyypiä, T., King, A.M.Q., Lindberg, M., Pallansch, M.A., Palmenberg, A.C., Simmonds, P., Skern, T., Stanway, G., Yamashita, T. and Zell, R. 2011**.** *Picornaviridae.* In: *Virus taxonomy: classification and nomenclature of viruses: Ninth Report of the International Committee on Taxonomy of Viruses.* (King, A.M.Q., Adams, M.J., Carstens, E.B. and Lefkowitz, E.J., eds). pp 855 – 880. Elsevier Academic Press, London.

56. Kost, T.A., Condreay, J.P. and Jarvis, D.L. 2005. Baculovirus as versatile vectors for protein expression in insect and mammalian cells. *Nature Biotech.* **23,** 567 – 575.

57. Kozak, M. 1987. An analysis of 5'-noncoding sequences from 699 vertebrate messenger RNAs. *Nucleic Acids Res.* **15,** 8125 – 8148.

58. Kramvis, A. and Kew, M.C. 1998. Structure and function of the encapsidation signal of *Hepadnaviridae*. *Journal of Virus Hepatitis.* **5,** 357 – 367.

59. Krishna, N.K., Marshall, D. and Schneemann, A. 2003. Analysis of RNA packaging in wild type and mosaic protein capsids of *Flock House virus* using recombinant baculovirus vectors. *Virol.* **305,** 10 – 24.

60. Krol, M., Olson, N.H., Tate, J., Johsnon, J.E., Baker, T.S. and Ahlquist, P. 1999. RNA-controlled polymorphism in the *in vivo* assembly of 180-subunit

and 120-subunit virions from a single capsid protein. *Proc. Natl. Acad. Sci. (USA).* **96,** 13650 – 13655.

61. Laemmli, U. 1970. Cleavage of structural proteins during the assembly of the head of *bacteriophage T4*. *Nature.* **227,** 680 – 685.

62. Liljas, L. 1999. Virus Assembly. *Curr. Opin. Struc. Biol.* **9,** 129 – 134.

63. Lukas, R.W., Kuznetsov, Y.G., Larson, S.B. and McPherson, A. 2005. Crystallization of *Brome mosaic virus* and *T*=1 *brome mosaic virus* particles following structural transition. *Virol.* **286,** 290 – 303.

64. Maree, H.J., Van der Walt, E., Tiedt, F.A.C., Hanzlik, T.N. and Appel, M. 2006. *J. Virol. Methods.* **136,** 283 – 288.

65. Marshall, D. and Schneemann, A. 2001. Specific packaging of nodaviral RNA 2 requires the N-terminus of the capsid protein. *Virol.* **285,** 165 – 175.

66. Matsui, T., Lander, G. and Johnson, J.E. 2009. Characterization of large conformational changes and autoproteolysis in the maturation of a *T*=4 virus capsid. *J. Virol.* **83,** 1126 – 1134.

67. Miller, D.J., Schwartz, M.D. and Ahlquist, P. 2001. *Flock House virus* RNA replicates on outer mitochondrial membranes in *Drosophila* cells. *J. Virol.* **75,** 11664 – 11676.

68. Molenkamp, R. and Spaan, J.M. 1997. Identification of a specific interaction between the coronavirus *mouse hepatitis virus* A59 nucleocapsid protein and packaging signal. *Virol.* **239,** 78 – 86.

69. Mori, K., Nakai, T., Muroga K., Arimoto, M., Mushiake, K. and Furusawa, I. 1992. Properties of a new virus belonging to *Nodaviridae* found in larvak striped jack (*Pseudocaranax dentex*) with nervous necrosis. *Virol.* **187,** 368 – 371.

70. Munshi, S., Liljas, L., Cavarelli, J., Bomu, W., McKinney, B., Reddy, V. and Johnson, J.E. 1996. The 2.8 Å structure of a *T*=4 animal virus and its implications for membrane translocation of RNA. *J. Mol. Biol.* **261,** 1 – 10.

71. Natarajan, P., Lander, G.C., Shepherd, C.M., Reddy, V.S., Brooks, C.L. and Johnson, J.E. 2005. Exploring icosahedral virus structure with VIPER. *Nature Rev. Microbiol.* **3,** 809 – 817.

72. Osman, F., Grantham, G.L. and Rao, A.L.N. 1997. Molecular studies of bromovirus capsid protein. *Virol.* **238,** 452 – 459.

73. Pringle, F.M., Johnson, K.N., Goodman, C.L., McIntosh, A.H. and Ball, L.A. 2003. *Providence virus*: a new member of the *Tetraviridae* that infects cultured insect cells. *Virol.* **306,** 359 – 370.

74. Qi, N., Cai, D., Qiu, Y., Xie, J., Wang, Z., Si, J., Zhang, J., Zhou, X. and Hu, Y. 2011. RNA binding by a novel helical fold of b2 protein from *wuhan nodavirus* mediates the suppression of RNA interference and promotes b2 dimerization. *J. Virol.* **85,** 9543 – 9554.

75. Reichsteiner, M. and Rogers, S.W. 1996. PEST sequences and regulation by proteolysis. *Trends Biochem. Sci.* **21,** 267 – 271.

76. Rao, A.L.N. 2006. Genome packaging by spherical plant RNA viruses. *Ann. Rev. Phytopathol.* **44,** 61 – 87.

77. Rossmann, M.G. and Johnson, J.E. 1989. Icosahedral RNA virus structure. *Annu. Rev. Biochem.* **58,** 533 – 573.

78. Sambrook, J., Fritsch, E.F. and Maniatis, T. 1989. Molecular Cloning: A laboratory manual, 2nd edition. New York: Cold Spring Harbor Laboratory.

79. Schneemann, A. 2006. The structural and functional role of RNA in icosahedral virus assembly. *Annu. Rev. Microbiol.* **60,** 51 – 67.

80. Schneemann, A. and Marshall, D. 1998. Specific encapsidation of nodavirus RNAs in mediated through the C terminus of capsid precursor protein alpha. *J. Virol.* **72,** 8738 – 8746.

81. Schneemann, A., Dasgupta, R., Johnson, J.E. and Rueckert, R.R. 1993. Use of recombinant baculovirus in synthesis of morphologically distinct virus-like particles of *Flock House virus*, a nodavirus. *J. Virol.* **67,** 2756 – 2763.

82. Schneemann, A., Gallagher, T.M. and Rueckert, R.R. 1994. Reconstitution of *Flock House virus*: a model system for studying structure and assembly. *J. Virol.* **68,** 4547 – 4556.

83. Schneemann, A., Zhong, W., Gallagher, T.M. and Rueckert, R.R. 1992. Maturation cleavage required for infectivity of a nodavirus. *J. Virol.* **66,** 6728 – 6734.

84. Schneider, P.A., Schneemann, A. and Lipkin, W.I. 1994. RNA splicing in *Borna-disease virus*, a nonsegmented, negative strand RNA virus. *J. Virol.* **68,** 5007 – 5012.

85. Short, J.R., Knox, C. and Dorrington, R.A. 2010. Subcellular localisation and live cell imaging of the *Helicoverpa armigera stunt virus* replicase in mammalian and *Spodoptera frugiperda* cells. *J. Gen. Virol.* **91,** 1514 – 1523.

86. Speir, J.A., Bothner, B., Qu, C., Willits, D.A., Young, M.J. and Johnson, J.E. 2006. Enhanced local symmetry interactions globally stabilize a mutatnt virus capsid that maintains infectivity and capsid dynamics. *J. Virol.* **80,** 3582 – 3591.

87. Speir, J.A., Munshi, S., Wang, G., Baker, T.S. and Johnson, J.E. 1995. Structures of the native and swollen forms of *Cowpea chlorotic mottle virus* determined by X-ray crystallography and cryo-electron microscopy. *Structure.* **3,** 63 – 78.

88. Speir, J.A., Taylor, D.J., Natarajan, P., Pringle, F.M., Ball, L.A. and Johnson, J.E. 2010. Evolution in action: N and C termini of subunits in related *T*=4 viruses exchange roles as molecular switches. *Structure.* **18,** 700 – 709.

89. Studier, F.W. and Moffat, B.A. 1986. Use of *bacteriophage T7* RNA polymerase to direct selective high-level expression of cloned genes. *J. Mol. Biol.* **189,** 113.

90. Sullivan, C. and Ganem, D. 2005. A virus-encoded inhibitor that blocks RNA interference in mammalian cells. *J. Virol.* **79,** 7371 – 7379.

91. Tang, L., Johnson, K.N., Ball. A.L., Lin, T., Yeager, M. and Johnson, J.E. 2001. The structure of *Pariacoto virus* reveals a dodecahedral cage of duplex RNA. *Nature.* **8,** 77 – 83.

92. Taylor, D.J. 2003. Molecular and biophysical analysis of a conformational change in a nonenvoloped RNA virus. Doctor of Philosophy Thesis, University of California, San Diego, United States of America.

93. Taylor, D.J., Krishna, N.K., Canady, M.A., Schneemann, A. and Johnson, J.E. 2002. Large-scale pH-dependant, quaternary structure changes in an RNA virus capsid are reversible in the absence of subunit autoproteolysis. *J. Virol.* **76,** 9972 – 9980.

94. Thiéry, R., Johnson, K.L., Nakai, T., Schneemann, A., Bonami, J.R. and Lightner, D.V. 2011. *Nodaviridae*. In: *Virus taxonomy: classification and nomenclature of viruses: Ninth Report of the International Committee on Taxonomy of Viruses*. (King, A.M.Q., Adams, M.J., Carstens, E.B. and Lefkowitz, E.J., eds). pp 2011 – 2076. Elsevier Academic Press, London.

95. Tomasicchio, M., Venter, P.A., Gordon, K.H.J., Hanzlik, T.N. and Dorrington, R.A. 2007. Induction of apoptosis in *Saccharomyces cerevisiae* results in the spontaneous maturation of tetravirus procapsids *in vivo*. *J. Gen. Virol.* **88,** 1576 – 1582.

96. Towbin, H., Staehelin, T. and Gordon, J. 1979. Electrophoretic transfer of proteins from polyacrylamide gels to nitrocellulose sheets: procedure and some applications. *Proc. Natl. Acad. Sci.* **76,** 4350 – 4354.

97. Van Oers, M.M. 2011. Oppurtunities and challenges for the baculovirus expression system. *Journal of Inv. Pathol.* **107,** 53 – 515.

98. Venter, P.A. and Schneemann, A. 2007. Assembly of two independent populations of *Flock House virus* particles with distinct RNA packaging characteristics in the same cell. *J. Virol.* **81,** 613 – 619.

99. Venter, P.A., Krishna, N.K. and Schneemann, A. 2005. Capsid protein synthesis from replicating RNA directs specific packaging of the genome of a multipartite positive-strand RNA virus. *J. Virol.* **79,** 6239 – 6248.

100. Venter, P.A., Marshall, D. and Schneemann, A. 2009. Dual roles for an arginine-rich motif in specific genome recognition and localization of viral coat protein to RNA replication sites in *Flock House virus*-infected cells. *J. Virol.* **83,** 2872 – 2882.

101.   Vlok, M. 2009. Understanding the function of *Helicoverpa armigera stunt virus* p17 in the virus lifecycle.   Masters Thesis, Rhodes University, Grahamstown, South Africa.

102.   Walter, C.T. 2008. Establishing experimental systems for studying the replication biology of *Providence virus*. Doctor of Philosophy Thesis, Rhodes University, Grahamstown, South Africa.

103.   Walter, C.T., Pringle, F.M., Nakayinga, R., de Felipe P., Ryan, M.D., Ball, L.A. and Dorrington, R.A. 2010. Genome organisation and translation of *Providence virus*: Insight into a unique tetravirus. *J. Gen. Virol.* **91,** 2826 – 2835.

104.   Wien, M.W., Chow, M. and Hogle, J.M. 1996. *Poliovirus*: new insights from an old paradigm. *Structure.* **4,** 763 – 767.

105.   Yi, F., Zhang, J., Yu, H., Liu, C., Wnag, J. and Hu, Y. 2005. Isolation and identification of a new tetravirus from *Dendrolimus punctatus* larvae collected from the Yunnan province, China. *J. Gen. Virol.* **86,** 789 – 796.

106.   Yi, G., Letteney, E., Kim, C.H. and Kao, C.C. 2009. *Brome mosaic virus* capsid protein regulates accumulation of viral replication proteins by binding to the replicase assembly RNA element. *RNA.* **4**, 615 – 626.

107.   Yi, G., Vaughan, R.C., Yarbrough, I., Dharmaiah, S. and Kao, C.C. 2009. RNA bindind by the *Brome mosaic virus* capsid protein and the regulation of viral RNA accumulation. *J. Mol. Biol.* **391,** 314 – 326.

108.   Zhou, L., Zheng, Y., Jihang, H., Zhou, W., Lin, M., Han, Y., Cao, X., Zhang, J. and Hu, Y. 2008. RNA-binding properties of *Dendrolimus punctatus* tetravirus p17 protein. *Virus. Res.* **138,** 1 – 6.

109.   Zhou, X., Fox, J.M., Olson, N.H., Baker, T.S. and Young, M.J. 1995. *In vitro* assembly of *Cowpea chlorotic mottle virus* from the coat protein expressed in *Escherichia coli* and *in vitro*-transcribed viral cDNA. *Virol.* **207,** 486 – 494.

110.   Zhu, J., Gopinath, K., Mural, A., Yi, G., Diane Hayward, S., Zhu, H. and Kao, C. 2007. RNA-binding proteins that inhibit RNA virus infection. *Proc. Natl. Acad. Sci. (USA).* **104,** 3129 – 3134.